Celastrol, a proteasome inhibitor, can induce the expression of heat shock protein genes in *Xenopus* cultured cells

by

Shantel Walcott

A thesis
presented to the University of Waterloo
in fulfillment of the
thesis requirement for the degree of
Master of Science
in
Biology

Waterloo, Ontario, Canada, 2010

Author's Declaration

I hereby declare that I am the sole author of this thesis. This is a true copy of the thesis, including any required final revisions, as accepted by my examiners. I understand that my thesis may be made electronically available to the public.

Abstract

Heat shock proteins (HSPs) are stress-inducible and evolutionarily conserved molecular chaperones that are involved in protein binding and translocation. As molecular chaperones, HSPs bind to denatured proteins, inhibit their aggregation, maintain their solubility, and assist in refolding. This process inhibits the formation of protein aggregates which can be lethal to the cell. In eukaryotic cells, the ubiquitin-proteasome system (UPS) is responsible for the degradation of most non-native proteins. Furthermore, proteasome inhibition has been shown to induce *hsp* gene expression. Celastrol, a quinone methide triterpene, was shown to have an inhibitory effect on proteasome function in mammalian cells. The present study determined that celastrol induced the accumulation of ubiquitinated proteins and reduced proteasomal chymotrypsin-like activity in *Xenopus laevis* A6 kidney epithelial cells. In addition, incubation of A6 cells with celastrol induced the accumulation of HSP30 and HSP70 in a dose- and time-dependent manner with maximal levels of HSP accumulation occurring after 18 h of exposure. In A6 cells recovering from celastrol, the relative levels of HSP30 and HSP70 accumulation remained elevated for 18-24 h after removal of celastrol. The activation of heat shock factor 1 (HSF1) DNA-binding may be involved in celastrol-induced *hsp* gene expression in A6 cells, since the HSF1 inhibitor, KNK437, repressed the accumulation of HSP30 and HSP70. Exposure of A6 cells to simultaneous celastrol and mild heat shock treatment enhanced the accumulation of HSP30 and HSP70 to a greater extent than the sum of both stressors individually. Additionally, concurrent treatment of A6 cells with low concentrations of both celastrol and MG132 produced different patterns of HSP30 and HSP70 accumulation. While combined treatment with

celastrol and MG132 acted synergistically on HSP30 accumulation, relative levels of HSP70 were similar to those observed with MG132 alone. Immunocytochemical analysis of celastrol- or MG132-treated A6 cells revealed HSP30 accumulation in a punctate pattern primarily in the cytoplasm with some staining in the nucleus. Also, in some cells treated with celastrol or MG132 large HSP30 staining structures were observed in the cytoplasm. Lastly, exposure of A6 cells to celastrol induced rounder cell morphology, reduced adherence and disorganization of the actin cytoskeleton. In conclusion, this study has shown that celastrol inhibited proteasome activity in amphibian cultured cells and induced HSF1-mediated expression of *hsp* genes.

Acknowledgements

I have had an amazing experience in the Heikkila lab and I would like to start by thanking my supervisor Dr. John Heikkila for giving me this opportunity. Thank you John for your advice, patience and guidance over these past two years. I have learned a lot from you. In addition, I would like to thank my committee members, Dr. Vivian R. Dayeh and Dr. Matt M. Vijayan for taking time out of their busy schedules to review my work and provide helpful feedback. Also, thanks to all members of Club Heikkila past and present: Janine Voyer, Jessica Woolfson, Jordan Young (the "J" crew), Ashlee Rammeloo, Saad Khan, and Jara Brunt for making my Master's experience fun. I would also like to extend a big thank you to Linda Zepf for providing her administrative assistance and advice, whenever I needed it. I would like to acknowledge Dale Weber for his help with confocal microscopy, thank you for constantly checking in on me. Last but not least, I would like to thank my family, for providing continuous love and support throughout my undergraduate and Master's degree and for keeping me motivated.

Table of Contents

List of Figures

List of Abbreviations

ALS	amyotrophic lateral sclerosis
ANOVA	analysis of variance
APS	ammonium persulfate
ATCC	american type culture collection
BCA	bicinchoninic acid
BCIP	5-bromo-4-chloro-3-indolyl phosphate
BiP	immunoglobulin-binding protein
BSA	bovine serum albumin protein standard
BSA fraction V	bovine serum albumin fraction V
C	control
Cel	celastrol
CT-like	chymotrypsin-like
DAPI	4,6-diamidino-2-phenylindole
DEPC	diethylpyrocarbonate
DIG	digoxigenin
DMSO	dimethylsulphoxide
EDTA	ethylene-diamine-tetraacetic acid
EEVD	Glu-Glu-Val-Asp
EGTA	ethylene-glycol-tetraacetic acid
FBS	fetal bovine serum
HBSS	hank's balanced salt solution
HEPES	4-(2-hydroxyethyl)-1-piperazineethanesulfonic acid
HIF-1	hypoxia inducible factor 1
HIP	Hsp70 interacting protein
HOP	Hsp70/Hsp90 Organizing Protein
HR	hydrophobic repeats
HSC	heat shock cognate
HSE	heat shock element
HSF	heat shock factor
HSP	heat shock protein
hsp	heat shock protein gene
HSR	heat shock response
KNK437	N-formyl-3, 4-methylenedioxy-benzylidene-γ-butyrolactam
L-15	leibovitz-15 media
LB	luria-bertani
LSCM	laser scanning confocal microscopy
MBT	midblastula transition
MG132	carbobenzoxy-L-leucyl-L-leucyl-L-leucinal

MHC	major histocompatibility complex
NBT	4-nitro blue tetrazolium
NF-kβ	nuclear factor kappa beta
PBS	phosphate buffered saline
Rec.	recovery
SCA	spinocerebellar ataxias
SDS-PAGE	sodium dodecyl sulfate polyacrylamide gel electrophoresis
SSC	saline-sodium citrate
TBS-T	tris buffered saline solution – Tween20
TEMED	tetra-methyl-ethylene-diamine
Temp.	temperature
Tris buffer	tris(hydroxymethyl)aminomethane
TRITC	rhodamine-tetramethylrhodamine-5-isothiocyanate phalloidin
Ub	ubiquitin
UPS	ubiquitin-proteasome system

1 Introduction

1.1 Protein homeostasis and the heat shock response

The preservation of protein homeostasis is essential to cellular survival and is influenced by many molecular processes including protein synthesis, folding, translocation, disaggregation, and degradation (Morimoto and Santoro, 1998; Balch et al., 2008). Deficiencies in maintaining proteostasis are associated with a wide range of human disorders including amyotrophic lateral sclerosis (ALS), Huntington's, Parkinson's, Alzheimer's and prion diseases (Hartl, 1996; Kakizuka, 1998; Morimoto and Santoro, 1998; Westerheide and Morimoto, 2005; Balch et al., 2008).

Biochemical properties responsible for protein function and stability are disrupted as a result of exposure to chronic or acute stress conditions causing proteins to unfold into unstable conformations (Morimoto and Santoro, 1998; Morimoto, 1998; Balch et al., 2008). These non-native proteins possess exposed hydrophobic amino acid residues and regions of unstructured polypeptide backbone that can interact with neighbouring side chains to form large non-functional aggregates (Morimoto, 1998; Hartl, 1996; Hartl and Hayer-Hartl, 2009). Due to molecular crowding, large aggregates within the cytosol can become toxic and disrupt proper cellular functioning (Morimoto and Santoro, 1998; Morimoto, 1998; Balch et al., 2008).

Molecular chaperones are vital modulators of proteostasis that are abundantly expressed in multiple compartments of the cell. They prevent aggregation by maintaining misfolded proteins as soluble partially folded intermediates that are subsequently refolded by co-chaperones or targeted for degradation (Moriomoto, 1998; Westerheide and Morimoto, 2005; Morimoto, 2008).

In response to proteotoxic stress, cells utilize the heat shock response (HSR) to up-regulate molecular chaperones, proteases, and other cytoprotective agents to prevent and facilitate recovery from stress-induced cellular damage (Hartl, 1996; Morimoto and Santoro, 1998; Westerheide and Morimoto, 2005; Morimoto, 2008). The HSR is an evolutionarily conserved mechanism, first discovered by Ferrucio Ritossa in the salivary glands of *Drosophila* in 1962 (Jolly and Morimoto, 2000; Katschinski, 2004). Over the past 30 years, members of the heat shock protein (HSP) gene family have been characterised in most organisms ranging from archaebacteria to mammals (Parsell and Lindquist, 1993; Morimoto and Santoro, 1998; Jolly and Morimoto, 2000; Prahlad and Morimoto, 2009).

1.2 Heat shock proteins (HSPs)

HSPs are a family of molecular chaperones involved in the promotion of cellular viability in response to diverse environmental and physiological stressors such as elevated temperature, infection, oxidative stress, and exposure to heavy metals (Heikkila, 2004; Westerheide and Morimoto, 2005). As molecular chaperones, HSPs protect denatured proteins from aggregation while maintaining their solubility to assist in their refolding, once normal conditions have been re-established (Morimoto,1998; Heikkila, 2004). HSPs have been characterized into six major families based on size, including HSP100, HSP90, HSP70, HSP60, HSP40, and the small HSPs (Heikkila, 2004; Westerheide and Morimoto, 2005). They can be constitutively expressed, strictly stress inducible, or both inducible and constitutively regulated (Morimoto, 2008). The stress-induced transcription of *hsp* genes is mediated by interactions between heat shock transcription factors (HSFs) and the *cis*-acting heat shock element (HSE). The HSE

consists of multiple inverted repeats of the pentamer sequence 5`-nGAAn-3` and is found in the 5` upstream region of most stress-inducible *hsp* genes (Morimoto and Santoro, 1998; Heikkila, 2004; Westerheide and Morimoto, 2005).

1.3 Stress induced regulation of *hsp* gene expression

1.3.1 Heat shock transcription factors

Sacchromyces cerevisiae, *Caenorhabditis elegans*, and *Drosophila melanogaster* express a single type of HSF that mediates induction of the HSR, while plants and vertebrate animals express multiple HSFs with specialized and related functions (Morimoto and Santoro, 1998; Voellmy, 2004; Voellmy and Boellman, 2007). In addition to their role in stress resistance, *hsf* gene expression also contributes to cell maintenance and developmental processes under normal physiological conditions. For example, in *Drosophila,* HSF is essential for larval development and oogenesis independent of *hsp* gene expression (Jedlicka et al., 1997). Additionally, while yeast HSF is required for survival and regulates genes associated with metabolism and cell wall integrity (Yamamoto et al., 2005; Yamamoto et al., 2009), HSF1 is a maternal factor required for extra-embryonic development and female fertility in mice (Xiao et al., 1999; Christians et al., 2000; Kallio et al., 2002).

The expression of multiple HSFs in higher vertebrates likely serves as an additional mechanism to detect and respond to diverse forms of stress (Morimoto and Santoro, 1998). Thus far, four HSFs have been identified in vertebrates (HSF1-4). While HSF1, HSF2, and HSF4 are expressed in mammals, HSF3 appears to be an avian-specific transcription factor (Voellmy, 2004; Voellmy and Boellman, 2007; Yamamoto et al., 2009). HSF1 is functionally equivalent to yeast and *Drosophila* HSF and is considered

the primary eukaryotic transcription factor responsible for the stress-induced expression of *hsp* genes (Morimoto, 1998; Heikkila, 2004).

Detectable levels of HSF2 activity only occur in embryonic tissues and specifically contribute to the developmental regulation of *hsp* gene expression (Rallu et al., 1997; Voellmy, 2004). Recent data collected using chromatin immunoprecipitation (ChIP) showed that both HSF1 and HSF2 are recruited to the *hsp70* promoter in response to heat shock and hemin treatment (Ostling et al., 2007). In addition, evidence acquired using RT-PCR suggested that in the presence of HSF1, HSF2 contributes to the transcriptional regulation of multiple *hsp* genes including mouse *hsp25*, *hsp40*, *hsp70*, and *hsp110* in response to heat shock and proteasome inhibition (Ostling et al., 2007). In avian cells, HSF3 is required for stress-induced *hsp* gene expression and the combined functional roles of avian HSF1 and HSF3 seem to be equivalent to mammalian HSF1 activity (Nakai, 1999; Voellmy, 2004). Lastly, HSF4 is expressed in a tissue-specific manner and has two isoforms; HSF4a and HSF4b. HSFa appears to function as a repressor of *hsp* gene expression while, HSF4b is capable of activating transcription. Whether HSF4 is stress-inducible remains unclear (Tanabe, 1999; Pirkkala, 2001).

1.3.2 HSF1 structure and regulation

Exposure to proteotoxic stress results in the conversion of HSF1 from its inactive monomeric form to an active trimer with DNA binding capabilities. Following activation, HSF1 undergoes nuclear localization and associates with HSE to up regulate *hsp* gene expression (Morimoto and Santoro, 1998; Holmberg et al., 2002). HSF1 activity is regulated by various mechanisms including; intramolecular interactions between conserved hydrophobic domains, chaperone-mediated repression, and posttranslational

modifications (Morimoto and Santoro, 1998). Previous studies have found that certain chemicals can induce HSF1 trimerization and DNA binding activity without enhancing HSP accumulation. This suggests that the acquisition of HSE DNA-binding activity and transcriptional activation are two independently regulated steps required for HSF1 activation (Bruce et al., 1993; Zuo et al., 1995; Voellmy, 2004).

Through analyses of HSF1 structure and sequence conservation, several domains involved in the regulation of HSF1 activation have been identified including; the helix-turn-helix DNA binding domain, an adjacent hydrophobic repeat sequence (HR-A/B) essential for trimerization, and a carboxy-terminal transcriptional activation domain (Morimoto, 1998; Voellmy, 2004) (Fig.1). An additional hydrophobic repeat sequence (HR-C) absent in yeast HSF and mammalian HSF4 is located adjacent to the transcription activation domain (Morimoto, 1998; Voellmy, 2004) (Fig. 1). Under normal conditions interactions between HR-A/B and HR-C contribute to the suppression of HSF1 trimerization, while a conserved sequence located between HR-A/B and HR-C is thought to negatively regulate DNA-binding and transcriptional activation (Fig. 1) (Morimoto, 1998; Voellmy, 2004).

Figure 1. General structure of HSF1. Schematic representation of HSF1 structural motifs that correspond to the helix-turn-helix DNA binding domain, hydrophobic repeat sequences (HR-A/B and HR-C), the carboxy terminal transcription activation domain, and regulatory domains associated with the suppression of HSF1 activity (adapted from Voellmy, 2004).

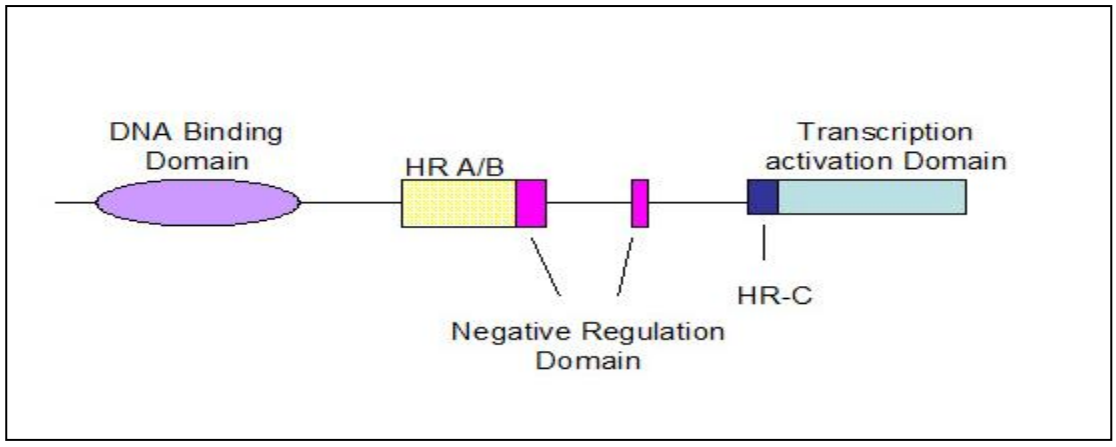
DNA Binding
Domain
HR A/B
Transcription
activation Domain
HR-C
Negative Regulation
Domain

Immunodepletion experiments have shown that under non-stressful conditions, HSF1 trimerization and DNA binding activity is repressed through interactions with various HSPs and co-chaperones including HSP70, HSP90, HSP40, HIP, HOP, and P23 (Bharadwaj et al., 1999; Voellmy, 2004). These chaperones form a multimeric complex with HSF monomers in which HSP90 functions as the primary inhibitor. During stress, this complex is disrupted as a result of increased levels of denatured protein enabling unbound HSF1 monomers to trimerize (Morimoto, 1998; Bharadwaj et al., 1999; Voellmy, 2004) (Fig. 2 & 3). HSF1 trimers subsequently relocalize to the nucleus and associate with HSE to facilitate *hsp* gene expression (Morimoto and Santoro, 1998; Heikkila, 2004; Voellmy, 2004; Westerheide and Morimoto, 2005).

Once activated HSF1 is further modified post-translationally by phosphorylation, sumoylation, and/or acetylation at conserved amino acid residues, providing an additional step of regulation (Holmberg et al., 2002; Morimoto, 2008). Conserved serine residues are both inducible and constitutively phosphorylated. The mechanism responsible for HSF1 phosphorylation is unknown but in general, constitutively phosphorylated serine residues appear to suppress HSF1 activation under normal conditions whereas, the inducible phosphorylation of serine residues is associated with the promotion of HSF1 activity in response to stress (Holmberg et al., 2002; Morimoto, 2008). Additionally, the ratio between activated and repressed phosphorylation sites likely varies in accordance to levels of HSF1 transcriptional activity (Holmberg et al., 2002; Voellmy, 2004). Sumoylation at conserved lysine residues also occurs in response to stress, this process occurs in a phosphorylation dependent manner and plays a role in regulating HSF1 DNA binding activity and transcriptional activation (Hong et al., 2001; Heitakangas et al.,

Figure 2. Chaperone mediated repression of HSF1 trimerization. The current model for the regulation of HSF1 activity suggests that the inactive form of HSF1 is associated with an HSP90 multicomplex that inhibits trimerization under normal conditions. The initial binding of HSP70 and HSP40 is thought to recruit HSP90 with the help of the cochaperones HOP and P23 (adapted from Voellmy, 2004).

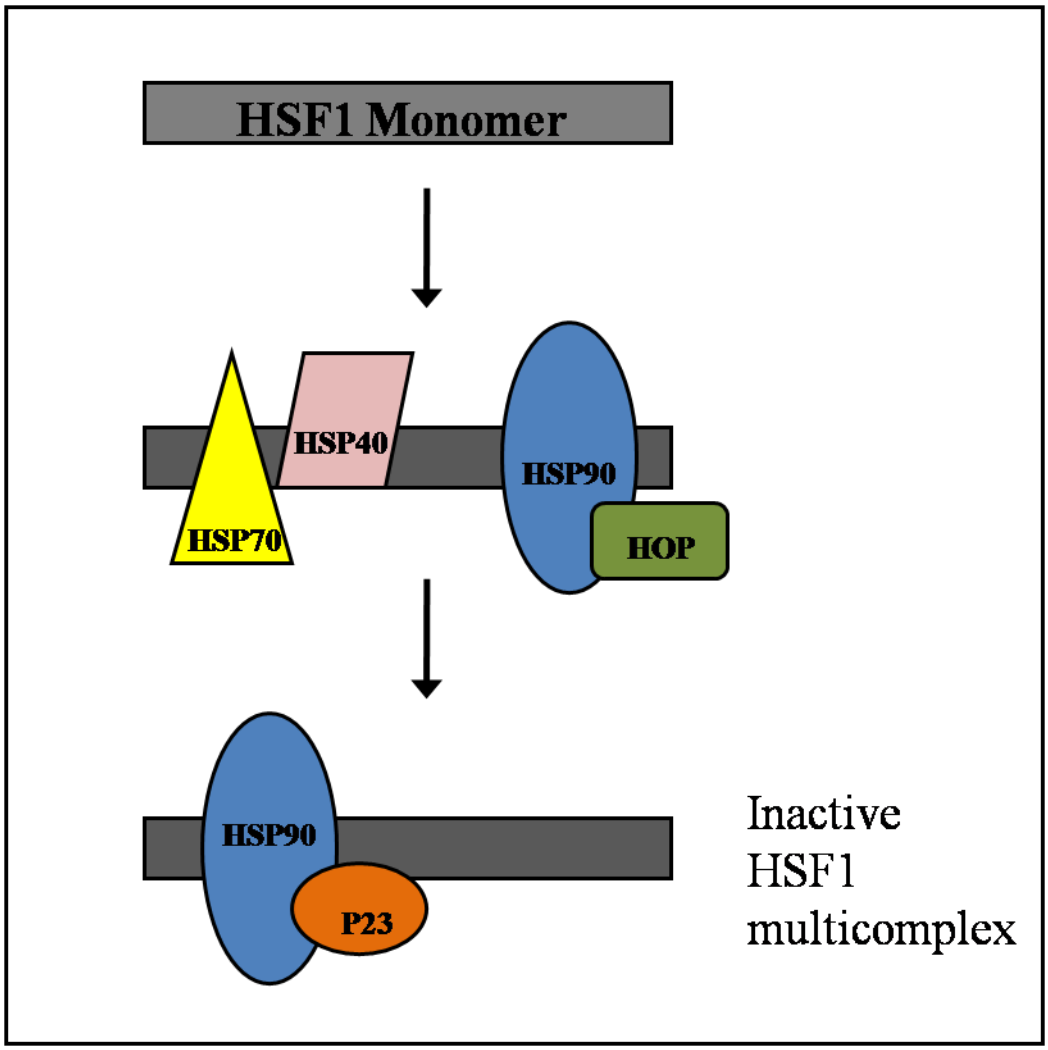
HSF1 Monomer
HSP40
HSP70
HSP90
HOP
HSP90
P23
Inactive
HSF1
multicomplex

Figure 3. Competitive binding of molecular chaperones to non-native proteins. An increase in the level of non-native proteins in response to stress, results in the disassembly of the HSF1-HSP90 multicomplex, causing HSF1 monomers to trimerize (adapted from Voellmy, 2004).

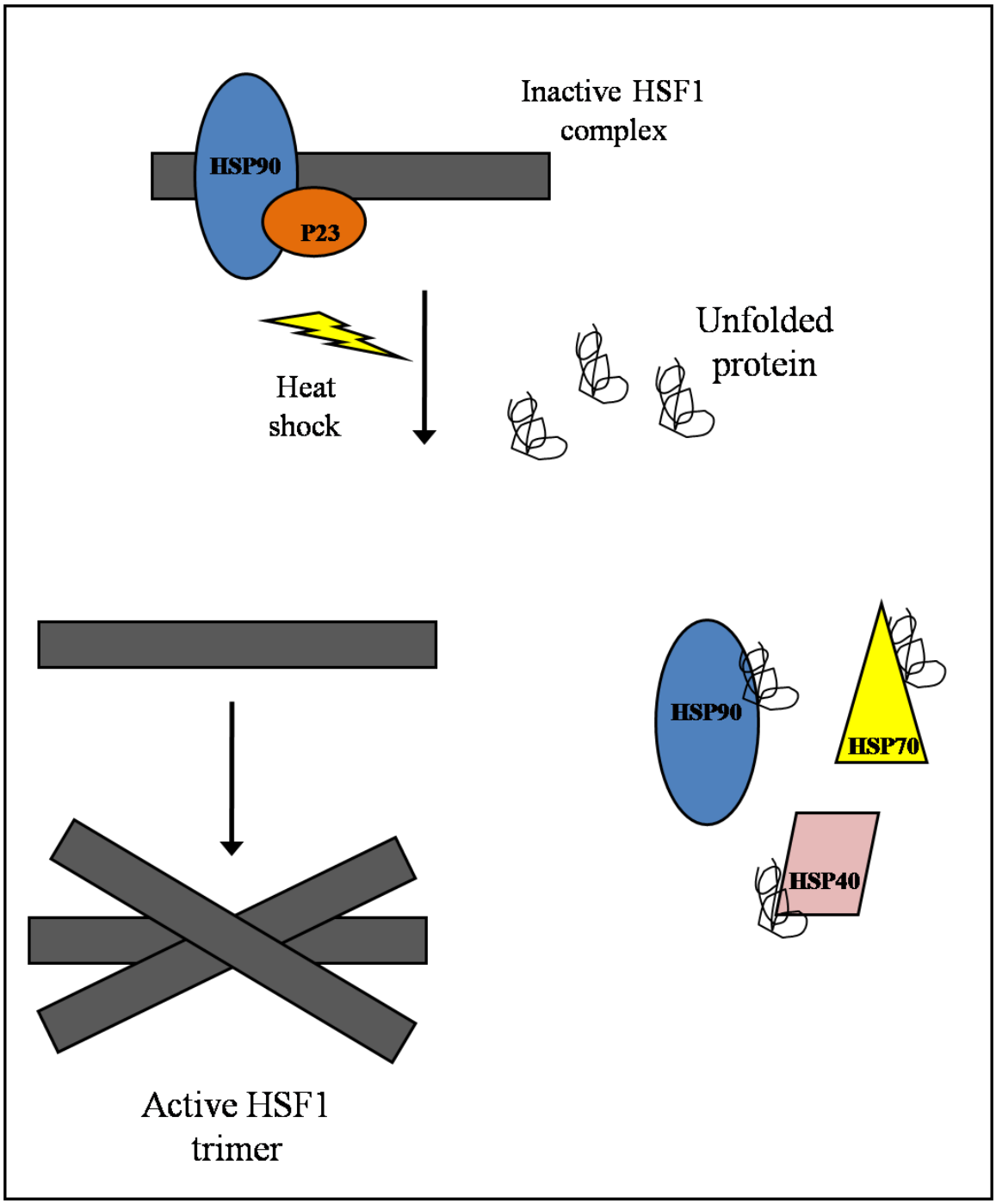
Inactive HSF1
complex
HSP90
P23
Heat
shock
Unfolded
protein
HSP90
HSP70
HSP40
Active HSF1
trimer

2003; Anckar et al., 2006). Lastly, recent studies suggest that the inducible acetylation of HSF1 negatively regulates DNA binding activity and plays a role in the attenuation of the HSR (Westerheide et al., 2009).

1.4 Small heat shock proteins

Members of the small HSP family, which includes the stress-inducible lens protein α-crystallin, range in size from 12 to 43 kDa (MacRae, 2000; Van Montfort et al., 2001; Heikkila, 2003). Small HSPs form high molecular weight complexes up to 1 Mda in size that are necessary for chaperone activity in response to heat shock and other stressors (Heikkila, 2003; Sun and MacRae, 2005). Sequence similarities between members of the small HSP family are generally restricted to an 80-100 amino acid sequence termed the α-crystallin domain that is flanked by two poorly conserved terminal extensions (Sun and MacRae, 2005). The N-terminal extension of the small HSP amino acid sequence influences oligomer formation and chaperone activity, while stabilization of quaternary structure and protein solubility occurs at the C-terminal extension (Sun and MacRae, 2005). The secondary structure of the α-crystallin domain primarily consists of β-strands organized into β-sheets required for dimer formation, the basic functional units of small HSPs (MacRae, 2000). Small HSPs bind partially denatured proteins in an energy-independent manner, keeping them in a folding competent state so that they may be refolded by other ATP-dependent chaperones such as HSP70. These actions protect proteins from irreversible aggregation during various stress conditions (MacRae, 2000; Sun and MacRae, 2005).

In vivo experiments have suggested various functions for small HSPs including actin polymerization, cellular differentiation, modulation of redox parameters, interactions with pro- and anti-apoptotic signalling factors, and the acquisition of thermotolerance (Arrigo, 1998; MacRae, 2000; Van Montfort et al., 2001; Paul et al., 2002; Rane et al., 2003). As a result, the role of small HSP activity in several medical conditions such as multiple sclerosis, cancer, neurodegenerative disorders, and muscle myopathy are currently being investigated (Birnbaum and Kotilinek, 1997; Clark and Muchowski, 2000; Jolly and Morimoto, 2000; Westerheide and Morimoto, 2005).

1.5 Heat shock protein 70

The *hsp70* gene family is highly conserved and is involved in regulating protein folding during normal and stress conditions (Katschinski, 2004). In general, eukaryotes possess multiple species of HSP70 capable of exhibiting both redundant and gene-specific functional properties (Daugaard et al., 2007). The HSP70 amino acid sequence consists of a highly conserved N-terminal ATPase domain that is involved in the binding and release of non-native proteins (Katchinksi, 2004; Daugaard et al., 2007). Additionally, an EEVD motif present in the C-terminal region, allows cytoplasmic HSP70 to interact with other HSPs and cochaperones such as HIP, HOP, and HSP40 (Katchinksi, 2004; Daugaard et al., 2007). Binding at this motif may be responsible for HSP70 function and target protein specificity (Katchinksi, 2004; Daugaard et al., 2007). Examples of essential housekeeping functions performed by HSP70 family members include the translocation of proteins across cell membranes, protein folding, and the degradation of denatured and misfolded proteins (Katschinksi, 2004; Daugaard et al., 2007).

1.6 *Xenopus laevis* as a model organism

As aquatic animals, amphibians have a high tolerance for dynamic environmental conditions and are a popular experimental system used to study eukaryotic stress response and embryonic development. They possess physiological traits common to most other vertebrates and data collected using amphibian systems are often applicable to mammals (Burggren and Warburton, 2007). The South African Clawed frog, *Xenopus laevis,* has been utilized as a model system in cell and developmental biology for many decades. They are completely aquatic and utilize both cutaneous and pulmonary forms of respiration (Heikkila, 2003; Burggren and Warburton, 2007). Studies using *X. laevis* have provided insight into the various mechanisms of HSR regulation and the characterization of eukaryotic HSPs (Heikkila, 2003; Heikkila et al., 2007).

1.6.1 *X. laevis* A6 kidney epithelial cell line

The *X. laevis* A6 kidney epithelial cell line is a popular system used for *in vitro* analysis of the HSR. This continuous cell line was initiated by Keen Rafferty (1968) and was derived from the renal uriniferous tubule of the adult male *Xenopus*. At confluence, A6 cells form an epithelial monolayer and adapt a dome-like morphology. This cell line is easy to maintain and has been used to study a variety of biological mechanisms including renal sodium transport, cell differentiation, and cellular gravitational responses (Tanaka et al., 2003;Verrey et al., 2003). Induction of the HSR following exposure to environmental stressors such as heat shock, sodium arsenite, cadmium, hydrogen peroxide and herbimycin A have been well characterised in *X. laevis* A6 kidney epithelial cells (Tam and Heikkila, 1995; Briant et al., 1997; Ohan et al., 1998; Phang et al., 1999; Muller et. al, 2004; Gellalchew and Heikkila, 2005; Woolfson and Heikkila, 2009).

Additionally, recent studies have shown that the HSF1 inhibitor, KNK437, can suppress the HSR and HSP-mediated acquisition of thermotolerance in A6 cells (Manwell and Heikkila, 2007; Voyer and Heikkila, 2008).

1.6.2 Developmentally-regulated *hsp* gene expression

X. laevis is a desirable model organism for embryo development because their eggs are easily obtainable in large quantities, they can be fertilized *in vitro*, and their oocytes and eggs are suitable for microinjection due to their large size (1-1.2 mm in diameter) (Heikkila, 2003). *X. laevis* embryos go through cleavage, midblastula, gastrula, neurula, tailbud, and tadpole stages of development (Heikkila et al., 1997; Heikkila, 2003). The midblastula transition (MBT) is an important point in development in which the embryonic genome becomes transcriptionally active. MBT is also associated with an increase in the duration of the cell cycle, loss of synchronous cell division, and a reduced rate of DNA synthesis (Heikkila et al., 1997; Hair et al., 1998). Although constitutive levels of *hsp27*, *hsp70*, and *hsp90* mRNA was detected at earlier stages of development, they were not heat inducible until after MBT (Heikkila et al., 1997; Heikkila, 2003). In contrast, *hsp30* was not stress inducible until the late neurula/early tailbud stages of development (Heikkila et al., 1997; Heikkila, 2003; Tuttle et. al., 2007).

1.6.3 *X. laevis* Heat shock protein 30

Members of the *hsp30* gene family are the most extensively investigated amphibian small HSPs and have been isolated in both *X. laevis* and the American bullfrog, R*ana catesbeiana* (Heikkila, 2003; Mulligan-Tuttle and Heikkila, 2007). Multiple HSP30 isoforms detected using 2-D SDS page and immunoblot analyses suggested a relatively large *hsp30* gene family (Tam and Heikkila, 1995). In *Xenopus*,

two *hsp30* gene clusters have been isolated containing *hsp30* genes A to E. The first cluster isolated by Bienz (1984) was comprised of *hsp30A* and *hsp30B* while, the second cluster identified in our laboratory contained *hsp30C*, *hsp30D* and a portion of *hsp30E* (Krone et al., 1992; Tam and Heikkila, 1995; Heikkila, 2003). While *Hsp30A* contains a 21 bp insertional mutation with a stop codon in its coding region, *hsp30B* is a pseudogene. Less is known about *hsp30E* since only a partial gene sequence was isolated (Krone et al., 1992; Heikkila, 2004).

Previous experiments done in our laboratory have characterized *hsp30C* and *hsp30D* gene expression. Both *hsp30C* and *hsp30D* are intronless genes that share a high degree of similarity and encode 24 kDa proteins containing the conserved α-crystallin domain found in other small HSPs (Krone et al., 1992). *Hsp30C* is first heat inducible at the late neurula/early tailbud stage of development while *hsp30D* is not heat inducible until midtailbud (Heikkila et al., 1997; Heikkila, 2003). Additionally, *in vitro* and *in vivo* analyses of chaperone function have found that HSP30C and HSP30D were capable of molecular chaperone activity by inhibiting heat-induced target protein aggregation and maintaining heat or chemically denatured luciferase in a folding competent state (Fernando and Heikkila, 2000; Fernando et al., 2002; Abdulle et al., 2002).

In A6 cells, HSP30 accumulation was induced by heat shock, sodium arsenite, herbimycin A, hydrogen peroxide, and cadmium treatment (Briant et al., 1997; Fernando et al., 2003; Muller et al., 2004; Woolfson and Heikkila, 2009). Differences in the heat shock induced proteins recognized by the HSP30C antibody in A6 cells compared to heat shocked embryos suggested that *Xenopus* embryos and cultured cells exhibited unique patterns of *hsp30* gene expression in response to stress (Tam and Heikkila, 1995). In

addition, studies in our laboratory using confocal laser scanning microscopy have found that in response to 33˚C and 35˚C heat shock, A6 cells exhibit a punctate pattern of HSP30 accumulation that was primarily localized in the cytoplasm (Gellalchew and Heikkila, 2004; Manwell and Heikkila, 2007). Similar findings with respect to HSP30 localization were observed in cadmium or sodium arsenite-treated A6 cells (Voyer and Heikkila, 2008; Woolfson and Heikkila, 2009).

1.6.4 *X. laevis* Heat shock protein 70

In *Xenopus*, several members of the HSP70 family have been analyzed including the stress-inducible HSP70, constitutively expressed heat shock cognate 70 (HSC70) and immunoglobulin-binding protein (BiP) (Ali et al., 1997; Briant et al., 1997; Miskovic and Heikkila, 1999; Ali and Heikkila, 2002). HSC70 and HSP70 reside in the cytosol and contain functional nuclear localization signals while, BiP is confined to the lumen of the endoplasmic reticulum (Goldfarb et al., 2006; Heikkila et al., 2007). Recent investigations on the differential effects of HSC70 and HSP70 on the formation of epithelial sodium channels, suggested that although they are very similar, these proteins do not possess identical functional properties (Goldfarb et al., 2006). To date, four members of the stress-inducible *Xenopus hsp70* genes (*hsp70A, hsp70B, hsp70C, and hsp70D*) have been isolated and sequence analysis revealed that their coding regions were highly conserved (Bienz, 1984). In developmental studies, *hsp70* mRNA was determined to be heat inducible after MBT (Heikkila et al., 1997; Lang et. al, 2000). Additionally, whole mount *in situ* hybridization analysis previously carried out in our laboratory demonstrated that heat shock-induced *hsp70* mRNA accumulation preferentially occurred in the lens placode, cement gland, heart, somites, spinal cord, and proctodeum (Lang et

al., 2000). Previous experiments suggested that the heat-induced preferential expression of HSP70 and HSP30 in selected tissues was due to a lowered set point temperature for HSF1 activation compared to other tissue types (Lang et al., 1999; Lang et al., 2000). This type of thermosensitivity was also reported in adult *Xenopus* heart tissue (Ali et al., 1997). The treatment of *X. laevis* A6 cells with various stressors including herbimycin A, hydrogen peroxide, ethanol and cadmium also induced *hsp70* mRNA and protein accumulation (Darasch et al.,1988; Briant et al., 1997; Muller et al., 2004; Gauley and Heikkila, 2006; Woolfson and Heikkila, 2009).

1.7 HSPs and their association with cancer and neurodegenerative disease

The overexpression of cytoprotective HSPs like HSP27 and HSP70 have been implicated in a variety of human cancers including lung, breast and prostate cancer (Malusecka et al., 2001; Melendez et al., 2006; So et al., 2007). For example, the inhibition of HSP70 and HSP90 by antisense RNAs inhibited growth and induced apoptosis in transformed cells (Whitesell, 1994; Nylandsted, 2000; Westerheide and Morimoto, 2005). Additionally, it has been proposed that higher levels of *hsp* gene expression likely contribute to the acquisition of chemoresistance in certain types of cancer (So et al., 2007). This may occur because tumor cells rely on elevated levels of HSPs in order to counteract cell cycle regulators normally involved in programmed cell death and to resist various forms of cancer treatment (Westerheide and Morimoto 2005). Thus, the utilization of inhibitors of the HSR in combination with chemotherapy may prove to be beneficial in the treatment of various types of cancer.

A large number of neurodegenerative disorders are associated with the expression of misfolded proteins that form cytotoxic aggregates (Westerheide et al., 2004; Zhang

and Sarge, 2007). Examples of these disorders include Alzheimer's, Parkinson's, amyotrophic lateral sclerosis (ALS), and polyglutamine diseases such as Huntington's disease and spinocerebellar ataxias (SCAs) (Fujikake et al., 2008). Therapeutic approaches against neuronal degeneration must therefore involve the suppression of unfolded proteins in order to inhibit the downstream effects of protein aggregation that cause neuronal dysfunction (Fujikake et al., 2008). In fact, previous studies have suggested that the chaperone activity provided by overexpression of HSPs can inhibit aggregate formation and cellular toxicity in cells expressing polyglutamine proteins (Zhang and Sarge, 2007). For the above reasons, there is a great amount of interest in the characterisation of various inducers of the HSR for therapeutic purposes.

1.8 Protein degradation

Eukaryotes possess two major systems for protein degradation that are significant mediators of cellular homeostasis. The first to be discovered was the lysosomal degradation pathway. It plays a minor role in the non-specific degradation of cellular proteins and is primarily responsible for the hydrolysis of extracellular or membrane associated proteins taken up by endocytosis (Lee and Goldberg, 1998a). Protein breakdown within the lysosome is facilitated by multiple acidic proteases referred to as cathepsins. Although lysosomal degradation is an important cellular process, the ATP dependent ubiquitin-proteasome system (UPS), is responsible for the majority (80-90 %) of protein hydrolysis occurring in the cell (Lee and Goldberg, 1998a).

1.8.1 The ubiquitin-proteasome system

The UPS is a degradation pathway that plays an essential role in multiple biological processes including; development, differentiation, cell cycle progression,

proliferation, and apoptosis (Yang et al., 2008; Lehman, 2009). In addition to the general proteolysis of mutant, unfolded or damaged proteins, the UPS can also function as a molecular switch that rapidly blocks the activity of target proteins involved in various signalling pathways including nuclear factor kappa beta (NF-kβ), Notch and hypoxia inducible factor 1 (HIF-1) (Leung et al., 2005; Lathia et al., 2008; Rekwirowicz and Marzalek, 2009). As its name suggests, the UPS consists of the ubiquitin (Ub) conjugating system that regulates protein degradation by the multicatalytic proteasome (Yang et al., 2008; Lehman, 2009).

1.8.2 Protein ubiquitination

Ubiquitin is an evolutionarily conserved 76 amino acid protein that serves as a marker for proteasome degradation when it is covalently attached to lysine residues of target proteins. The ubiquitination of proteins destined for degradation is a multistep process controlled by various ubiquitin-activating enzymes (E1-E4) (Yang et al., 2008; Lehman, 2009). Initially, ubiquitin is activated in an ATP-dependent manner by the ubiquitin-activating enzyme (E1) through adenylation and formation of a thiol-ester bond at its C-terminal. Following activation, ubiquitin is transferred to a cysteine residue within one of several distinct ubiquitin-conjugating enzymes (E2). Subsequently, the ubiquitin bound E2 associates with an ubiquitin ligase (E3) capable of transferring activated ubiquitin to the lysine residue of a specific target protein. In some cases, additional ubiquitin monomers are added to the ubiquitinated target to form polyubiquitin chains that contain 4 to 7 monomers (Hershko and Ciechanover, 1998), E4 enzymes facilitate the formation of these polyubiquitin chains (Koegl et al., 1999). Following ubiquitination, ubiquitin receptor proteins act as carriers to deliver polyubiquitinated

proteins to the proteasome. Ubiquitin monomers are then released from the target protein prior to degradation and are subsequently recycled for future use (Hershko and Ciechanover, 1998).

1.8.3 The Proteasome

The proteasome (also known as the 26S proteasome) is a multicatalytic enzyme complex that contains a 20S catalytic core that serves as its central processing subunit (Groll et al., 1997; Baumeister et al., 1998). The 20S proteasome is capable of hydrolyzing most unfolded protein substrates and is composed of two catalytic β rings (with 7 subunits) surrounded by two non-catalytic α rings (with 7 subunits) that are stacked to form a barrel-like structure with a narrow central catalytic cavity (Groll et al., 1997). The catalytic activity of the β ring occurs within the β1, β2, and β5 subunits that posses caspase-like, trypsin-like, and chymotrypsin-like proteolytic activities, respectively (Groll et al., 1997; Lehman, 2009).

Proteasomal activity is modified by the regulatory 19S and 11S subcomplexes that bind to either end of the 20S proteasome. The 700 kDa 19S regulator contains at least 17 different subunits and guides access to the 20S proteasome through recognition, binding, unfolding, and de-ubiquitination of tagged proteins (Hershko and Ciechanover, 1998; Nandi et al., 2006). Due to the narrow cylindrical shape of the inner 20S cavity proteins must be unfolded before degradation. The 19S proteasome contains 6 ATPase subunits that provide the energy required to unfold these protein substrates and feed them through the 20S core. Remaining 19S subunits contribute to 19S assembly and de-ubiquitination (Hershko and Ciechanover, 1998; Nandi et al., 2006). Lastly, the 11S activator stimulates the peptidase activity of the 20S core and regulates the proteasome-mediated production

of antigenic peptides that are presented to the immune system on MHC class I molecules (Whitby et al., 2000). The 11S subcomplex associates with one or both ends of 20S proteasome and can bind in the absence or presence of the 19S subcomplex. Since the 11S proteasome is unable to recognize or degrade ubiquitinated proteins, researchers have suggested that it functions as an adapter between the 20S proteasome and cytosolic chaperones (Hershko and Ciechanover, 1998; Nandi et al., 2006; Yang et al., 2008; Lehman, 2009).

1.8.4 Proteasome inhibitors

Many low-molecular weight proteasome inhibitors have been identified, and peptide aldehydes such as carbobenzoxy-L-leucyl-L-leucyl-L-leucinal (MG132), are among the most popular. They are substrate analogues that primarily inhibit proteasomal chymotrypsin-like activity (Rock et al., 1994; Lee and Goldberg, 1998b). Lactacystin and its derivative *clasto* lactacystin β-lactone, have also been identified as natural inhibitors of the proteasome. Lactacystin binds covalently to the hydroxyl groups of β subunits in the 20S proteasome, subsequently inactivating chymotrypsin- and trypsin-like proteasomal activities (Fenteany et al., 1995; Lee and Goldberg, 1998a). While the effects of MG132 are reversible, lactacystin is an irreversible modifier of proteasome activity (Lee and Goldberg, 1998b).

1.9 Celastrol

Extracts from the *Celastraceae* family have been used in traditional Chinese medicine as anti-inflammatory agents to treat rheumatoid arthritis, bacterial infection, and fever, for hundreds of years (Westerheide et al., 2004). Celastrol is a quinone methide triterpene derived from root bark extracts of *Tripterygium wilfordii* Hook F., an ivy-like

vine belonging to the *Celastraceae* family of plants. Celastrol was identified in 2002 as a biological agent that suppressed toxic cellular properties associated with ALS and Huntington's disease (Westerheide et al., 2004; Kim et al., 2009). For example, experiments employing SDS solubility analysis and fluorescence microscopy demonstrated that celastrol was capable of suppressing protein aggregation and toxicity in HeLa cells expressing polyglutamine aggregates (Zhang and Sarge, 2007). Additionally, treatment with celastrol was found to be neuroprotective and improved general brain function in rodent models for Huntington's, Parkinson's, and ALS (Kiaei et al., 2005; Cleren et al., 2005). Additionally, in mammalian cells celastrol induced the HSR and activated HSF1 with kinetics similar to those observed with heat shock, such as rapid activation and comparable magnitudes of induction (Westerheide et al., 2004; Trott et al., 2008). The chemical mechanism by which celastrol elicited the HSR remains unclear. However, data collected by Yang et al. (2006) suggested that celastrol might have an inhibitory effect on proteasome activity. Thus, it is possible that the accumulation of ubiquitinated proteins within the cell in response to proteasome inhibition may contribute to celastrol-mediated induction of the HSR. Recently, the induction of *hsp* gene expression in response to proteasome inhibition has been described in amphibian cells (Young and Heikkila, 2009). The potential advantages of using celastrol as a small molecule regulator of the HSR include; the rapid activation of HSF1 similar to heat shock, low dosage requirements, and potential cytoprotective properties against a variety of stressors (Westerheide et al., 2004). Additionally, since medicinal extracts containing celastrol have been used as a natural remedy for many years without reported instances of

severe adverse effects, *in vivo* implications for celastrol are promising (Westerheide et al., 2004).

Proteasome inhibition has a great potential for use in cancer treatment and prevention (An et al., 1998; Orlowski et al., 1999; Drexler et al., 2000; Li et al., 2000; Soligo et al., 2001). Previous studies determined that celastrol is an inhibitor of chymotrypsin-like activity of the 20S proteasome (Yang et al., 2006). It was also suggested that the conjugated ketone carbons C2 and C6 of celastrol may facilitate celastrol-induced proteasomal inhibition by associating with β5 subunits of the 20S proteasome (Fig. 4) (Yang et al., 2006). Several studies have demonstrated that celastrol inhibits proliferation and induces apoptosis in a wide range of cancer cell lines including; A549 lung, MCF-7 breast, and PC-3 prostate cancer cell lines (Chang et al., 2003; Yang et al., 2008). Additionally, treatment of PC-3 tumor bearing mice with celastrol for 1 to 31 days suppressed tumor growth (Yang et al., 2006), while the treatment of human lung adenocarcinoma H1299 cells with celastrol in combination with other chemotherapeutic agents inhibited tumor invasion (Sethi et al., 2007). Accumulating evidence suggests that the celastrol-mediated induction of apoptosis occurs through inhibition of the NF-kβ signalling pathway (Jin et al.,2002; Lee et al., 2006; Sethi et al., 2007), which regulates anti-apoptotic responses (Ghosh et al., 1998; Baldwin, 2001).

Figure 4. Chemical structure of celastrol. The molecular formula for celastrol is $C_{29}H_{38}O_4$ (Cayman Chemical, 2010).

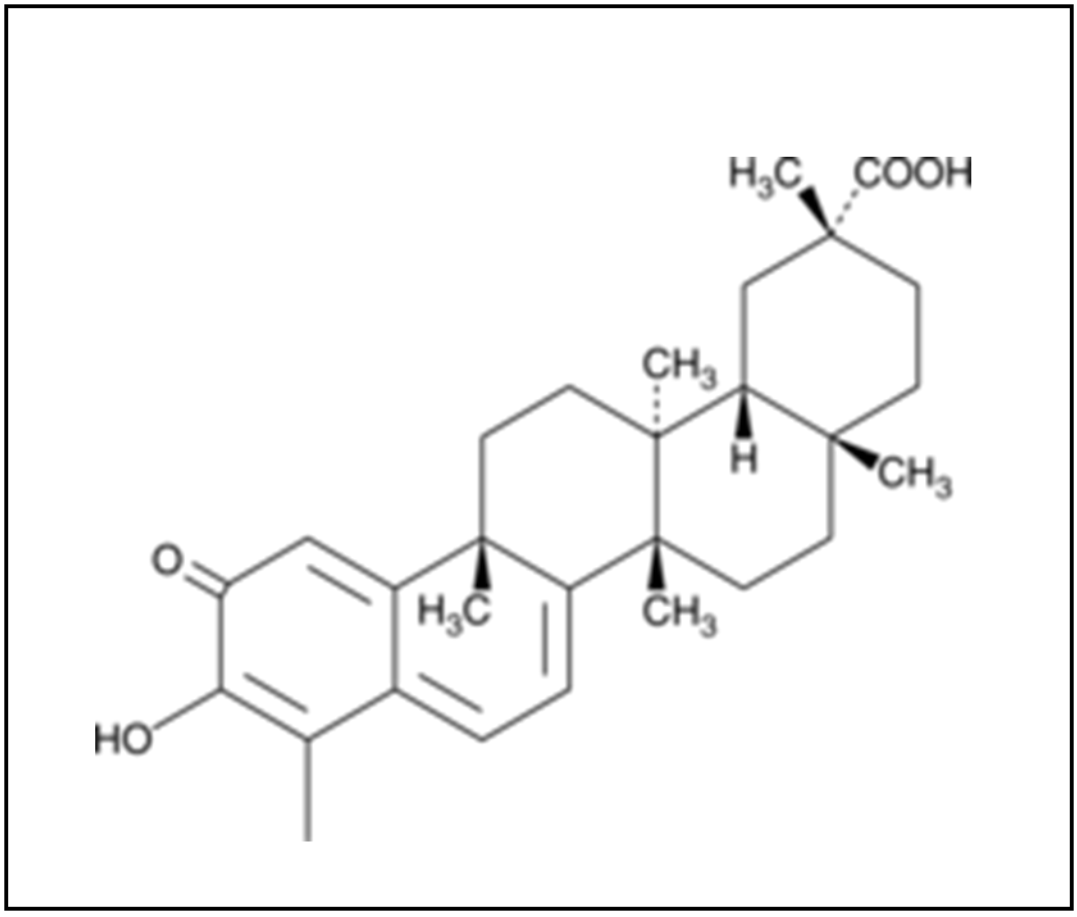
H3C
COOH
CH3
H
CH3
O
H3C
CH3
HO

1.10 Objectives

Thus far, the effects of celastrol have been partially characterized in yeast and mammalian systems. However, there is no available information on the impact of celastrol in amphibian cells. The primary goal of this thesis was to determine the effect of celastrol on proteasome activity and *hsp* gene expression in *Xenopus laevis* A6 kidney epithelial cells. The objectives for this study are as follows:

- To analyze the accumulation of cellular protein conjugated to ubiquitin in *Xenopus* A6 cells treated with celastrol or MG132
- To examine proteasomal chymotrypsin-like activity in celastrol- or MG132-treated *Xenopus* A6 cells
- To determine the effect of celastrol on the expression of *hsp30* and *hsp70* genes in *Xenopus* A6 cells
- To determine whether HSF1 activation was involved in celastrol-induced accumulation of HSP30 and HSP70 *Xenopus* A6 cells
- To examine the pattern of HSP30 and HSP70 accumulation in *Xenopus* A6 cells simultaneously exposed to both celastrol and a mild heat shock simultaneously
- To determine the effect of incubating *Xenopus* A6 cells concurrently with celastrol and MG132 on HSP30 and HSP70 accumulation
- To analyze the celastrol-induced localization of HSP30 accumulation in *Xenopus* A6 cells
- Lastly, to examine the effects of celastrol on *Xenopus* A6 cell morphology and cytoskeleton organization

2 Materials and Methods

2.1 Treatment and maintenance of *Xenopus laevis* A6 cells

Xenopus laevis A6 kidney epithelial cells were acquired from the American Type Culture Collection (ATCC, Rockville, Maryland). Cells were cultured in 55 % Leibovitz L-15 media (Sigma; Oakville, ON) supplemented with 10 % fetal bovine serum (FBS; Sigma) and 1 % penicillin (100 U/mL) and streptomycin (100 µg/mL)(Sigma) and were grown at 22 ºC in T-75 cm^2 flasks. Upon confluency, cells were washed with 1 mL of versene [0.02 % (w/v) KCl, 0.8 % (w/v) NaCl, 0.02 % (w/v) KH_2PO_4, 0.115 % (w/v) Na_2HPO_4, 0.02 % (w/v) sodium ethylenediaminetetraacetic acid (Na_2 EDTA)], followed by a 1 min incubation with 2 mL of fresh versene. Then 1 mL of 1X trypsin (Sigma) diluted in 100 % Hank's balanced salt solution (HBSS; Sigma) was added until cells began to detach from the flask. Ten mL of fresh L-15 media was then added to the detached cells. The cell suspension was then divided evenly into additional flasks. Cell treatments were performed 2 days after cell splitting to allow the cells to reach 90-100 % confluence.

Celastrol ($\geq$ 98 % purity) (Cayman chemical, Ann Arbor, MI) was dissolved in dimethylsulphoxide (DMSO; Sigma) to make a stock solution of 10 mg/mL. The stock was then diluted further to make a 1 mg/mL working solution. This working stock was used to prepare 1, 2.5, 5, or 7.5 µM concentrations of celastrol used for subsequent experiments. MG132 (Sigma) and KNK437 (N-formyl-3, 4-methylenedioxy-benzylidene-γ-butyrolactam; Calbiochem, Gibbstown, New Jersey) were also dissolved in DMSO to prepare 5 mg/mL stock solutions. Experiments with MG132 used 5, 10, or 30 µM concentrations while all treatments with KNK437 used 100 µM concentrations.

For A6 cell treatments, appropriate volumes of each chemical were added to fresh L-15 media followed by gentle shaking to ensure even distribution prior to adding each treatment to tissue culture flasks containing A6 cells. Treatments with 100 µM KNK437 were performed 6 h prior to treatment with 2.5 µM celastrol. Heat shock treatments at 33 ˚C were for 2 h, followed by a 2 h recovery period at 22 ˚C for protein isolation and without a recovery period for the isolation of RNA. Combined treatments with celastrol and mild 30 ˚C heat shock did not include a recovery period. Immediately following treatment, A6 cells were harvested by washing in 2 mL of 65 % HBSS, and were then removed with a cell scraper and suspended in 1 mL of 100 % HBSS. The cells were centrifuged at 14,000 rpm for 1 min and stored at -80 ˚C until protein or RNA isolation.

2.2 Detection of chymotrypsin-like activity in A6 cells

Chymotrypsin-like activity was detected from cultured A6 cells using the Promega Proteasome-Glo cell based luminescent assay kit (Promega Corp., Madison, WI) according to the manufacturer's recommendations as outlined below. The Proteasome-Glo Cell-Based Reagents each contain a specific luminogenic proteasome substrate (Suc-LLVY-Glo substrate for chymotrypsin-like activity) in a buffer optimized for cell permeabilization, proteasome activity and luciferase activity. The proteasome cleavage generates an aminoluciferin substrate that is consumed by luciferase to produce a luminescent signal at a rate proportional to proteasome activity (Promega Corp., 2009). After thawing the Proteasome-Glo cell based buffer, both the buffer and lyophilized Luciferin detection reagent were equilibrated to room temperature in the dark before use. It should be noted that the Suc-LLVY-Glo substrate was also thawed and equilibrated to room temperature in the dark. Once at room temperature the lyophilized Luciferin

detection buffer was reconstituted in Proteasome-Glo cell based buffer in an amber bottle provided by the manufacturer. Then 50 µL of the Suc-LLVY-Glo substrate was vortexed to remove any precipitate that may have formed. The substrate was then added to the amber bottle containing lyophilized Luciferin detection reagent reconstituted in Proteasome-Glo cell based buffer. To remove any free aminoluciferin and reduce background luminescence, the contents of the bottle (prepared proteasome-glo cell based reagent) were then mixed gently and stored at room temperature in the dark for 30 min before use.

A6 cells were cultured in L-15 media supplemented with 10 % FBS and 1 % penicillin and streptomycin (as described in section 2.1). Following chemical treatment, cells were washed with 2 mL of versene and then with 1 mL of 1X trypsin until the cells began to detach from the flask. Nine mL of fresh L-15 media was then added to the flask. The media was pipetted up and down to rinse the flask surface and allow for even distribution. The cell suspension was then removed from the flask and placed into a 15 mL Falcon tube. Cells were pelleted at 4 ˚C by gentle centrifugation at 4,000 rpm for 5 min. Following centrifugation excess media was removed and pellets were washed in 5 mL of fresh L-15 media and then centrifuged again at 4,000 rpm for 5 min at 4 ˚C. A6 cells were then resuspended in 5 mL of fresh L-15 media. For each sample, the total number of cells per mL was determined using a Bright-Line haemocytometer (Hausser Scientific, Horsham, PA). Approximately 15,000 were suspended in 100 µL of L-15 media for the chymotrypsin-like assay.

For the chymotrypsin-like activity assay, 100 µL of each sample were added to the wells of a white-walled 96-well plate. Then 100 µL of Proteasome-Glo cell-based

reagent (prepared previously) was added to each sample. The plate was then covered with foil and samples were mixed gently on a rocking platform for 2 min. The samples were then incubated at room temperature for 45 min in the dark, prior to measuring chymotrypsin-like activity. The luminescence of each sample was measured using the Victor^3 luminometer (PerkinElmer Inc., Waltham, MA). Values were then compared to a blank control (Proteasome-Glo cell-based reagent + L-15 media) and a no-treatment control (Proteasome-Glo cell-based reagent + L-15 containing DMSO).

2.3 Antisense riboprobe production and northern blot hybridization analysis

2.3.1 *Hsp30C* template construction

The open reading frame of the *hsp30C* gene was previously inserted into the pRSET expression vector (Invitrogen, Carlsbad, CA) by Pasan Fernando (Fernando and Heikkila, 2000). Plasmids containing the *hsp30C* insert were transformed into *Escherichia coli* DH5α cells. Individual colonies were inoculated in 5 mL of LB broth [1 % (w/v) tryptone-peptone, 0.5 % (w/v) yeast extract, 1 % (w/v) NaCl, pH 7.5] containing 100 μg/mL ampicillin (Bioshop, Burlington, ON) and grown overnight in at 37 ˚C for 14-16 h.

2.3.2 *Hsp70* template construction

The coding region of *hsp70* genomic DNA was previously isolated (Lang et al., 2000) and inserted into the plasmid pSP72 (Promega, Napean, ON). Plasmids containing the *hsp70* insert were also inoculated in 5 mL of LB broth containing 100 μg/mL ampicillin and grown overnight in 5 mL of LB broth containing 100 μg/mL ampicillin at 37 ˚C for 14-16 h.

2.3.3 Isolation of plasmid DNA

After overnight incubation, bacterial cells were centrifuged (Eppendorf Centrifuge 5810R, Brinkmann Instruments Ltd., Mississauga, ON) at 5,000 rpm for 5 min at 4 ˚C. Plasmid DNA was then isolated by resuspending the pelleted cells in 200 µL of ice-cold alkaline lyisis solution #1[50 mM glucose, 25 mM Tris (pH 8.0) and 1 mM EDTA (pH 8.0)] and then transferring the mixture into a microcentrifuge tube. The cells were then lysed by mixing them gently with 200 µL of alkaline lysis solution #2 [0.2 M NaOH and 1 % (w/v) SDS (sodium dodecyl sulfate)]. The microcentrifuge tubes were kept on ice for the remainder of the experiment. After adding 200 µL of ice-cold alkaline solution #3 [3 M potassium acetate and 5 M glacial acetic acid] the tubes were mixed gently and placed on ice for 5 min. Next, the samples were centrifuged at 14,000 rpm for 5 min at 4 ˚C, the supernatant was then transferred to fresh microcentrifuge tubes. This was followed by a 2 h RNase A treatment (10 µg/mL; BioShop, Burlington, ON) at 37 ˚C to eliminate RNA from the samples.

After a 2 h incubation, 600 µL of phenol:chloroform (1:1) was added and the samples were vortexed. The samples were then centrifuged at 14,000 rpm for 3 min at 4 ˚C and the upper aqueous layer was transferred to new microcentrifuge tubes. The phenol/chloroform step was repeated. Next, a 600 µL solution of isoamyl alcohol:chloroform (1:24) was prepared and added to the microcentrifuge tubes which were then vortexed and centrifuged at 14,000 rpm for 3 min at 4 ˚C. Again the upper aqueous layer was transferred to fresh microcentrifuge tubes. To precipitate the nucleic acids, 600 µL of isopropanol was added to each microcentrifuge tube. The samples were then vortexed and incubated at room temperature for 2 min. Followed by centrifugation at

14,000 rpm for 5 min at room temperature. The supernatant was removed and 500 µL of 70 % ethanol was added to wash the pellets. The samples were then centrifuged at 14,000 rpm for 2 min at 4 ˚C. Then the ethanol was removed and the previous step was repeated. The pellets were allowed to air dry and were then resuspended in 50 µL distilled water and stored at -20 ˚C.

2.3.4 *In vitro* transcription

The plasmid containing the *hsp30C* or *hsp70* insert as mentioned above was linearized using the *Pvu*II or *Mlu*NI restriction enzymes, respectively (Roche, Laval, Quebec). The linearized plasmid was then electrophoresed on a 1 % (w/v) agarose gel in 1X modified tris-acetate EDTA buffer (TAE)(Millipore corp., Bedford, MA). The DNA band corresponding to the *hsp30C* or *hsp70* insert was visualized using a UV lamp. The DNA band was then cut out using a razor blade. Plasmid DNA was extracted from the gel using the Montage DNA gel Extraction Kit (Millipore). The gel slice containing the plasmid DNA was placed into a gel nebulizer containing a microporous membrane filter (Millipore). The nebulizer tube was then centrifuged at 5,000 rcf for 10 min at 4 ˚C. The filter was then removed and the DNA was precipitated by adding 100 % ice-cold ethanol (2X volume) and 3 M sodium acetate (pH 5.2, 1/10 volume). The tube was then placed at -80 ˚C for 30 min and then centrifuged at 14,000 rpm for 10 min at 4 ˚C. The supernatant was discarded and the pellet was washed in 1 mL of 70 % ice-cold ethanol and centrifuged at 14,000 rpm for 10 min at 4 ˚C. The ethanol was removed and the previous step was repeated. The pellet was then air dried and resuspended in 20 µL of sterile water and kept at -20 ˚C.

In vitro transcription was used to generate digoxygenin (DIG)-labelled riboprobes. Each *in vitro* transcription reaction contained 4 µL of linearized DNA template, 4 µL of rNTP mix [2.5 mM rGTP, 2.5 mM rATP, 2.5 mM rCTP, 1.625 mM rUTP (Promega, Nepean, ON), 0.875 mM DIG-11-UTP (Roche), 1.5 µL diethylpyrocarbonate (DEPC, Sigma)-treated water, 4 µL of 100 mM (Promega), 4 µL of 5X transcription buffer (Fermentas, Burlington, ON), 0.5 µl RNase inhibitor (Fermentas) and 40 IU of SP6 RNA polymerase (Roche)]. The *in vitro* transcription reaction was performed for 1 h at 37 ˚C. To remove any remaining DNA template, 2 µL of RNase-free DNase 1 (Roche) was added for 10 min at 37 ˚C. *In vitro* transcripts were then precipitated with the addition of 10 µL of 3 M sodium acetate (pH 5.2), 80 µL of TES [10 mM Tris-HCl (pH 7.4), 5 mM EDTA (pH 8.0), 1 % (w/v) SDS] and 220 µL of ice-cold 100 % filtered ethanol. The reaction was incubated at -80 ˚C for 30 min and then centrifuged at 14,000 rpm for 15 min at 4 ˚C. The supernatant was removed and the pellet was air dried and resuspended in 21 µL of DEPC-treated water. Two µL of the sample was electrophoresed to verify the presence of the *in vitro* transcript. The remaining 19 µL was stored at -80 ˚C until northern blot hybridization analysis.

2.3.5 RNA isolation

RNA was isolated from pelleted A6 cells using the Qiagen RNeasy Mini Kit (Qiagen; Mississauga, ON) according to the manufacturer's protocol outlined in the RNeasy Mini Handbook (2009). Isolated RNA was suspended in 30-40 µL of DEPC-treated water and quantified using the NanoDrop ND-1000 (NanoDrop, Waltham, MA) spectrophotometer. Prior to northern blot analysis, RNA integrity was analysed by electrophoresing 2 µg of each RNA sample on a 1.2 % formaldehyde agarose gel [1.2 %

(w/v) agarose, 10 % (v/v) 10X MOPS, 16 % (v/v) formaldehyde]. Before the samples were electrophoresed, they were dissolved in 10 µL of loading buffer [1 µL 10X MOPS, 1.6 µL formaldehyde, 2 µL RNA loading dye (0.2 % bromophenol blue, 1 mM EDTA (pH 8.0), 50 % (v/v) glycerol), 5 µL formamide, 0.5 µg/mL ethidium bromide] and then heat denatured in a 68 ˚C water bath and immediately cooled on ice for 5 min. The samples were then electrophoresed at 90-100 V for approximately 1 h.

2.4 Northern blot hybridization analysis

Ten µg of RNA was electrophoresed for 3 h at 65 V on a 1.2 % formaldehyde agarose gel as described above with the exception that ethidium bromide was not added to the loading buffer. Following electrophoresis the gel was soaked in 0.05 NaOH for 20 min to denature RNA. Next, the gel was rinsed in DEPC-treated water and soaked twice for 20 min each in fresh 20X SSC buffer [3 M sodium chloride, 300 mM sodium citrate]. The RNA was then transferred overnight to a positively charged nylon membrane (Roche) by capillary action. A piece of 3MM Whatman filter paper, which served as a wick, was pre-soaked in 20X SSC and placed on a plexiglass support over a Pyrex dish containing approximately 500 mL of 20X SSC. The inverted gel was placed onto the wick, followed by a piece of nylon membrane slightly larger in size than the gel. This was then covered by two pieces of 3MM Whatman filter paper cut to the size of the gel. Paper towels (same size as gel) were then stacked about 6-7 cm high on top of the blotting paper. A plexiglass support and a weight of approximately 250 g were placed on top of the apparatus to aid transfer. After overnight transfer the RNA was UV-crosslinked to the membrane using a UVC-515 Ultraviolet Multilinker at 12,000 MicroJ/CM^2. The membrane was then soaked in 10 % (v/v) glacial acetic acid for 5 min.

The quality of the transfer was checked using 1X reversible blot stain (Sigma). The membrane was stained for approximately 10 min and then rinsed with DEPC-treated water. The stained membrane was then scanned using a Hewlett Packard ScanJet 3300C. Next, the membrane was incubated in 50 mL of pre-heated prehybridization buffer [50 % (v/v) formamide, 5X SSC, 0.02 % (w/v) SDS, 0.01 % (w/v) N-lauryl sarcosine, 2 % (w/v) blocking reagent (Roche)] in a hybridization bag at 68 ˚C for 4 h in a pre-heated hybridization oven.

After 4 h, the prehybridization buffer was replaced with hybridization buffer (same components as prehybridization buffer) containing 20 µL of either *hsp30* or *hsp70* DIG-labelled antisense riboprobe. The membrane was then returned to the hybridization oven for overnight incubation at 68 ˚C.

Next, the membrane was washed to remove any unbound probe. First it was washed twice in 2X SSC at room temperature for 5 min, then once each in 0.5X SSC and 0.1X SSC, both at 68 ˚C for 15 min. All three SSC washing solutions contained 0.1 % (w/v) SDS. The blot was then equilibrated for 1 min at room temperature in washing buffer [100 mM maleic acid buffer, 0.3 % (v/v) Tween-20] and blocked using blocking solution [2 % (w/v) blocking reagent (Roche), 10 % (v/v) maleic acid buffer] for 1 h at room temperature. The blot was then incubated in blocking solution containing 1:8000 alkaline phosphatase conjugated anti-DIG-Fab fragments (Roche) for 30 min. The membrane was then washed twice in washing buffer for 10 min each and then equilibrated in detection buffer [0.1 M Tris-HCl (pH 9.5), 0.1 M NaCl] for 2 min prior to detection using CDP-star (Roche), a chemiluminescent reagent, which was applied to the membrane and allowed to develop in a hybridization bag for 10 min in the dark. The

membrane was then visualized on a DNR Chemiluminescent Imager (DNR Bioimaging Systems, Kirkland, QU) for up to 12 min depending on the strength of the signal.

2.5 Western blot analysis

2.5.1 Protein isolation from A6 cells

Pelleted A6 cells were thawed on ice prior to the addition of 500 µL of lysis buffer containing 1 % SDS, 1X complete protease inhibitor cocktail (Roche) and homogenization buffer [200 mM sucrose, 2 mM EGTA, 1 mM EDTA, 40 mM NaCl, 30 mM HEPES]. It should be noted that the lysis buffer used for samples in preparation for immunoblotting with a mouse anti-ubiquitin antibody contained 10 mM N-ethylmaleimide (Sigma) to inhibit ubiquitin conjugating enzymes. After adding lysis buffer the cells were subjected to sonication (output 4.5, 60 % duty cycle) for 15-20 bursts using a Fisher Scientific Sonic Dismembrator 100 (Fisher Scientific). The homogenate was then centrifuged at 14,000 rpm for 1 h at 4 ˚C. The supernatant was then transferred to a new microcentrifuge tube and stored at -20 ˚C until use.

2.5.2 Protein quantification

Protein was quantified using a bicinchoninic acid (BCA) Protein Assay Kit (Pierce, Rockford, Illinois). A bovine serum albumin (BSA; Bioshop) protein standard was created by diluting BSA in distilled water at concentrations ranging from 0 to 2 mg/mL. Protein samples were diluted to a concentration of 1:2 in milliQ water. Ten µL of BSA standards and protein samples were transferred in triplicate into a 96 well plate. Then 80 µL of BCA reagent A and B (Pierce) at a ratio 50:1 was added to the BSA and protein samples. The plate was tapped lightly on the side to mix samples, covered with foil and then incubated at 37 ˚C for 30 min. The plate was then read at 562 nm using

a Versamax microplate reader (Molecular Devices, Sunnyvale, CA). A standard curve was created in Microsoft Excel using the BSA protein standards which was used to determine the concentration of each protein sample.

2.5.3 Western blot analysis

Immunoblot analysis was performed using 20 or 60 μg of protein (depending on the primary antibody used) and sodium dodecyl sulfate polyacrylamide gel electrophoresis (SDS-PAGE). For SDS-PAGE, gels were electrophoresed on a BioRad TETRA cell electrophoresis system (BioRad; Mississauga, ON). Separating gels [10-12 % (v/v) acrylamide, 0.32 % (v/v) n'n'-bis methylene acrylamide, 0.375 M Tris (pH 8.8), 1 % (w/v) SDS, 0.2 % (w/v) ammonium persulfate (APS), 0.14 % (v/v) tetramethylethylenediamine (TEMED)] were prepared, poured and allowed to polymerize for 30 min with 100 % ethanol layered on top. Next, ethanol was poured off and the stacking gel [4 % (v/v) acrylamide, 0.11 % (v/v) n'n'-bis methylene acrylamide, 0.125 M Tris (pH 6.8), 1 % (w/v) SDS, 0.4 % (w/v) APS, 0.21 % (v/v) TEMED] was prepared, poured and allowed to polymerize for 30 min. Protein samples were then aliquoted and added to 1X loading buffer [0.0625M Tris (pH 6.8), 10 % (v/v) glycerol, 2 % (w/v) SDS, 5 % (v/v) β-mercaptoethanol, 0.0125 % (w/v) bromophenol blue]. Samples were then heat denatured in a boiling water bath for 10 min, immediately cooled on ice for 5 min and pulse-centrifuged (6 sec at 9 rpm) prior to loading. Gels were electrophoresed with 1X running buffer [25mM Tris, 0.2M glycine, 1 mM SDS] at 90 V until samples reached the separating gel, at which time the voltage was turned up to 160-170 V until the dye front reached the bottom of the gel.

Pure nitrocellulose transfer blot membranes (BioRad) and filter paper (BioRad) were cut to 5.5 cm x 8.5 cm, and membranes were incubated for 30 min in transfer buffer [25 mM Tris, 192 mM glycine, 20 % (v/v) methanol]. After electrophoresis, the stacking gel was cut away and the remainder of the gel was soaked in transfer buffer for 15 min. Protein was transferred to the nitrocellulose membrane with a Trans-Blot Semi-Dry Transfer Cell (BioRad) at 20 volts for 25 min. Blots were then stained with Ponceau-S stain [0.19 % (w/v) Ponceau-S, 5 % (v/v) acetic acid] for 12 min to determine the success of the transfer and equal loading. The membrane was then rinsed with MilliQ water and scanned with a Hewlett Packard ScanJet 3300C. The membrane was incubated in 5 % blocking solution [20 mM Tris (pH 7.5), 0.1 % Tween 20 (Sigma), 300 mM NaCl, 5 % (w/v) Nestle® Carnation skim milk powder] for 1 h to prevent nonspecific binding. The membrane was then incubated for 1 h in blocking solution containing the primary polyclonal antibody. The antibodies used were either mouse anti-ubiquitin (Zymed, San Francisco, CA), rabbit anti-HSP30 (Fernando and Heikkila, 2000), anti-HSP70 (Gauley and Heikkila) or anti-actin (Sigma) antibodies at dilutions of 1:150; 1:1000, 1:250 and 1:200, respectively.

Excess unbound antibody was removed by rinsing the membrane with 1X Tris-buffered saline with Tween 20 (TBS-T) [20 mM Tris, 300 mM NaCl, (pH 7.5), 0.1 % Tween 20 (Sigma)]. The membrane was washed with fresh TBS-T for 15 min, followed by two 10 min washes with fresh TBS-T. The membrane was then incubated for 1 h with blocking solution containing the secondary antibody conjugate, AP-conjugated goat-anti-rabbit (BioRad) at a 1:3000 dilution or AP-conjugated goat-anti-mouse (BioRad) at a 1:1000 dilution. The membrane was then rinsed with TBS-T and then washed with fresh

TBS-T for 15 min, followed by two 5 min washes with fresh TBS-T. The membrane was incubated in alkaline phosphatase detection buffer [alkaline phosphatase buffer (100 mM Tris base, 100 mM NaCl, 50 mM $MgCl_2$ (pH 9.5)), 0.3 % 4-nitro blue tetrazolium (NBT; Roche), 0.17 % 5-bromo-4-chloro-3-indolyl phosphate, toluidine salt (BCIP; Roche)] until the bands were visible. Images were scanned using a Hewlett Packard ScanJet 3300C.

2.5.4 Densitometric statistical analysis

Densitometry was performed using Image J (1.38) software on individual blots. Experiments were repeated in triplicate, and the average densitometric values were expressed as a percentage of the maximum hybridization band or as a percent inhibition for KNK437 experiments. The data were graphed with standard error, represented as vertical error bars. The level of significance of the differences between the samples was calculated using Microsoft Excel, by one-way analysis of variance (ANOVA) with a Tukey's post-test. With the exception of KNK437 experiments in which two-tailed paired *t*-tests were performed to analyze the differences between samples. Confidence levels used were 95 % ($p < 0.05$).

2.6 Immunocytochemistry and laser scanning confocal microscopy

A6 cells were prepared for imaging by laser scanning confocal microscopy (LSCM) on base-washed glass coverslips in Petri dishes. Coverslips were placed in small Coplin jars to ensure full contact with the base solution [49.5 % (v/v) ethanol, 0.22 M NaOH] for 30 min with periodic shaking at room temperature. The coverslips were then rinsed under running distilled water for 3 h and dried on 3MM Whatman paper. Finally, the coverslips were stored in Petri plates sealed with parafilm and flamed in the laminar

flow hood prior to use. To prepare A6 cells for an experiment, coverslips were placed in new sterile Petri dishes and the cell suspension was added to the dish.

The cells were then allowed to attach to the coverslips for 24 h at 22 ˚C. For chemical treatments, A6 cells were treated directly in the Petri dishes at 22 ˚C. In heat shock experiments, the Petri dishes were wrapped with parafilm, sealed in a plastic bag and then placed in a heated water bath. After treatment, the L-15 media was removed and the cells were washed twice in phosphate-buffered saline [PBS; 1.37 M NaCl, 67 mM Na_2HPO_4, 26 mM KCl, 14.7 mM H_2PO_4, 1 mM $CaCl_2$, 0.5 mM $MgCl_2$, pH 7.4] and the coverslips were transferred to new small Petri dishes. The cells were fixed with 3.7 % (w/v) paraformaldehyde (pH 7.4 in PBS) for 10-15 min and then washed 3 times in PBS for 5 min. It should be noted that for treatments with celastrol washes were performed with minimal shaking to reduce impact on cell adherence. Next, the cells were permeabilized using 0.3 % Triton X-100 (Sigma) in PBS for 10 min and then washed 3 times in PBS for 5 min. Finally, the cells were blocked with 3.7 % (w/v) bovine serum albumin fraction V (BSA fraction V; Sigma) in PBS for 1 h or overnight at 4 ˚C. The BSA fraction V was filter-sterilized using a 0.45 μm filter to remove debris that might negatively affect imaging. Cells were then incubated in primary antibody (rabbit anti-HSP30C at 1:500 in blocking solution) for 1 h. After three 5 min washes in PBS, the cells were indirectly labelled by incubation in a fluorescent-conjugated secondary antibody (goat-anti rabbit Alexa Fluor 488 (Molecular Probes, Eugene, OR) at 1:2,000 in blocking solution) for 30 min, in the dark, to avoid photo-bleaching of the fluorescent signal.

Cells were then probed for actin with rhodamine-tetramethylrhodamine-5-isothiocyanate phalloidin (TRITC; Molecular Probes) at 1:60 in PBS for 15 min, in the

dark. The cells were then washed three times for 5 min in PBS. The coverslips were mounted (cell side down) in one drop of VectaShield containing 4,6-diamidino-2-phenylindole (DAPI; Vector Laboratories Inc, Burlingame, CA) on a glass slide and sealed with clear nail polish. Once dried, the slides were visualized with a Zeiss Axiovert 200 microscope and LSM 510 META software (Carl Zeiss Canada Ltd., Mississauga, ON). The 63X oil immersion objective was utilized along with the 405 nm (for DAPI), 488 nm (for Alexa-488) and 533 nm (for TRITC) scanning lasers. Between uses, the slides were stored at 4 ˚C for no longer than 3 weeks.

3 Results

3.1 Analysis of heat shock induced *hsp30* gene expression and HSP30 accumulation in *Xenopus* cultured cells

A number of studies conducted in our laboratory using *X. laevis* A6 cells have shown that both *hsp30* mRNA and HSP30 accumulate in response to elevated temperatures (Ohan et al., 1998; Phang et al., 1999; Fernando and Heikkila, 2000; Gellalchew and Heikkila, 2004; Young et al., 2009). Examples of northern blot hybridization and immunoblot analyses demonstrating heat shock-induced *hsp30* gene expression are shown in Figure 5. In contrast to control cells, detectable levels of *hsp30* mRNA were present in cells subjected to heat shock at 33 ˚C or 35 ˚C for 2 h (Fig. 5A). The relative levels of *hsp30* mRNA were greater in cells incubated at 35 ˚C than those heat shocked at 33 ˚C. Similar findings were observed with the effect of heat shock on HSP30 accumulation in A6 cells. HSP30 levels were detected in cells heat shocked at 33 ˚C and were relatively greater at 35˚C (Fig. 5B). It should be noted that the anti-HSP30 antibody utilized in this study, which was prepared against the entire coding sequence of HSP30C, detected multiple members of the HSP30 family in immunoblot analysis (Fernando and Heikkila, 2000).

The present study also examined heat shock-induced localization of HSP30 using immunocytochemistry and LSCM (Fig. 6). While there was no detectable HSP30 in control cells maintained at 22 ˚C, A6 cells heat shocked at 33 ˚C displayed a punctate pattern of HSP30 accumulation primarily in the cytoplasm. These results are in agreement with previous studies conducted in our laboratory on HSP30 localization in

Figure 5. The effect of heat shock on *hsp30* gene expression in *X. laevis* A6 cells. **A)** The effect of heat shock on *hsp30* mRNA levels. Cells were maintained at 22 ˚C or subjected to a 2 h heat shock at 33 ˚C or 35 ˚C. After treatment, total RNA was isolated from A6 cells and quantified as described in the Materials and Methods section. Ten µg of total RNA was examined via northern blot hybridization analysis using an *hsp30* antisense riboprobe. Reversible blot staining was utilized to confirm equal loading and efficiency of transfer. The positions of 28S and 18S ribosomal RNAs are indicated with black arrows. These data are representative of three separate experiments. **B)** Effect of heat shock on HSP30 and actin protein levels. Cells were maintained at 22 ˚C or subjected to a 2 h heat shock at 33 ˚C or 35 ˚C followed by a 2 h recovery period at 22 ˚C. After treatment, cells were harvested and total protein was isolated. Twenty µg of protein was transferred to nitrocellulose membranes from SDS-polyacrylamide gels and probed with anti-HSP30 or anti-actin polyclonal antibodies. A section of a representative Ponceau S stained membrane that brackets a 42-kDa band (asterisk) is shown to demonstrate equal loading and efficiency of transfer. These data are representative of five separate experiments.

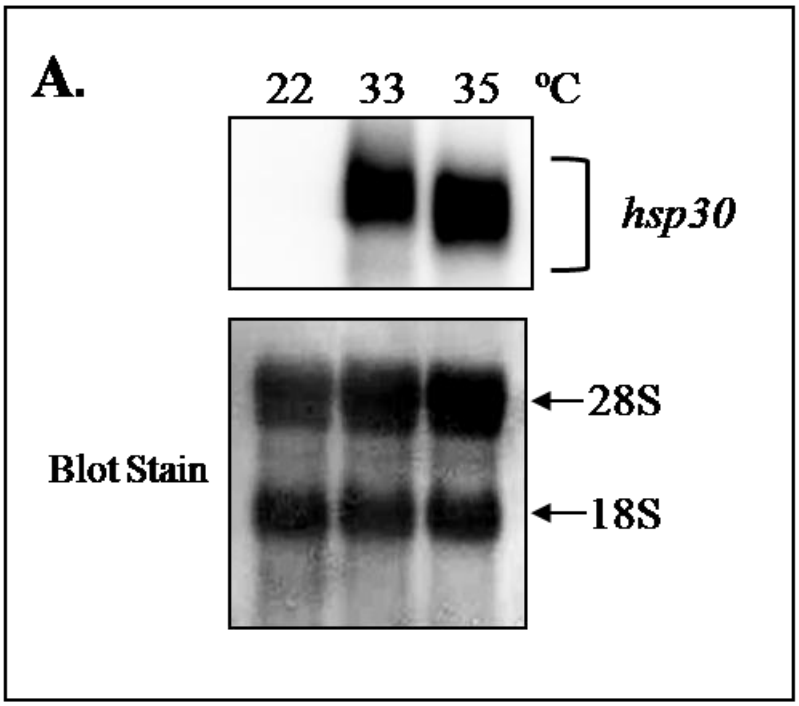
A.
22 33 35 ℃
hsp30
Blot Stain
28S
18S

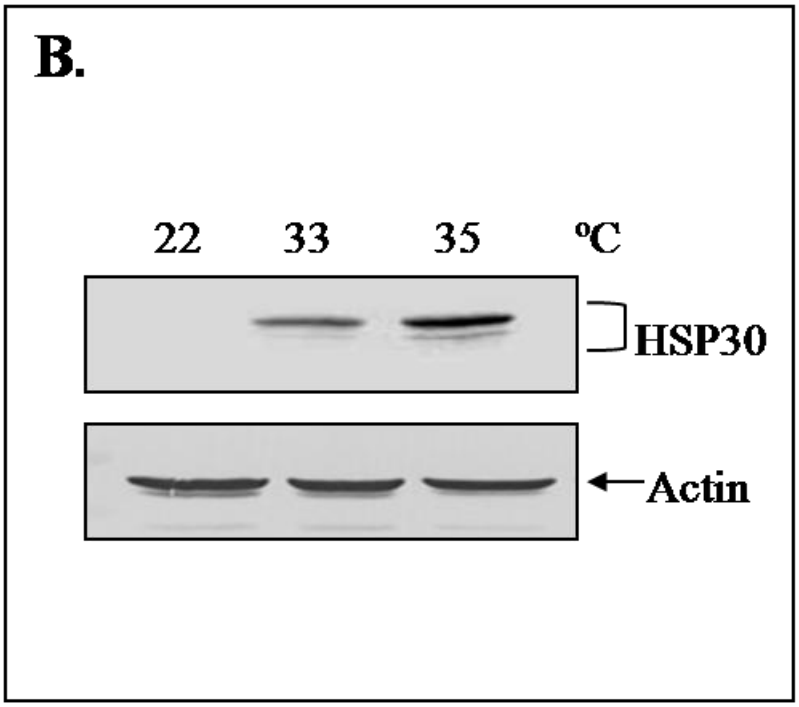
B.
22 33 35 ℃
HSP30
Actin

Figure 6. The effect of heat shock on the localization of HSP30 in A6 cells.

Cells were grown on base-washed glass coverslips and maintained at either 22 ˚C or incubated at 33 ˚C for 2 h followed by a 2 h recovery period at 22 ˚C. Actin and nuclei were stained directly with phalloidin conjugated to TRITC (red) and DAPI (blue), respectively. HSP30 was indirectly detected with an anti-HSP30 antibody and a secondary antibody conjugated to Alexa-488 (green). The 10 µm white scale bars are indicated at the bottom right section of each panel. These data are representative of five separate experiments.

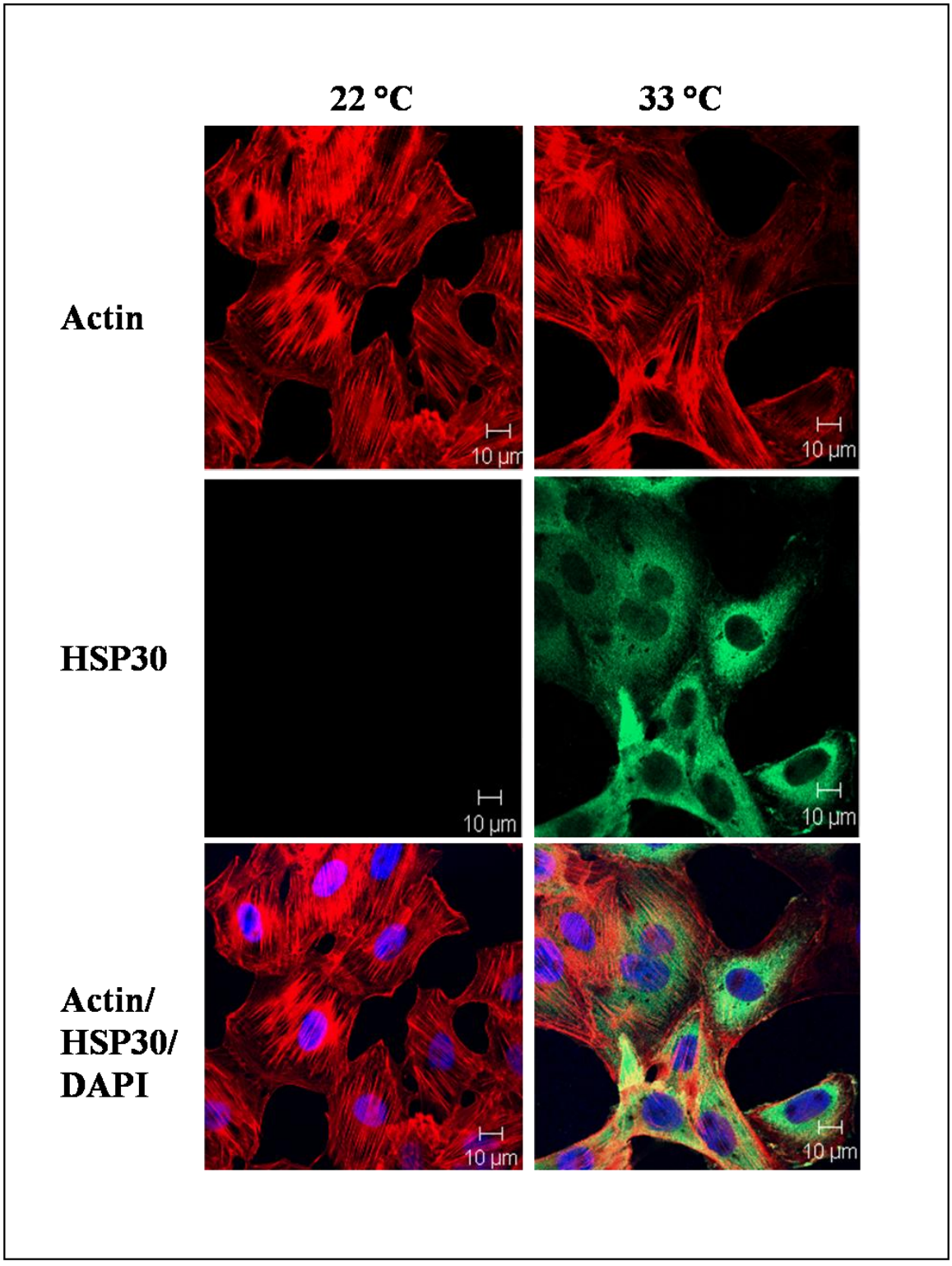
22 °C
33 °C
Actin
HSP30
Actin/
HSP30/
DAPI
10 µm
10 µm
10 µm
10 µm
10 µm
10 µm

response to heat shock (Gellalchew and Heikkila, 2004; Manwell and Heikkila, 2007). It should be noted that HSP70 was not investigated using this technique because the affinity purified, polyclonal anti-HSP70 antibody, that was utilized successfully in immunoblot analysis, was unable to specifically detect HSP70 by immunocytochemistry (Gauley et al., 2008).

3.2 Effect of celastrol and MG132 on proteasome activity in *Xenopus* A6 cells

Previous studies suggested that celastrol may have an inhibitory effect on proteasome activity in mammalian cells (Yang et al., 2006; Yang et al., 2008; He et al., 2009). To assess the impact of celastrol on proteasome activity in *Xenopus* A6 cells, the relative levels of ubiquitinated protein and chymotrypsin-like activity were determined. These data were compared to the effects of the proteasome inhibitor, MG132, which was previously characterized in our laboratory (Young and Heikkila, 2009). The relative levels of ubiquitinated protein detected in heat shocked A6 cells were similar to control cells (Fig. 7). However, the relative accumulation of ubiquitinated protein was greater in cells treated with 2.5 µM celastrol for 12 or 24 h at 22 ˚C. Furthermore, cells treated with 2.5 µM celastrol for 24 h displayed levels of protein ubiquitination similar to cells treated with 30 µM MG132 for 24 h.

Figure 7. The effect of celastrol and MG132 on ubiquitinated protein levels.

A6 cells were maintained at either 22 ˚C (1), heat shocked for 2 h at 33 ˚C followed by a 2 h recovery period at 22 ˚C (2), treated with 30 µM MG132 for 24 h (3), or incubated with 2.5 µM celastrol for 12 h (4) or 24 h (5), respectively. After treatment, cells were harvested and total protein was isolated. Sixty µg samples of protein were subjected to immunoblot analysis employing a mouse anti-ubiquitin monoclonal antibody. The levels of ubiquitinated protein in heat shocked, celastrol- or MG132-treated cells were compared to control A6 cells. The positions of molecular mass standards in kDa are shown in the first lane (M). A section of a representative Ponceau S stained membrane that brackets a 42-kDa band (asterisk) is shown to demonstrate equal loading and efficiency of transfer. These data are representative of three separate experiments.

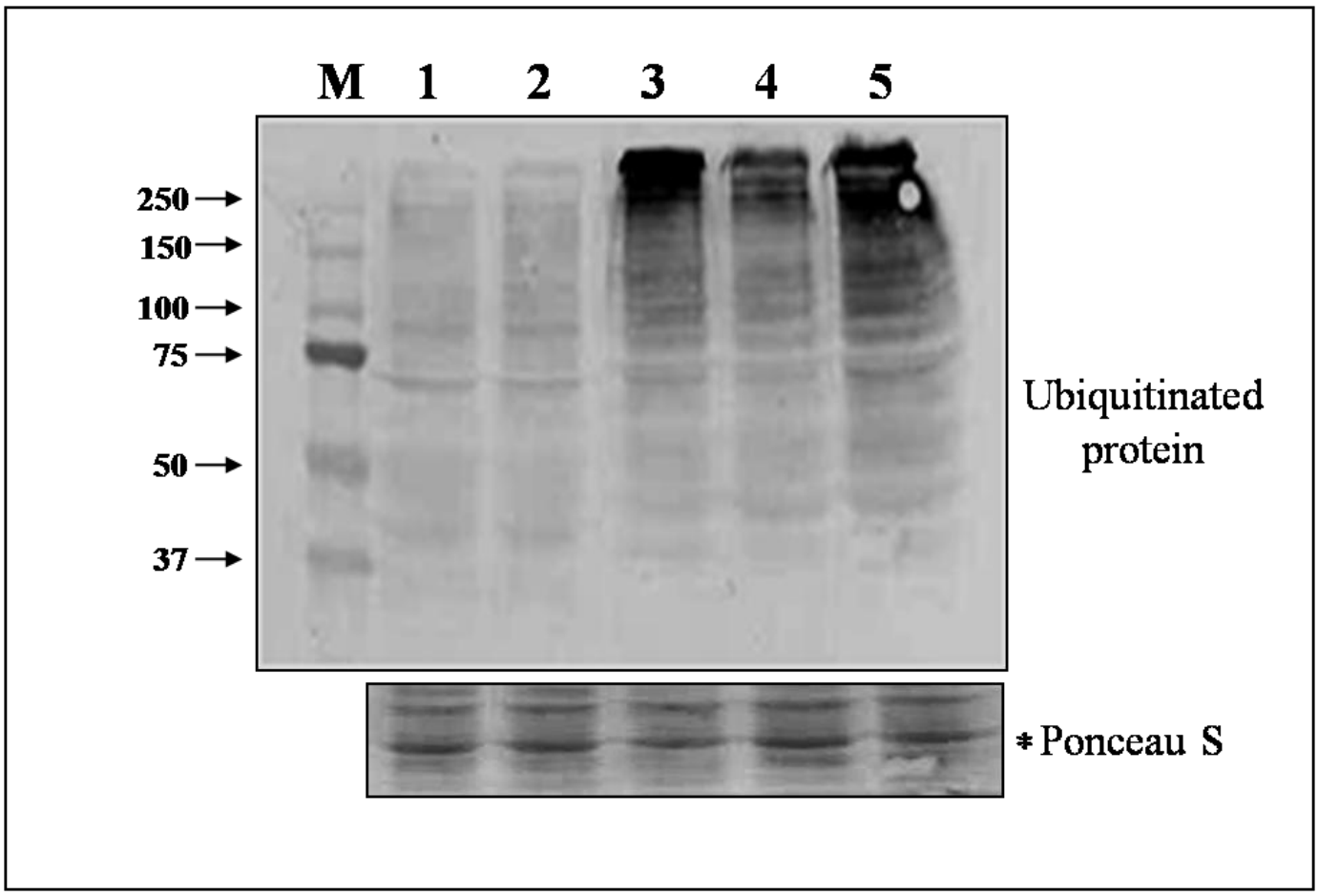
M
1
2
3
4
5
250
150
100
75
50
37
Ubiquitinated protein
* Ponceau S

Past studies reported that celastrol preferentially inhibits the chymotrypsin-like activity of the 20S proteasome in both the purified rabbit proteasome and human prostate cancer cells (Yang et al., 2006; Yang et al., 2008). To determine whether celastrol has a similar inhibitory effect on the proteasome in A6 cells, the proteasome-glo assay was employed to measure chymotrypsin-like activity. Compared to control cells, chymotrypsin-like activity decreased by approximately 61 %, in A6 cells treated with 2.5 µM celastrol for 12 h, and was reduced by 38 % in cells treated with celastrol for 24 h at 22 ˚C (Fig. 8). Celastrol-mediated proteasome inhibition was also compared to the effects of MG132, which acts a substrate analog of chymotrypsin-like activity in the 20S proteasome. An 85 % reduction in chymotrypsin-like activity occurred in cells treated with 30 µM MG132 for 24 h.

3.3 Characterization of celastrol-induced HSP accumulation

3.3.1 The effect of celastrol on HSP30 and HSP70 accumulation.

The next phase of this study examined the effect of celastrol on HSP30 and HSP70 accumulation in A6 cells. While cells treated with 1 µM celastrol for 8 h displayed relatively low levels of detectable HSP30, maximal levels of accumulation occurred in cells treated with 5 µM celastrol at 22 ˚C (Fig. 9A). Maximum HSP70 accumulation occurred in response to 5 µM celastrol for 8 h. Densitometric analysis revealed that in comparison to A6 cells incubated with 1 µM celastrol for 8 h, HSP30 accumulation increased 6-fold in cells that were treated with 5 µM celastrol (Fig. 9B). Similarly, levels of HSP70 increased 2.5-fold in cells incubated with 2.5 µM celastrol. Upon treatment with 7.5 µM celastrol for 8 h, A6 cells exhibited a 70 % decrease in

Figure 8. Celastrol and MG132-induced inhibition of proteasomal chymotrypsin-like activity. Cells were maintained at either 22 ˚C (Control) or treated with 30 μM MG132 for 24 h, 2.5 μM celastrol for 12 h, or 2.5 μM celastrol for 24 h at 22 ˚C. After treatment, proteasomal chymotrypsin-like activity was determined using the Promega Proteasome-Glo^{TM} chymotrypsin-like cell based assay as described in Materials and Methods. Results are expressed as a percentage of the chymotrypsin-like activity observed in control cells. These data are derived from four separate experiments. The level of significance of the differences between the samples was calculated by one-way ANOVA with a Tukey's post-test. Significant differences between control cells and A6 cells treated with MG132 (30 μM) or celastrol (2.5 μM) are indicated as * ($p < 0.05$).

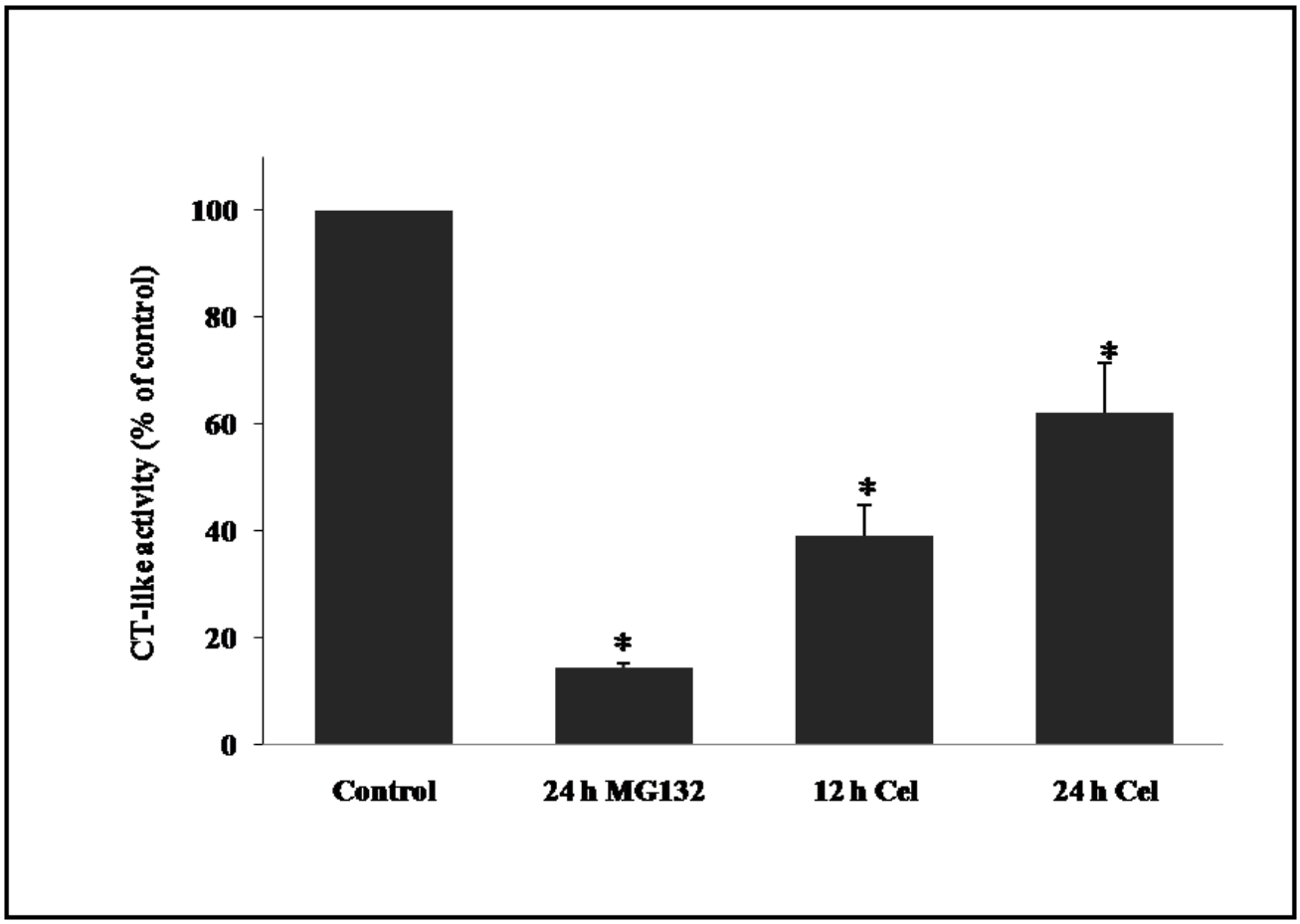
CT-like activity (% of control)
100
80
60
40
20
0
*
*
*
Control
24 h MG132
12 h Cel
24 h Cel

Figure 9. The effect of different celastrol concentrations on HSP30 and HSP70 accumulation. A) A6 cells were maintained at either 22 ˚C (C) or treated with various concentrations of celastrol ranging from 1 to 7.5 µM for 8 h at 22 ˚C. After treatment, cells were harvested and total protein was isolated. Twenty µg of protein was subjected to immunoblot analysis employing anti-HSP30, anti-HSP70 or anti-actin polyclonal antibodies. **B)** Image J software was used to perform densitometric analysis of the signal intensity for HSP30 (grey) and HSP70 (black) protein bands of western blot images. The data from three separate experiments are expressed as a percentage of the maximum bands (2.5 and 5 µM celastrol for HSP70 and HSP30, respectively). The standard error is represented by vertical error bars. The level of significance of the differences between the samples was calculated by one-way ANOVA with a Tukey's post-test. Significant differences between the maximum bands and other concentrations of celastrol are indicated as * ($p < 0.05$).

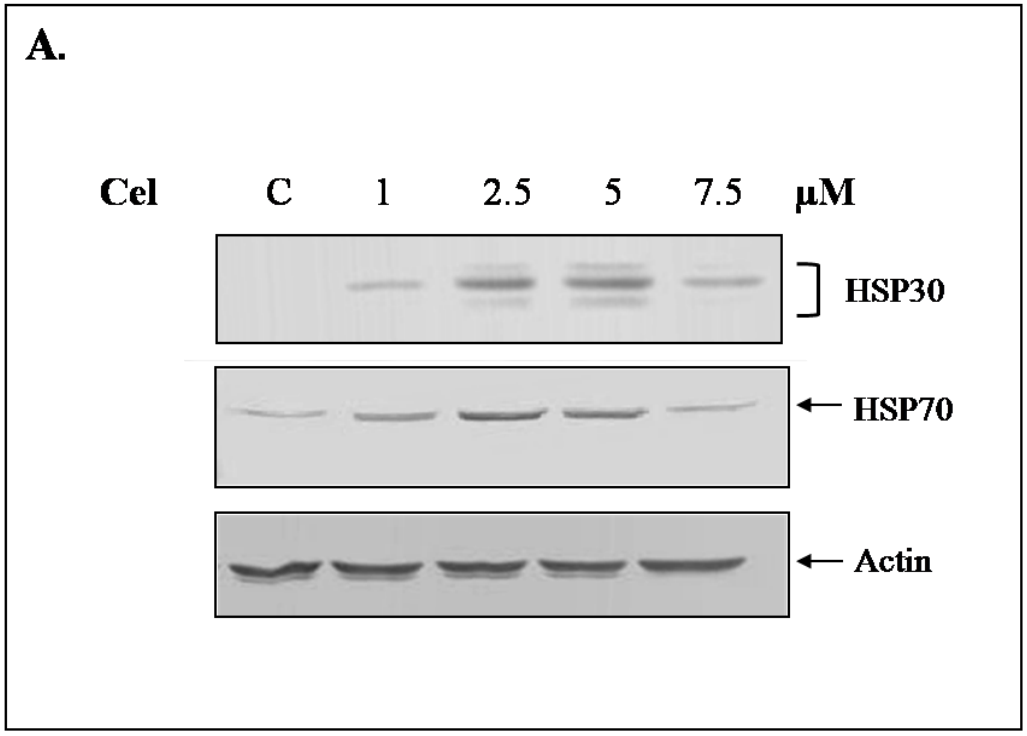
A.
Cel
C
1
2.5
5
7.5
µM
HSP30
HSP70
Actin

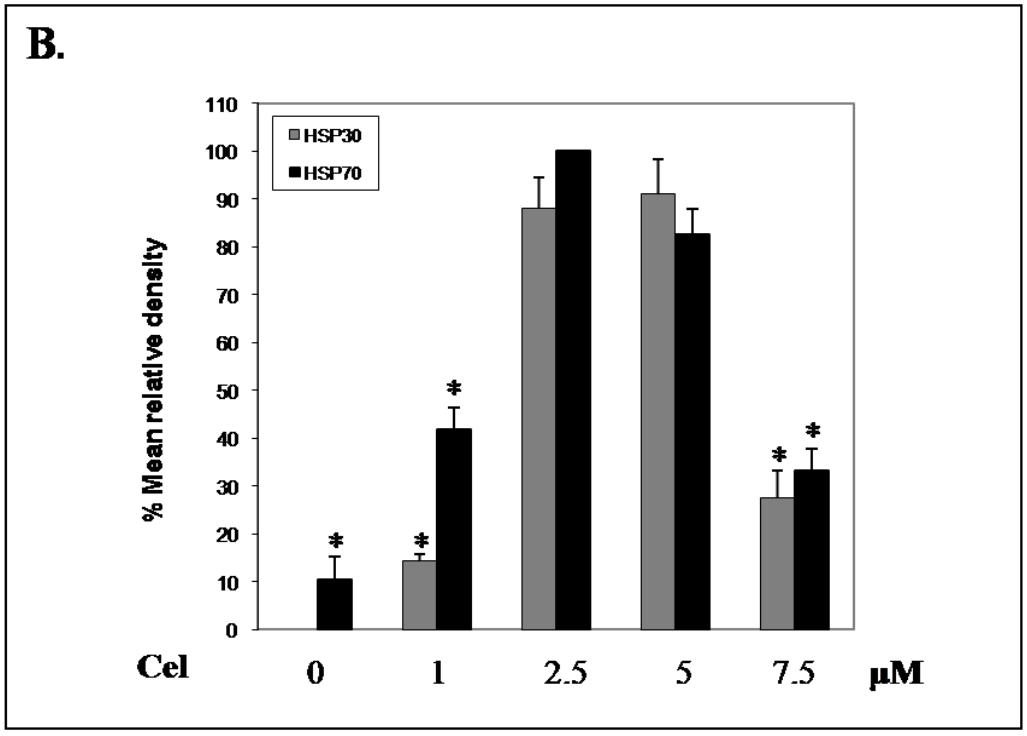
B.
HSP30
HSP70
% Mean relative density
110
100
90
80
70
60
50
40
30
20
10
0
Cel
0
1
2.5
5
7.5
µM

HSP30 accumulation compared to cells incubated with 5 µM celastrol. Similarly, the accumulation of HSP70 was reduced by 65 % in comparison to A6 cells exposed to 2.5 µM celastrol. To assess the effect of prolonged exposure of celastrol on HSP accumulation, A6 cells were subjected to different concentrations of celastrol for 18 h at 22 ˚C. For both HSP30 and HSP70, maximal levels of accumulation occurred in cells incubated with 2.5 µM celastrol (Fig. 10A). In comparison to A6 cells treated with 1 µM celastrol, a 50-fold increase in HSP30 occurred in response to 2.5 µM celastrol for 18 h, whereas HSP70 levels increased 4-fold (Fig. 10B). Similar to the results observed in 8 h celastrol treatments, cells incubated with 7.5 µM celastrol, displayed a 70 % and 65 % reduction in HSP30 and HSP70 levels, respectively compared to cells treated with 2.5 µM celastrol.

In time course studies, HSP30 accumulation was first detected in A6 cells treated with 2.5 µM celastrol for 6 h while HSP70 was detectable after 2 h. The relative levels of HSP30 and HSP70 increased with time reaching maximal levels in cells treated for 18 h (Fig. 11A). Densitometric analysis revealed that in comparison to cells treated with celastrol for 6 h, a 7.9-fold increase in HSP30 accumulation occurred in cells treated for 18 h (Fig. 11B) Similarly, in comparison to cells incubated with celastrol for 2 h, HSP70 levels increased 20-fold after 18 h. Additionally, the relative levels of HSP30 and HSP70 accumulation were reduced by approximately 30 % to 35 % in cells exposed to celastrol for 24 or 48 h, in comparison to cells incubated for 18 h. To determine whether A6 cells were able to recover from celastrol treatment, cells were incubated with 2.5 µM celastrol for 18 h and allowed to recover in fresh L-15 media for various periods of time (4-48 h).

Figure 10. The effect of prolonged exposure to various celastrol concentrations on HSP30 and HSP70 accumulation in A6 cells. A) Cells were maintained at 22 ˚C (C) or treated with different concentrations of celastrol ranging from 1 to 7.5 µM for 18 h at 22 ˚C. After treatment, cells were harvested and total protein was isolated. Twenty µg of protein was subjected to immunoblot analysis employing anti-HSP30, anti-HSP70 or anti-actin polyclonal antibodies. **B)** Image J software was used to perform densitometric analysis of the signal intensity for HSP30 (grey) and HSP70 (black) protein bands of western blot images. The data are expressed as a percentage of the maximum band (2.5 µM celastrol) . The standard error is represented by vertical error bars. The level of significance of the differences between the samples was calculated by one-way ANOVA with a Tukey's post-test. Significant differences between cells exposed to 2.5 µM celastrol and other concentrations of celastrol (1, 5 and 7.5 µM) are indicated as * ($p < 0.05$). These data are representative of three separate experiments.

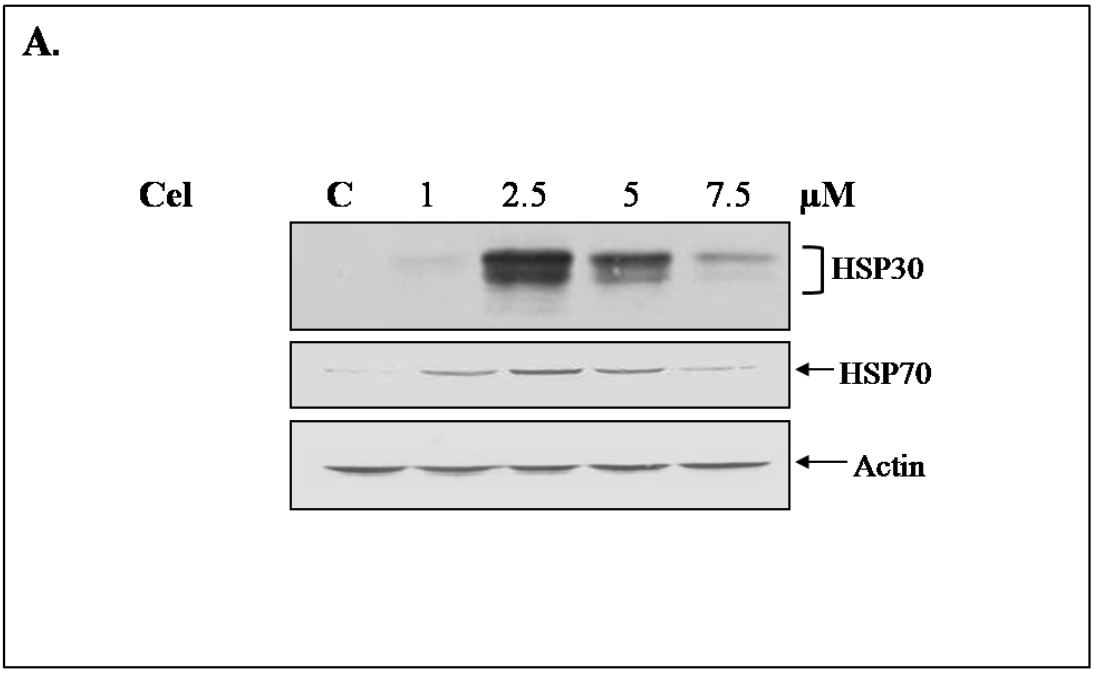
A.
Cel
C
1
2.5
5
7.5
μM
HSP30
HSP70
Actin

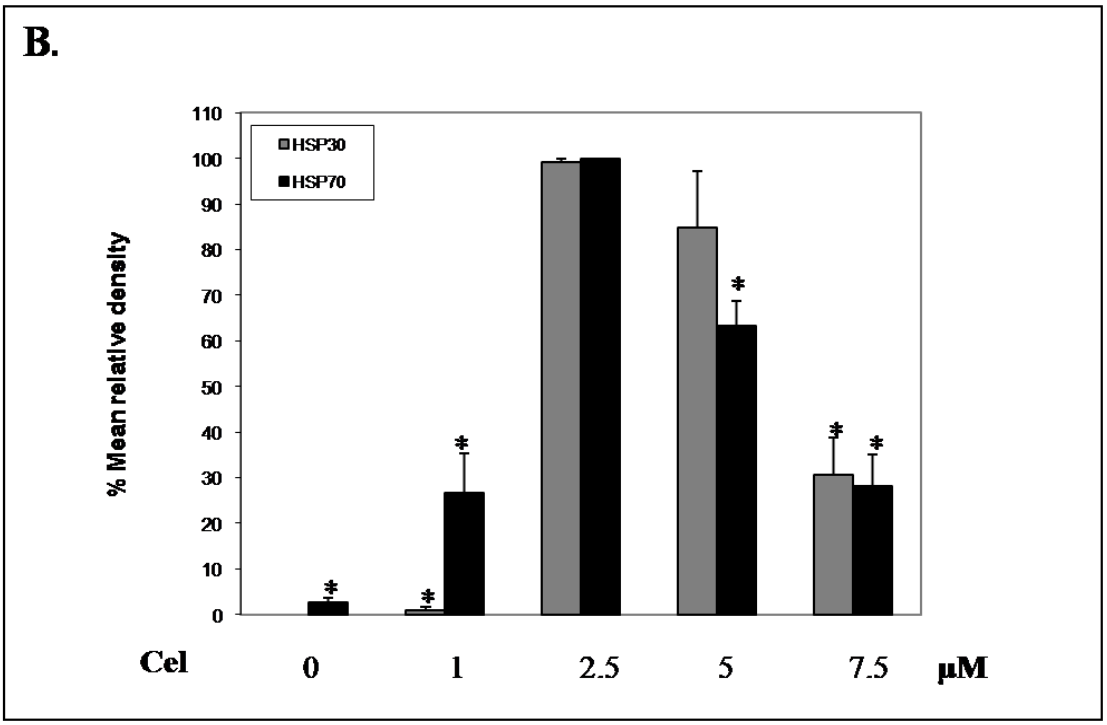
B.
% Mean relative density
HSP30
HSP70
110
100
90
80
70
60
50
40
30
20
10
0
Cel
0
1
2.5
5
7.5
μM

Figure 11. Time course of HSP30 and HSP70 accumulation in A6 cells treated with celastrol. A) Cells were maintained at 22 ˚C (C) or treated with 2.5 µM celastrol at 22 ˚C for various time periods ranging from 2 to 48 h. After treatment, cells were harvested and total protein was isolated. Twenty µg of protein was examined using immunoblot analysis employing anti-HSP30, anti-HSP70 or anti-actin polyclonal antibodies. **B)** Image J software was used to perform densitometric analysis of the signal intensity for HSP30 (grey) and HSP70 (black) protein bands of western blot images. The data are expressed as a percentage of the mean maximum band (2.5 µM celastrol for 18 h) while, the standard error is represented by vertical error bars. The level of significance of the differences between the samples was calculated by one-way ANOVA with a Tukey's post-test. Significant differences between cells exposed to 2.5 µM celastrol for 18 h and other time points (2 to 48 h) are indicated as * ($p < 0.05$). These data are representative of three separate experiments.

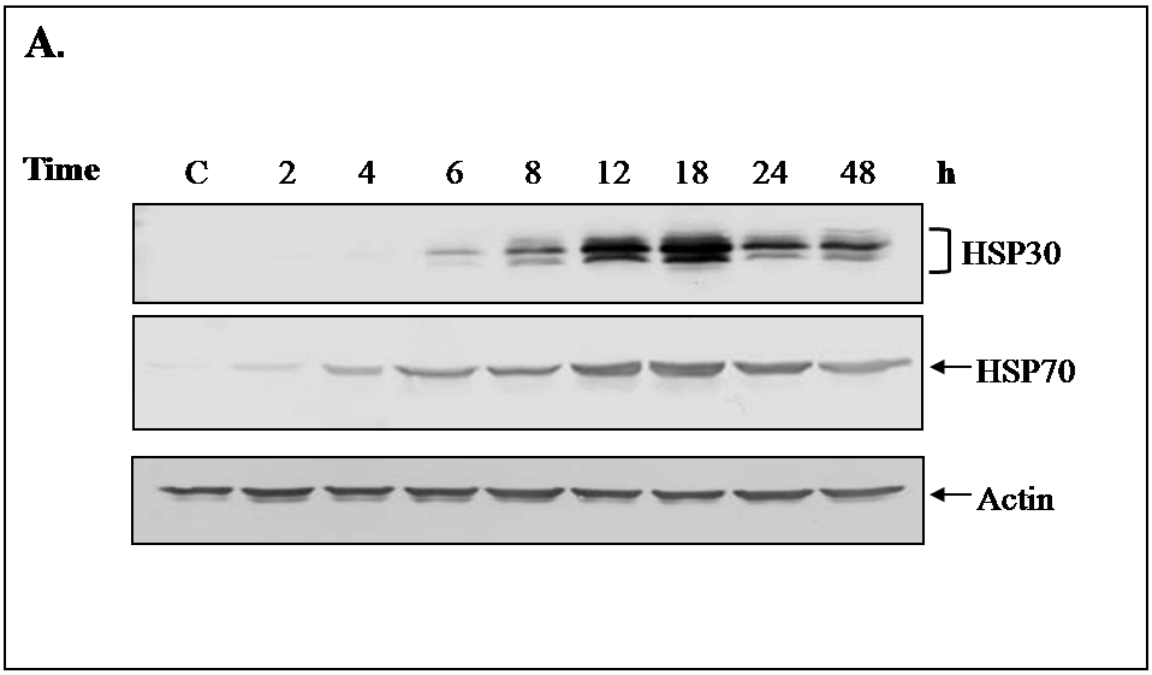
A.
Time
C
2
4
6
8
12
18
24
48
h
HSP30
HSP70
Actin

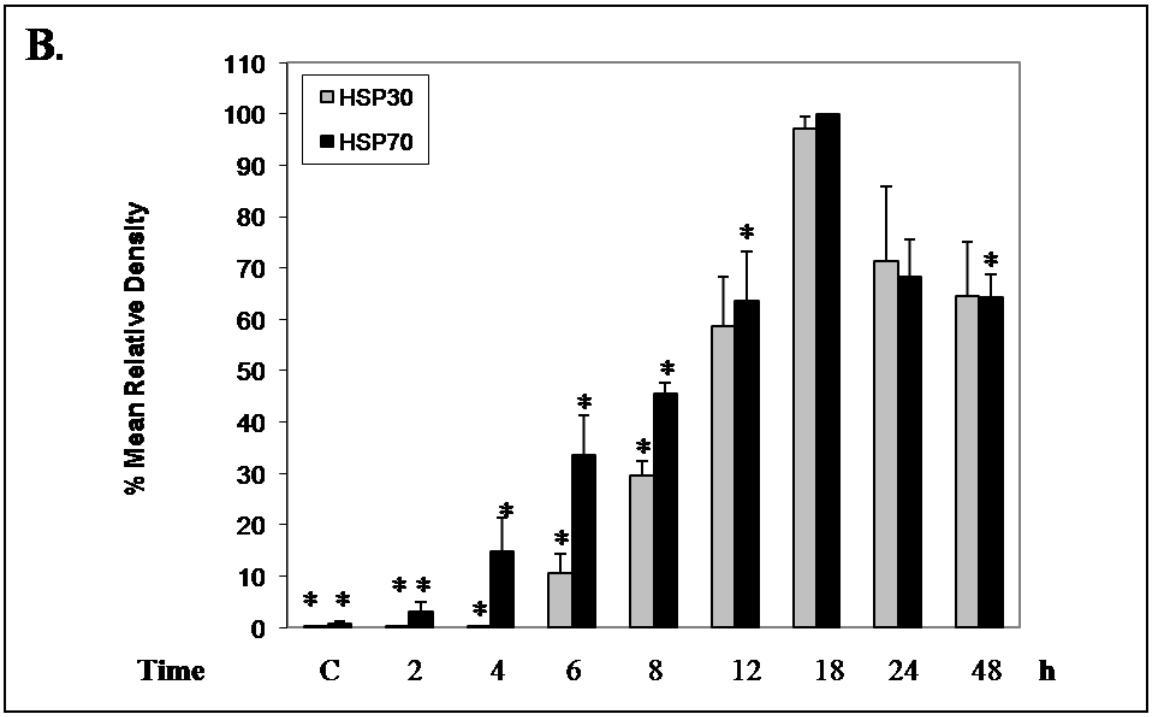
B.
HSP30
HSP70
% Mean Relative Density
110
100
90
80
70
60
50
40
30
20
10
0
Time
C
2
4
6
8
12
18
24
48
h

The levels of HSP30 in A6 cells recovering from celastrol treatment remained consistently high from 4 to 24 h of recovery, with reduced levels of HSP30 occurring in cells allowed to recover for 48 h (Fig. 12). HSP70 accumulation patterns were consistently high from 4 to 12 h of recovery and decreased after 18 h, with relatively low HSP70 levels occurring in cells allowed to recover for 48 h. Cells were also examined using phase contrast microscopy to detect morphological changes in cells treated with 2.5 µM celastrol for 18 h. Control cells displayed a slightly elongated and dome-like morphology and formed a confluent monolayer on the surface of tissue culture flasks (Fig.13). Upon treatment with celastrol for 18 h, most cells appeared round and were less confluent. Remaining A6 cells were allowed to recover in fresh L-15 media for 24 h, 48 h and 4 d at 22 ˚C. After 4 days of recovery, a portion of remaining cells were confluent and displayed typical epithelial morphology.

3.3.2 Analysis of the regulation of celastrol-induced *hsp30* and *hsp70* gene expression

Previous studies with *X. laevis* have shown that the induction of *hsp* genes by various stressors including heat shock and proteasomal inhibition are regulated, at least in part, at the level of transcription (Heikkila, 2003; Heikkila, 2004; Young and Heikkila, 2009). This phenomena involves HSF1-mediated synthesis of *hsp* mRNA. In the present study, northern blot hybridization analysis determined that celastrol treatment induced the accumulation of both *hsp30* and *hsp70* mRNA. For example, *hsp30* and *hsp70* mRNA accumulation was observed in cells exposed to 2.5 µM celastrol for 6, 8 and 12 h time periods. The relative levels of *hsp30* accumulation increased with increasing incubation

Figure 12. HSP30 and HSP70 protein levels in A6 cells recovering from celastrol treatment. Cells were maintained at 22 ˚C (C) or treated with 2.5 µM celastrol for 18 h followed by varying recovery periods in fresh L-15 media ranging from 4 to 48 h at 22 ˚C. After treatment, cells were harvested and total protein was isolated. Twenty µg of protein was examined using immunoblot analysis employing anti-HSP30, anti-HSP70 or anti-actin polyclonal antibodies. These data are representative of two separate experiments.

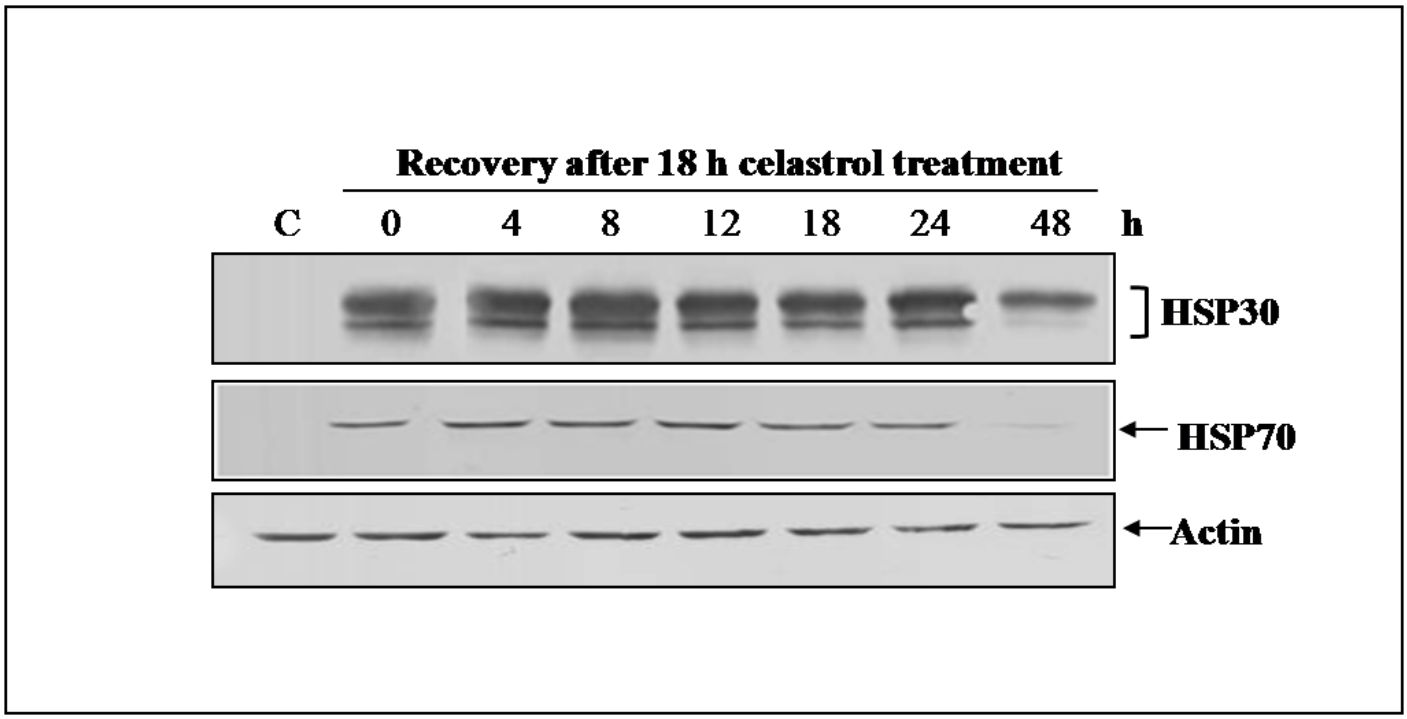
Recovery after 18 h celastrol treatment
C
0
4
8
12
18
24
48
h
HSP30
HSP70
Actin

Figure 13. Examination of the morphology of A6 cells recovering from celastrol treatment. A6 cells were cultured in FBS-supplemented L-15 media at 22°C in T-75cm^2 tissue culture flasks. Cells were then exposed to 2.5 µM celastrol for 18 h followed by a 24 h, 48 h, or 4 day recovery (Rec.) period in fresh L-15 media at 22 ˚C. Phase contrast microscopy was employed to examine the morphological changes occurring in cells recovering from celastrol treatment. Subsequently, A6 cells were photographed using a Nikon coolpix 995 digital camera (400X final magnification) and compared to control cells maintained at 22 ˚C.

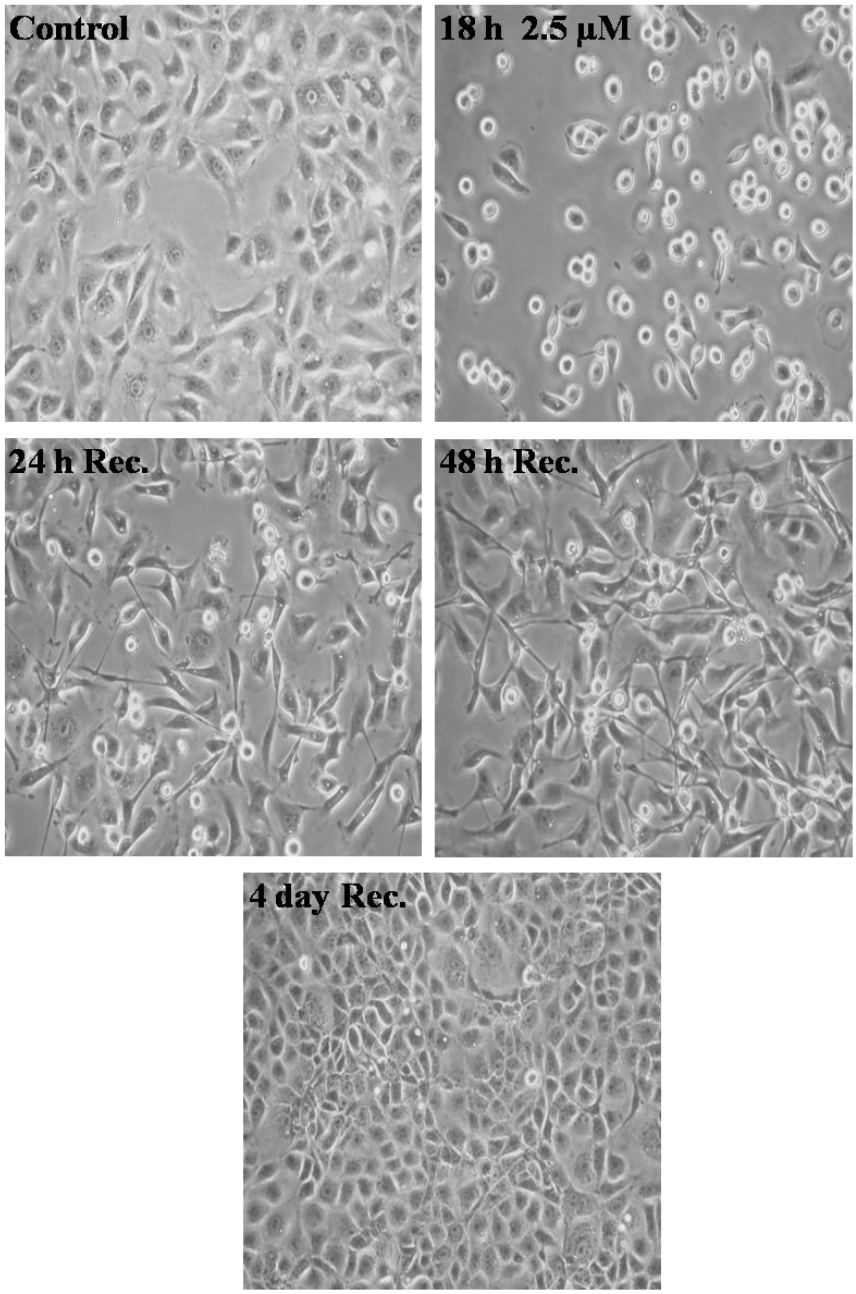
Control
18 h 2.5 µM
24 h Rec.
48 h Rec.
4 day Rec.

times, with the highest level of accumulation occurring in cells treated with celastrol for 12 h (Fig. 14). Additionally, in comparison to A6 cells treated with celastrol for 6 h, enhanced levels of *hsp70* mRNA accumulation were observed after 8 and 12 h incubation periods.

Additionally, past experiments in our laboratory employed the inhibitor, KNK437, to show that stress-induced *hsp* gene expression in *X. laevis* A6 cells was controlled at the level of HSF1 DNA binding (Manwell and Heikkila, 2007; Voyer and Heikkila, 2008). In the current study, relative levels of HSP30 and HSP70 in A6 cells treated with 2.5 µM celastrol alone, were compared to cells incubated with celastrol for 8, 12 or 18 h following a 6 h pre-treatment with 100 µM KNK437 (Fig. 15A). Densitometric analysis demonstrated that pre-treatment with KNK437, suppressed celastrol-induced HSP30 accumulation by 91 %, 86 %, and 73 % for cells treated with celastrol for 8, 12 and 18 h, respectively. Similarly, following pre-treatment with KNK437, a decrease in HSP70 by 88 %, 72 %, and 65 % occurred in cells incubated with celastrol for 8, 12 and 18 h, respectively (Fig. 15B).

3.4 The effect of mild heat shock on celastrol-induced HSP30 and HSP70 accumulation in A6 cells

The next sets of experiments were designed to investigate the effect of elevated temperatures on celastrol-induced *hsp* gene expression, in *X. laevis* A6 cells. In cells exposed to either mild heat shock (30 ˚C) or celastrol (2.5 µM) alone for 4 h, relatively low levels of HSP30 and HSP70 accumulation were detected (Fig. 16A). However, an enhancement in HSP30 and HSP70 accumulation occurred in A6 cells treated with both

Figure 14. Time course of *hsp30* and *hsp70* mRNA accumulation in A6 cells treated with celastrol. A6 cells were maintained at 22 ˚C (C) or incubated with 2.5 µM celastrol for 6, 8, or 12 h. After treatment, total RNA was isolated from A6 cells and quantified as described in the Materials and Methods section. Ten µg of total RNA was analyzed via northern hybridization analysis using *hsp30* and *hsp70* antisense riboprobes. Reversible blot staining was utilized to confirm equal loading and efficiency of transfer. The positions of 28S and 18S ribosomal RNAs are indicated with black arrows. These data are representative of two separate experiments.

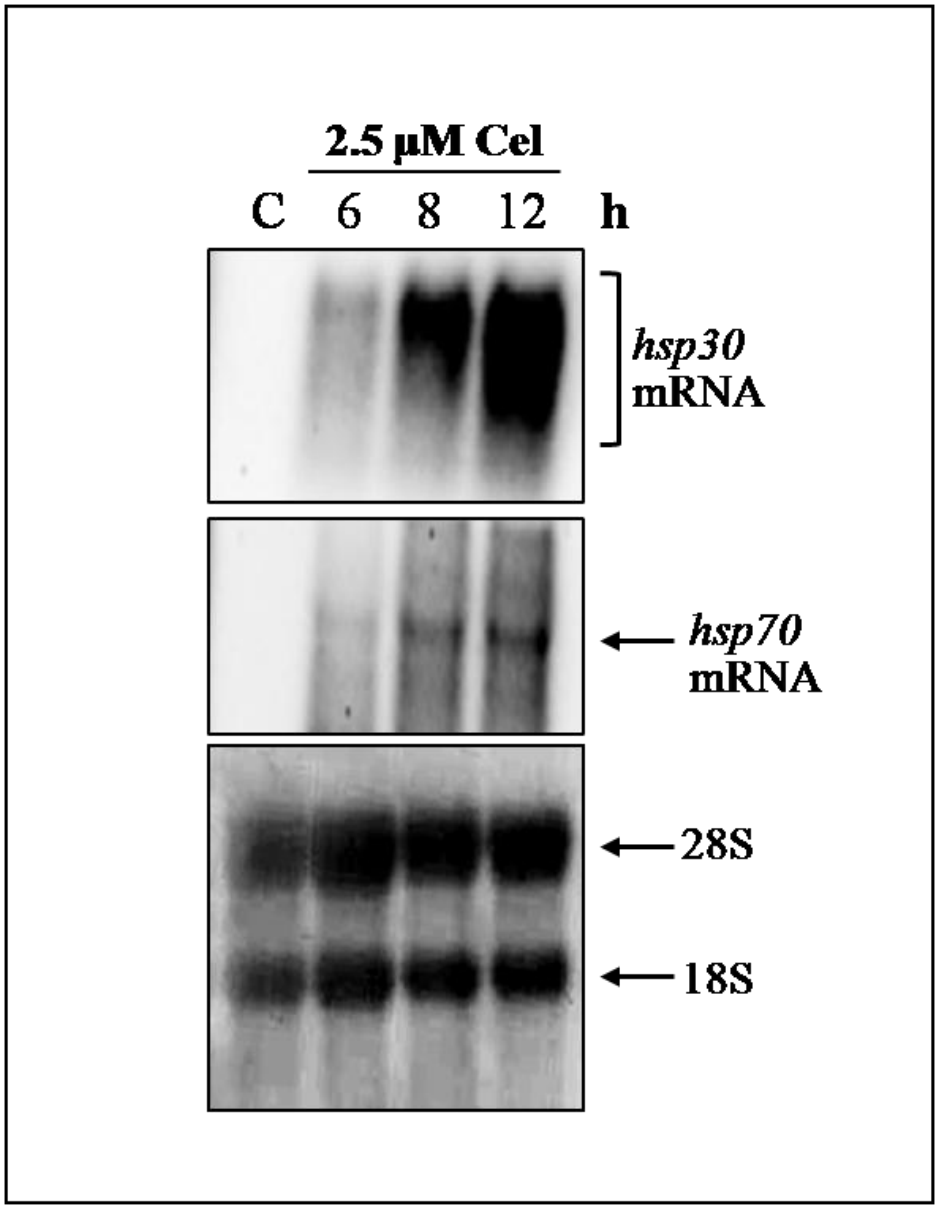
2.5 µM Cel
C 6 8 12 h
hsp30 mRNA
hsp70 mRNA
28S
18S

Figure 15. The effect of KNK437 on celastrol-induced HSP30 and HSP70 accumulation. A) Cells were treated with 2.5 µM celastrol for 8, 12, or 18 h with or without a 6 h pre-treatment with 100 µM KNK437 at 22 ˚C. After treatment, cells were harvested and total protein was isolated. Twenty µg of protein was subjected to immunoblot analysis employing anti-HSP30, anti-HSP70 or anti-actin polyclonal antibodies. **B)** Image J software was used to perform densitometric analysis of the signal intensity for HSP30 (grey) and HSP70 (black) protein bands of western blot images. The ability of KNK437 to inhibit celastrol-induced HSP30 and HSP70 accumulation at each time point was graphed as average percent inhibition. The standard error is represented by vertical error bars. Two-tailed, paired T-tests were performed to analyze the differences between samples. Significant differences between cells exposed to celastrol with or without a 6 h KNK437 pre-treatment are indicated as * ($p < 0.05$). These data are representative of three separate experiments.

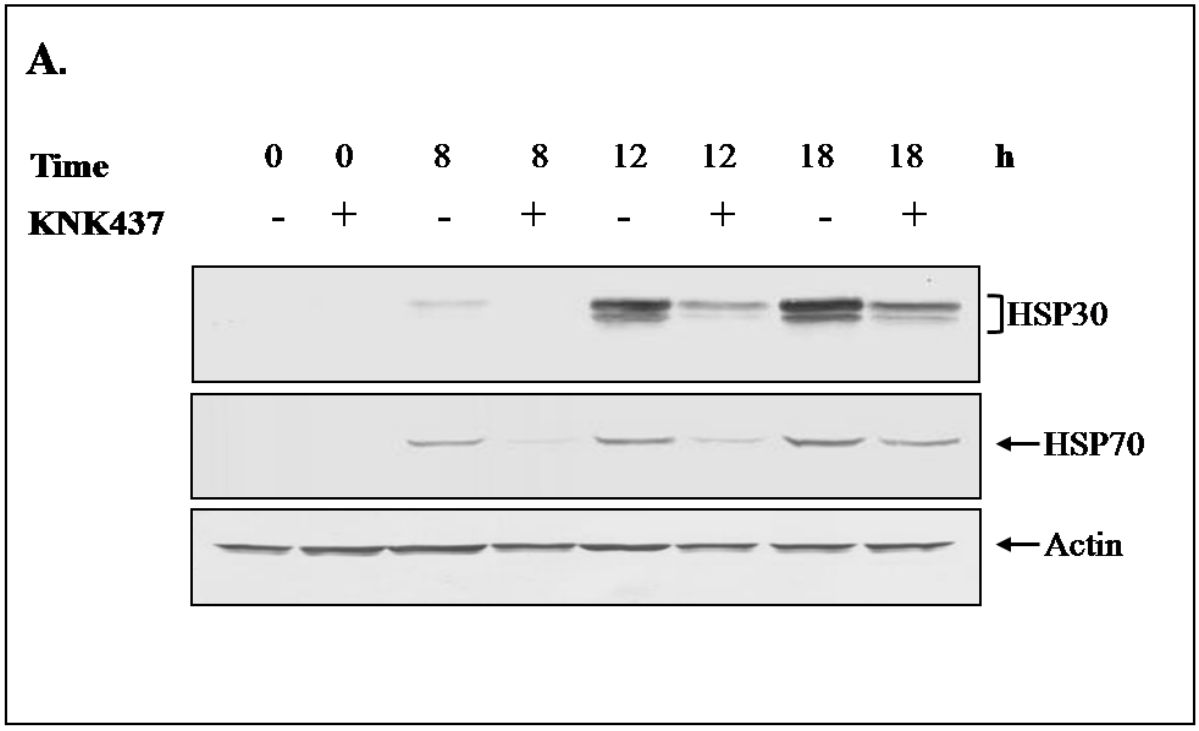
A.
Time
0 0 8 8 12 12 18 18 h
KNK437
- + - + - + - +
HSP30
HSP70
Actin

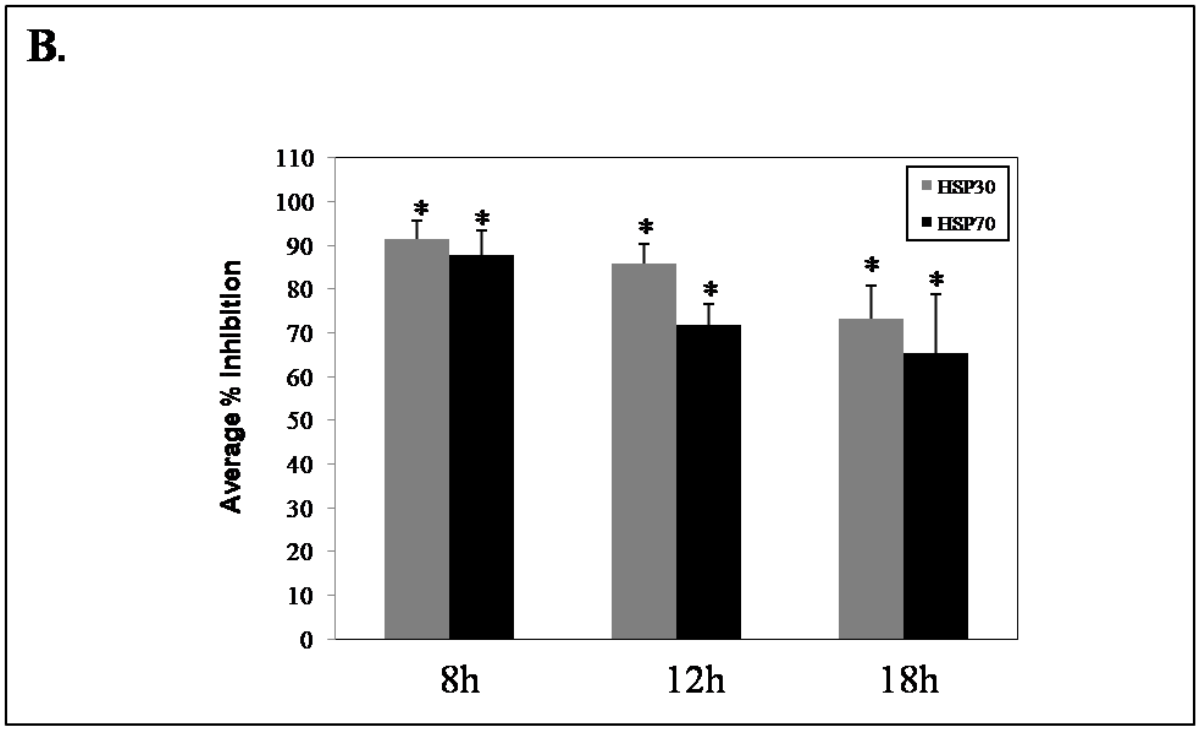
B.
Average % Inhibition
110
100
90
80
70
60
50
40
30
20
10
0
HSP30
HSP70
8h
12h
18h

Figure 16. The effect of mild heat shock on 2.5 µM celastrol-induced HSP30 and HSP70 accumulation. A) Cells were maintained at 30 ˚C, treated with 2.5 µM celastrol at 22 ˚C, or treated with 2.5 µM celastrol at 30 ˚C for 4 or 8 h. After treatment, cells were harvested and total protein was isolated. Twenty µg of protein was subjected to immunoblot analysis employing anti-HSP30, anti-HSP70 or anti-actin polyclonal antibodies. **B)** Image J software was used to perform densitometric analysis of the signal intensity for HSP30 (grey) and HSP70 (black) protein bands of western blot images. Data are expressed as a percentage of the maximum band (combined celastrol and mild heat shock treatment) at each time point. The standard error is represented by vertical error bars. The level of significance of the differences between the samples was calculated by one-way ANOVA with a Tukey's post-test. Significant differences between the maximum signal at each time point and other treatments (celastrol or mild heat shock alone) are indicated as * ($p < 0.05$). These data are representative of three separate experiments.

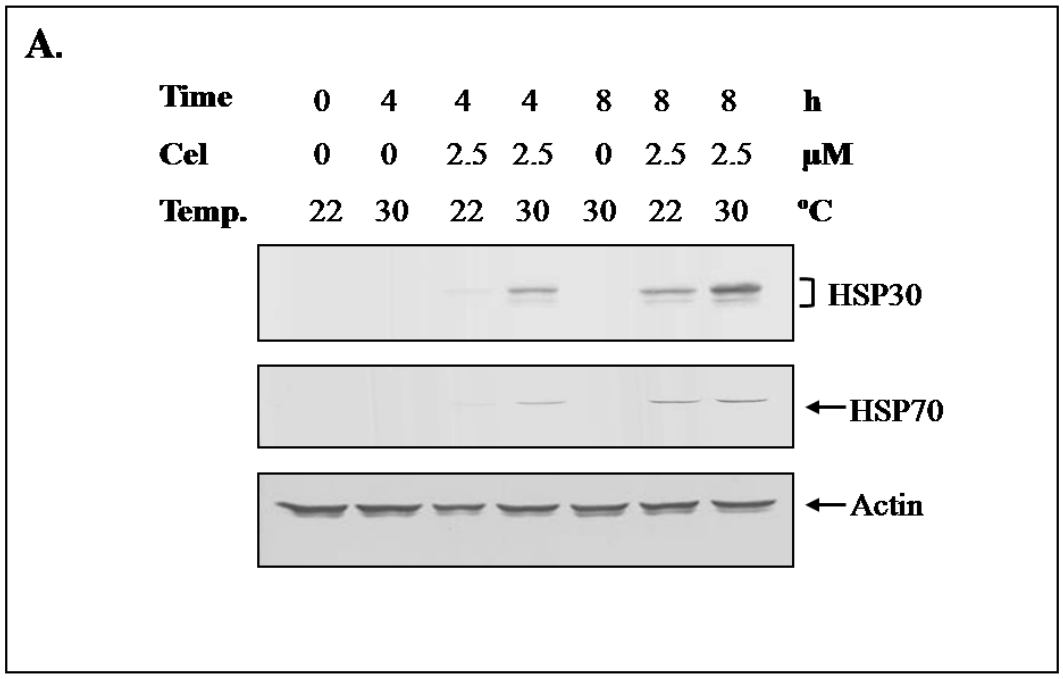
A.
Time 0 4 4 4 8 8 8 h
Cel 0 0 2.5 2.5 0 2.5 2.5 µM
Temp. 22 30 22 30 30 22 30 °C
HSP30
HSP70
Actin

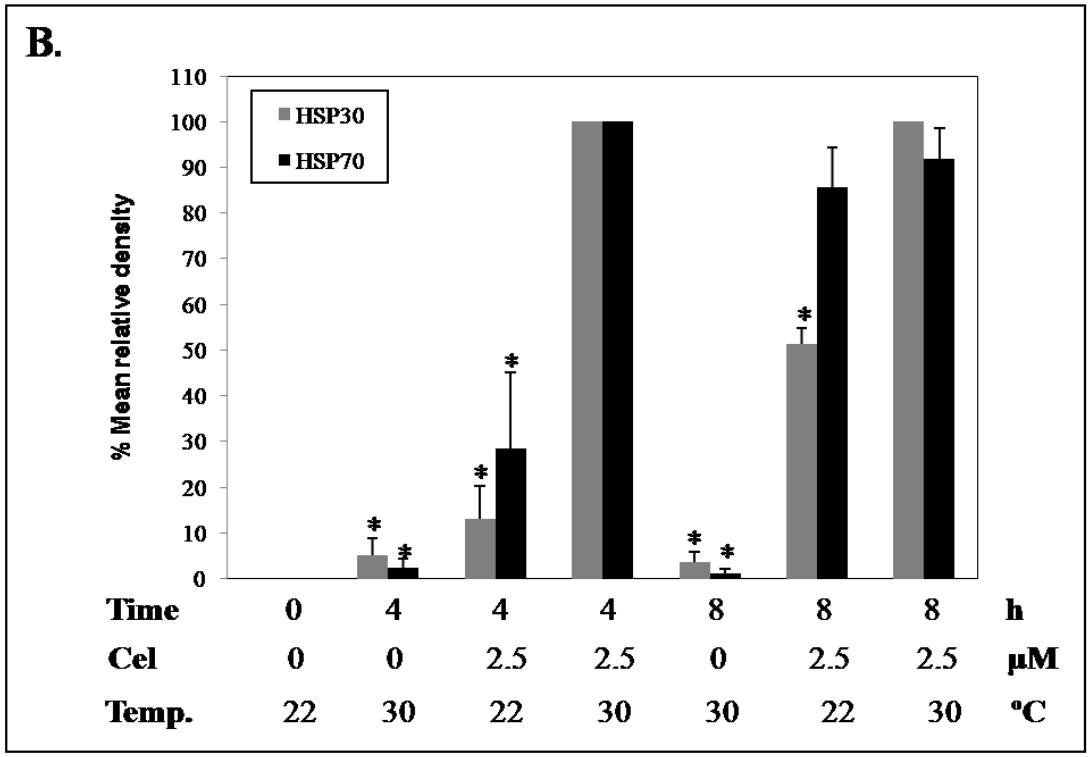
B.
% Mean relative density
HSP30
HSP70
110
100
90
80
70
60
50
40
30
20
10
0
Time 0 4 4 4 8 8 8 h
Cel 0 0 2.5 2.5 0 2.5 2.5 µM
Temp. 22 30 22 30 30 22 30 °C

stressors concurrently for 4 h. Densitometric analysis revealed that after 4 h of combined treatment, HSP30 and HSP70 levels were increased to values greater than the sum of the HSP levels induced by each stressor individually (Fig. 16B). Similarly, in cells treated with celastrol for 8 h, the relative accumulation of HSP30 in A6 cells treated with celastrol at 30 ˚C, was greater than the levels detected in response to each stress alone. Although they were slightly enhanced, the levels of HSP70 resulting from simultaneous exposure to both stresses for 8 h, were not greater than the sum of accumulation induced in A6 cells treated individually with either celastrol or mild heat shock.

3.5 The effect of combined exposure to celastrol and MG132 on HSP accumulation

To examine the effect of two different proteasome inhibitors on HSP30 and HSP70 accumulation in A6 cells, immunoblot analysis was carried out on cells exposed to low concentrations of both celastrol and MG132. While relatively low levels of HSP30 occurred in cells treated with celastrol (1 µM) or MG132 (5 µM) for 8 or 16 h individually, HSP30 levels were enhanced in cells treated with both stressors simultaneously for 8 or 16 h (Fig. 17A). Densitometric analysis revealed that the increased levels of HSP30 observed in cells treated with both stressors (1 µM celastrol and 5 µM MG132) concurrently, were greater than the sum of HSP30 caused by each stressor individually (Fig. 17B). To assess the impact of higher concentrations of MG132 on celastrol-induced HSP accumulation, A6 cells incubated with both 1 µM celastrol and 10 µM MG132 were examined. The combined stresses resulted in an increase in HSP30 accumulation that was greater than the sum of the responses induced by each individual

Figure 17. The effect of concurrent 1 µM celastrol and 5 µM MG132 exposure on HSP30 and HSP70 accumulation. A) A6 cells were incubated with 1 µM celastrol, 5 µM MG132, or both simultaneously for 8 or 16 h at 22 ˚C. After treatment, cells were harvested and total protein was isolated. Twenty µg of protein was subjected to immunoblot analysis employing anti-HSP30, anti-HSP70 or anti-actin polyclonal antibodies. **B)** Image J software was used to perform densitometric analysis of the signal intensity for HSP30 (grey) and HSP70 (black) protein bands of western blot images. Data are expressed as a percentage of the maximum band (combined 1 µM celastrol and 5 µM MG132 treatment) at each time point. The standard error is represented by vertical error bars. The level of significance of the differences between the samples was calculated by one-way ANOVA with a Tukey's post-test. Significant differences between the maximum signal at each time point and other treatments (celastrol or 5 µM MG132 alone) are indicated as * ($p < 0.05$). These data are representative of three separate experiments.

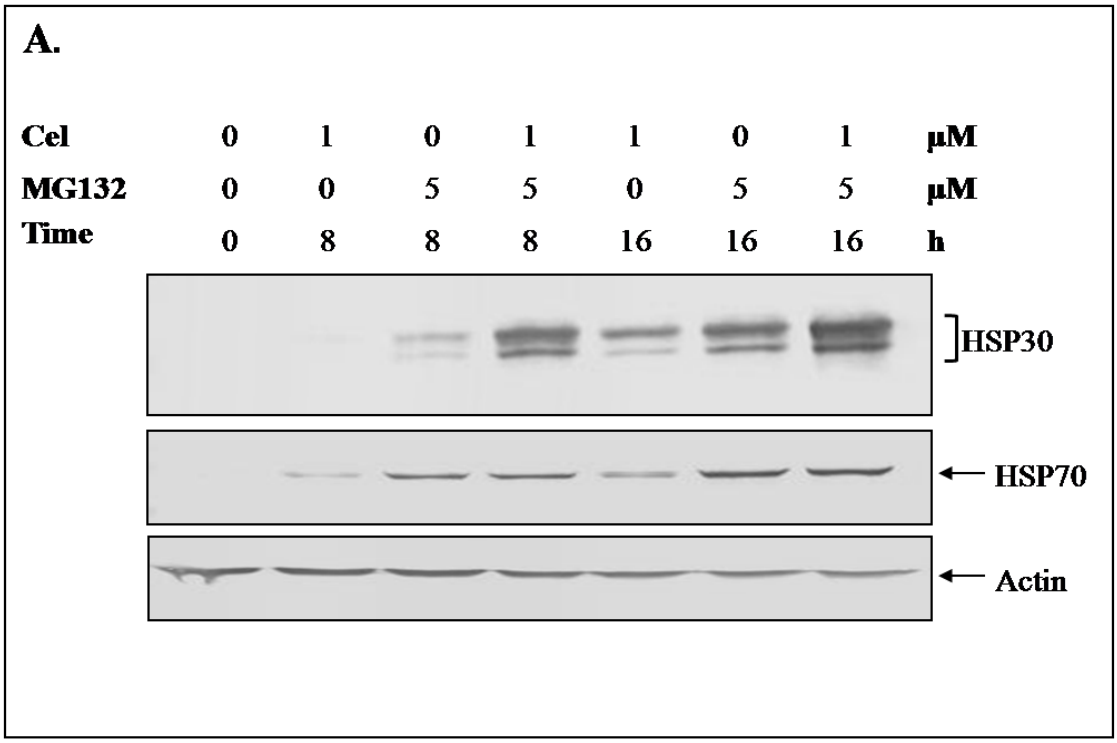
A.
Cel 0 1 0 1 1 0 1 µM
MG132 0 0 5 5 0 5 5 µM
Time 0 8 8 8 16 16 16 h
HSP30
HSP70
Actin

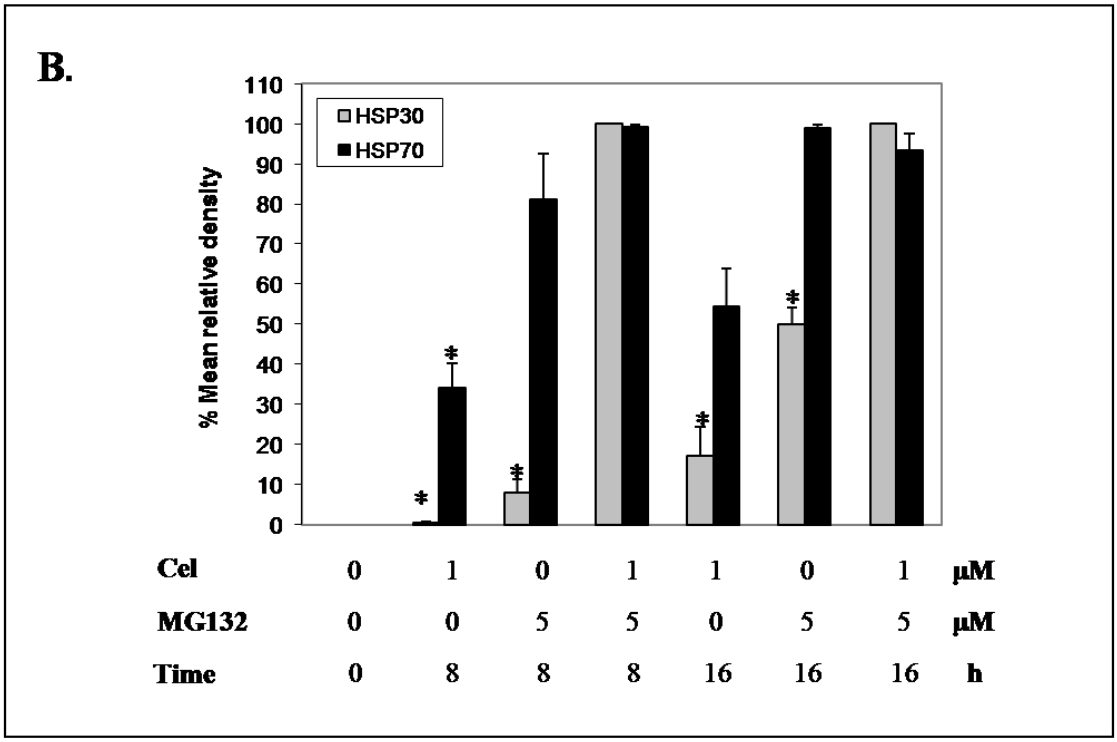
B.
% Mean relative density
HSP30
HSP70
Cel 0 1 0 1 1 0 1 µM
MG132 0 0 5 5 0 5 5 µM
Time 0 8 8 8 16 16 16 h

stressor (Fig. 18). In contrast to the synergistic effect that both stressors had on HSP30 levels in A6 cells, the patterns of HSP70 accumulation observed in cells treated with both celastrol and MG132 simultaneously for 8 or 16 h, were not significantly different from the HSP70 levels induced by MG132 (5 or 10 μM) treatment alone.

3.6 A comparison of celastrol-induced morphological changes in A6 cells grown in tissue-culture flasks or on glass coverslips.

A comparison of the morphology of celastrol-treated A6 cells grown in tissue culture flasks or on glass coverslips was carried out prior to immunocytochemistry and LSCM experiments. Cells were cultured in tissue culture flasks or on base-washed glass coverslips followed by treatment with 1, 2.5, or 5 μM celastrol for 4 or 8 h at 22 ˚C (Figs. 19 and 20). While cells incubated with 1 μM celastrol for 4 h appeared control-like with slightly reduced confluency, a small proportion of cells displayed a round morphology and were sparsely distributed after 8 h. Cells treated with 2.5 or 5 μM celastrol were sparsely distributed on the surface of both tissue culture flasks and coverslips after 4 and 8 h of treatment. The proportion of cells appearing round increased over time in response to 2.5 μM celastrol with the majority of cells displaying a circular morphology after 8 h. However, the majority of cells exposed to 5 μM celastrol became round after 4 h with no additional changes in appearance in response to 8 h treatments. Overall, A6 cells had less adherence to the surface of glass coverslips than they did to the surface of tissue culture flasks. Growing A6 cells on poly L-lysine coated or acid-washed coverslips in an attempt to increase cell adhesion was unsuccessful (data not shown). It should also be noted that

Figure 18. The effect of concurrent 1 µM celastrol and 10 µM MG132 exposure on HSP30 and HSP70 accumulation. A) Cells were subjected to 1 µM celastrol, 10 µM MG132, or both simultaneously at 22 ˚C for 8 or 16 h time periods. After treatment, cells were harvested and total protein was isolated. Twenty µg of protein was subjected to immunoblot analysis employing anti-HSP30, anti-HSP70, and anti-actin polyclonal antibodies. **B)** Image J software was used to perform densitometric analysis of the signal intensity for HSP30 (grey) and HSP70 (black) protein bands of western blot images. Data are expressed as a percentage of the maximum band (combined 1 µM celastrol and 10 µM MG132 treatment) at each time point. The standard error is represented by vertical error bars. The level of significance of the differences between the samples was calculated by one-way ANOVA with a Tukey's post-test. Significant differences between the maximum signal at each time point and other treatments (celastrol or 5 µM MG132 alone) are indicated as * ($p < 0.05$). These data are representative of three separate experiments.

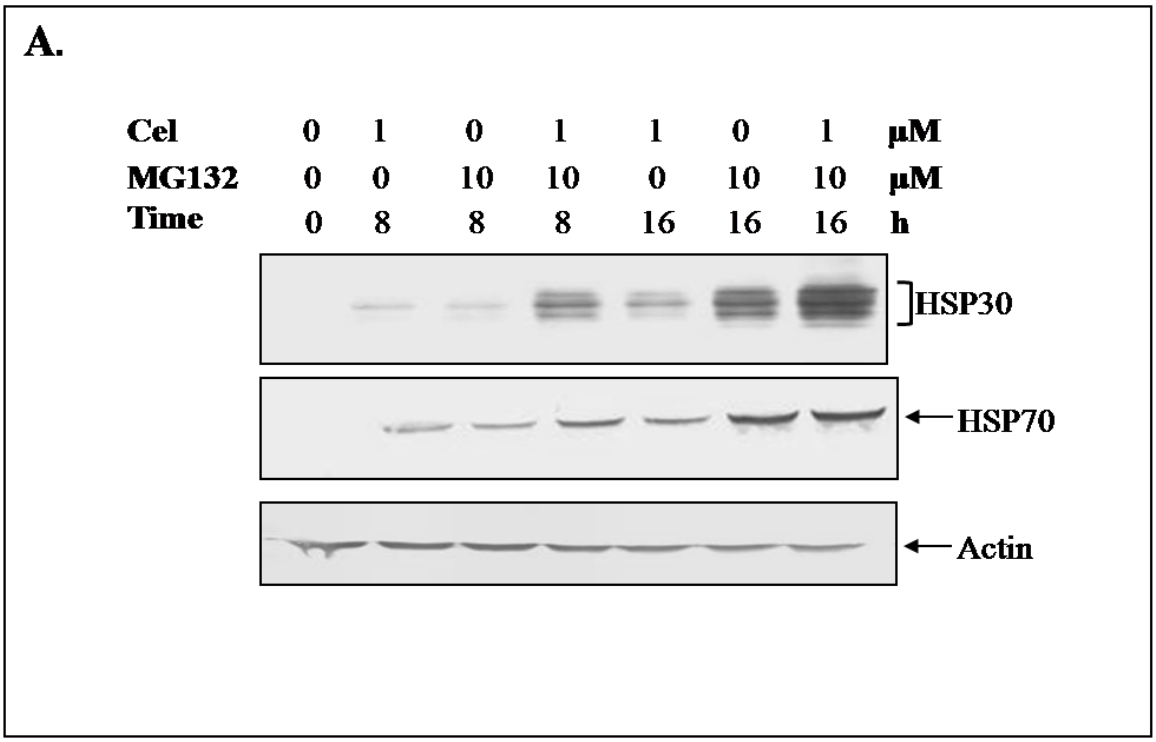
A.
Cel 0 1 0 1 1 0 1 µM
MG132 0 0 10 10 0 10 10 µM
Time 0 8 8 8 16 16 16 h
HSP30
HSP70
Actin

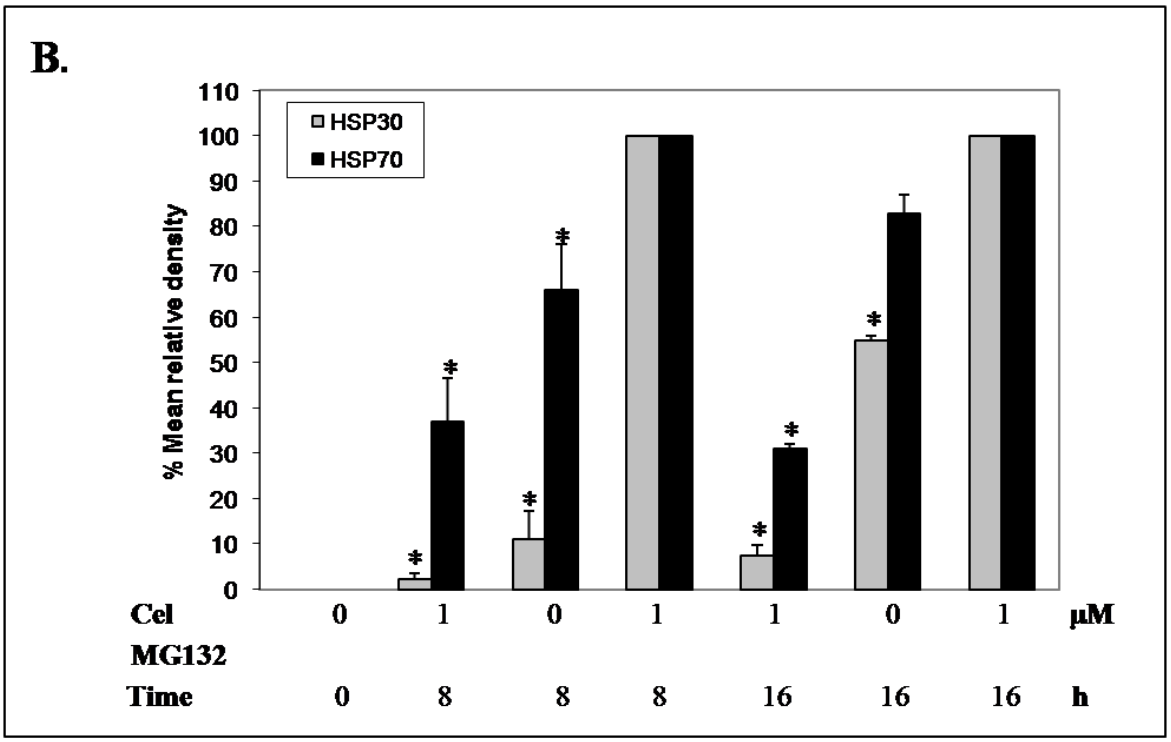
B.
% Mean relative density
HSP30
HSP70
110
100
90
80
70
60
50
40
30
20
10
0
Cel 0 1 0 1 1 0 1 µM
MG132
Time 0 8 8 8 16 16 16 h

Figure 19. Examination of the morphology of A6 cells treated with different concentrations of celastrol for 4 h. Cells were grown in tissue culture flasks or on base-washed glass coverslips at 22 ˚C in L-15 media containing FBS. A6 cells were then treated with 1, 2.5, or 5 µM celastrol for 4 h at 22 ˚C. Phase contrast microscopy was employed to examine the morphology of A6 cells exposed to celastrol for 4 h. Cells were then photographed using a Nikon coolpix 995 digital camera (400X final magnification) and compared to control cells maintained at 22 ˚C.

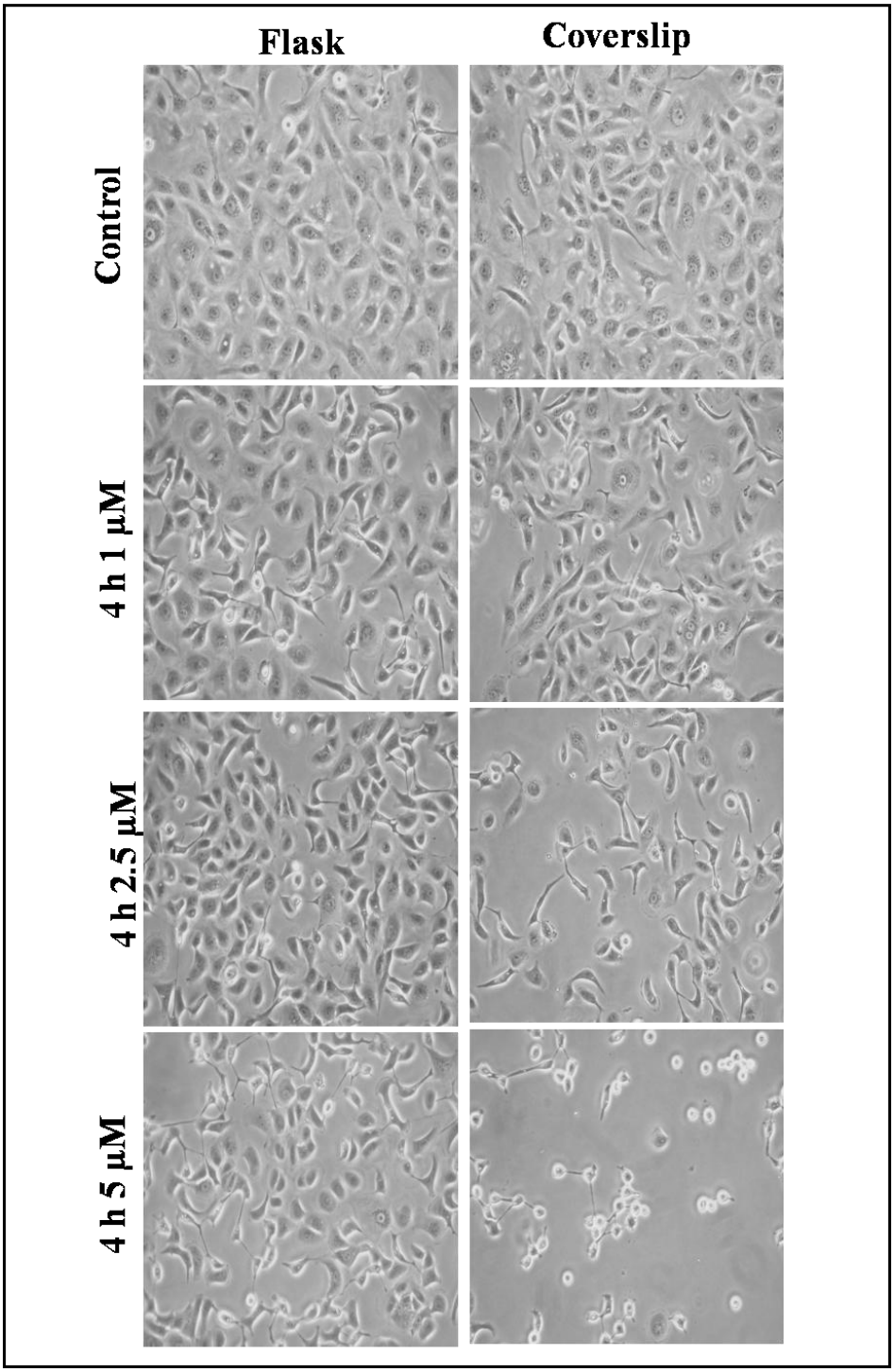
Flask
Coverslip
Control
4 h 1 µM
4 h 2.5 µM
4 h 5 µM

Figure 20. Examination of the morphology of A6 cells treated with different concentrations of celastrol for 8 h. A6 cells were cultured in tissue culture flasks or on base-washed glass coverslips at 22 ˚C in L-15 media containing FBS. Cells were then treated with 1, 2.5, or 5 µM celastrol for 8 h at 22 ˚C. Phase contrast microscopy was employed to examine A6 cell morphology following celastrol treatment. Cells were photographed using a Nikon coolpix 995 digital camera (400X final magnification) and compared to control cells maintained at 22 ˚C.

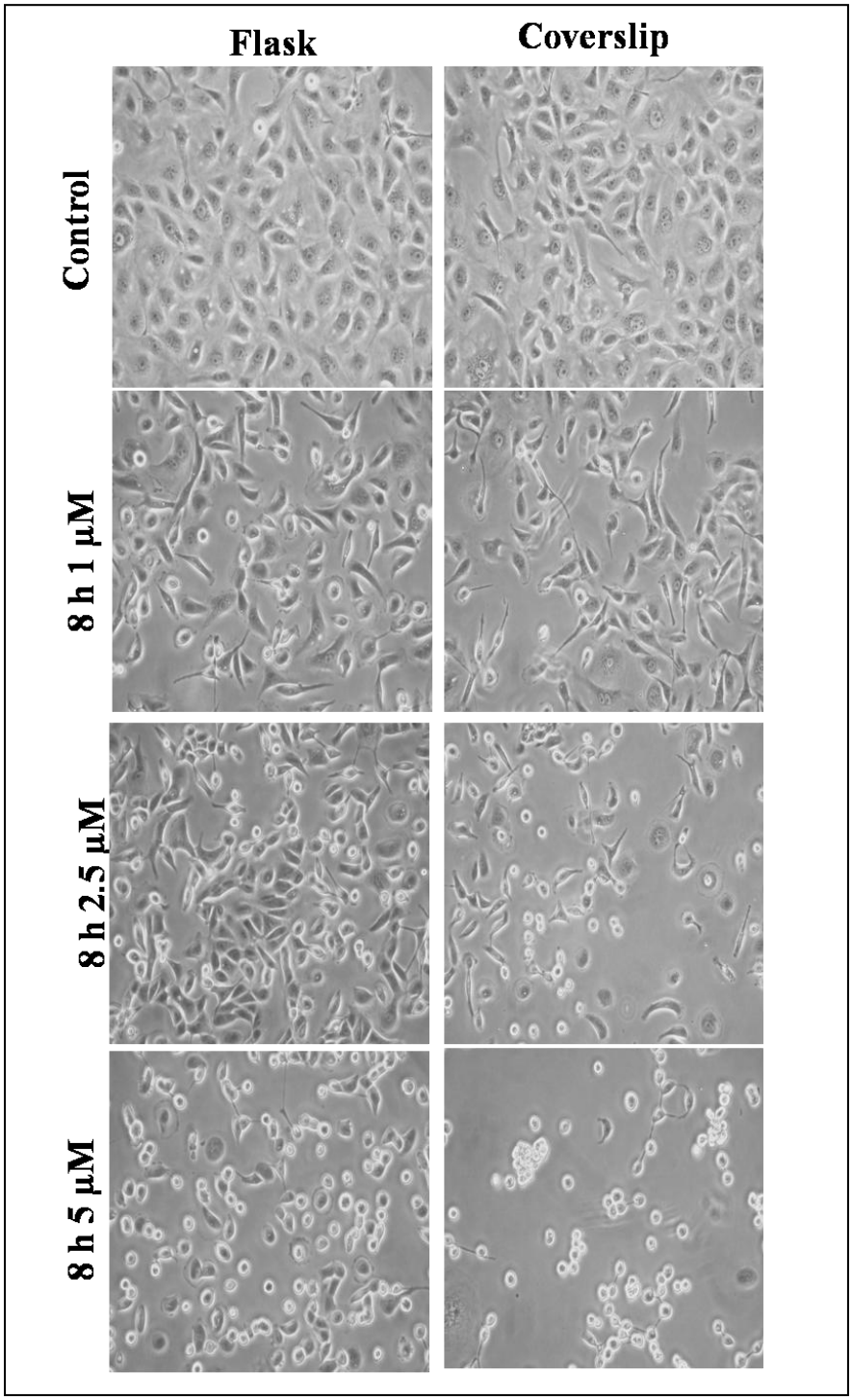
Flask
Coverslip
Control
8 h 1 µM
8 h 2.5 µM
8 h 5 µM

cells exposed to 2.5 or 5 µM celastrol for longer than 8 h (e.g. 12, 18 or 24 h) did not adhere to the coverslips after the fixation and protocol required for immunocytochemical analysis. Thus, subsequent experiments employed treatments of 1 or 2.5 µM celastrol for 4 or 8 h at 22 ˚C.

3.7 The localization of HSP30 in A6 cells treated with celastrol and MG132

As shown in Figure 21, preliminary experiments documented MG132-induced HSP30 localization in A6 cells. Cells incubated with 30 µM MG132 for 8 and 24 h, displayed levels of HSP30 accumulation primarily in the cytoplasm with some staining in the nucleus and no detectable levels in the nucleolus. While approximately 80 % of cells treated with MG132 for 8 h displayed detectable HSP30 accumulation, this value increased to 100 % in cells treated for 24 h. Relatively large circular HSP30 staining structures were observed in cells treated with MG132 for 8 h. In cells incubated for 8 h with MG132, a slight disorganization in actin cytoskeleton structure was observed. As shown in Figures 22 and 23, incubation with celastrol (1 µM and 2.5 µM) also resulted in the accumulation of HSP30 in the cytoplasm and nucleus but not in the nucleolus. In response to 1 µM celastrol, approximately 30 % and 35 % of A6 cells displayed HSP30 accumulation after 4 and 8 h, respectively. While HSP30 accumulation was detected in 45 % of cells treated with 2.5 µM celastrol for 4 h, the proportion of cells with HSP30 increased to 80 % after 8 h. Similar to the results found in cells treated with MG132, relatively large foci of HSP30 were detected within the cytoplasm of some cells treated with 1 and 2.5 µM celastrol for 8 and 4 h, respectively. Additionally, in comparison to

Figure 21. The effect of MG132 on the localization of HSP30 in A6 cells. Cells were grown on base-washed glass coverslips and either maintained at 22 ˚C or exposed to 30 μM MG132 for 8 or 24 h at 22 ˚C. Actin and nuclei were stained directly with phalloidin conjugated to TRITC (red) and DAPI (blue), respectively. HSP30 was indirectly detected with an anti-HSP30 antibody and a secondary antibody conjugated to Alexa-488 (green). The white arrows indicate large circular cytoplasmic foci of HSP30 observed in some cells treated with 30 μM MG132 for 8 h. The 10 μm white scale bars are indicated at the bottom right section of each panel. These data are representative of three separate experiments. It should be noted that colocalization of HSP30 with actin was not observed during confocal microscopy. However, the apparent colocalization in Figure 21 is an artifact of printing.

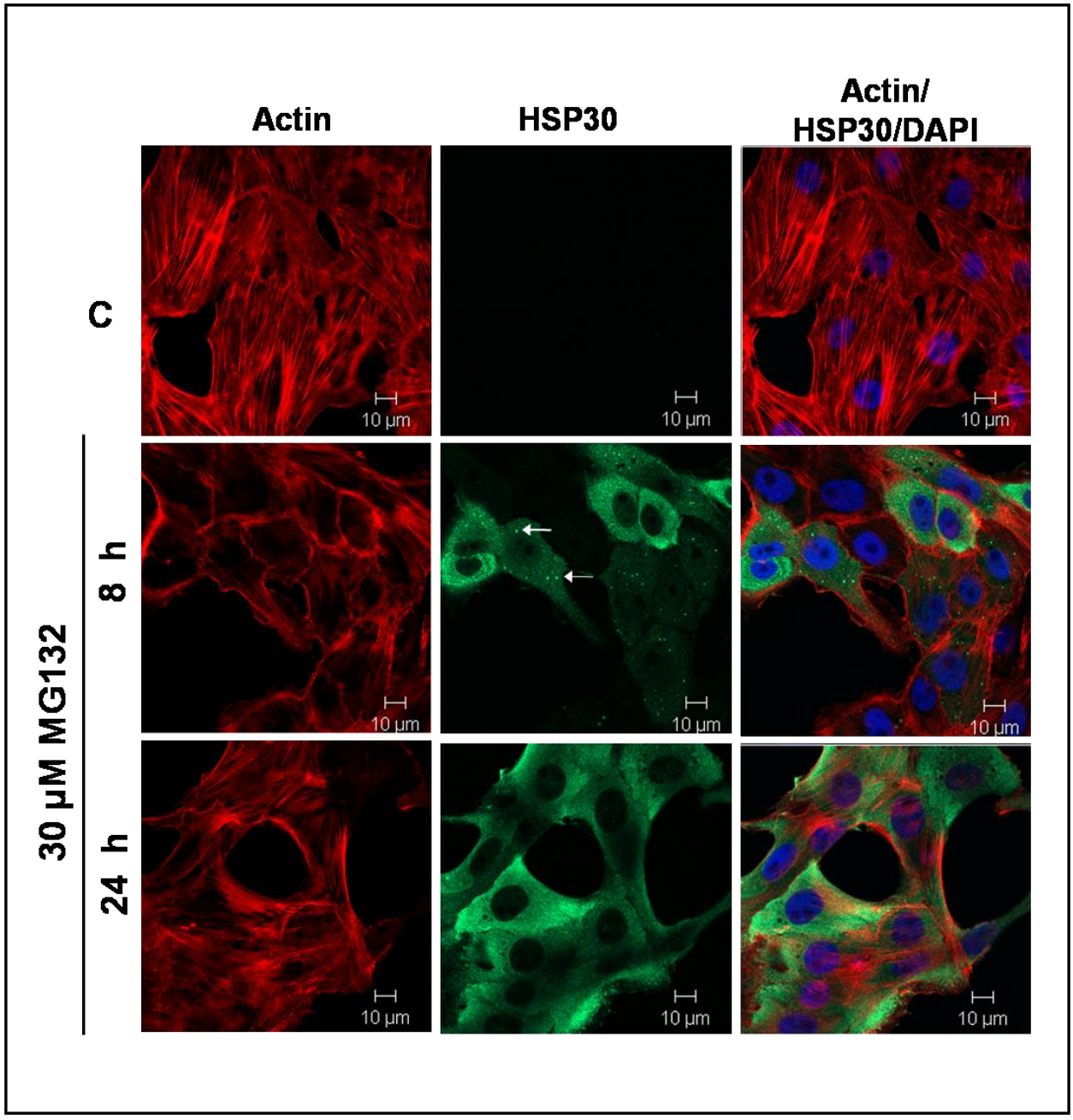
Actin
HSP30
Actin/
HSP30/DAPI
C
30 µM MG132
8 h
24 h
10 µm

Figure 22. The effect of 1 µM celastrol on the localization of HSP30 in A6 cells. Cells were cultured on base-washed glass coverslips and maintained at either 22 ˚C or incubated with 1 µM celastrol for 4 or 8 h at 22 ˚C. Actin and nuclei were stained directly with phalloidin conjugated to TRITC (red) and DAPI (blue), respectively. HSP30 was indirectly detected with an anti-HSP30 antibody and a secondary antibody conjugated to Alexa-488 (green). Large circular foci of HSP30 present in some cells treated with 1 µM celastrol for 8 h, are indicated by the white arrows. The 10 µm white scale bars are indicated at the bottom right section of each panel. These data are representative of five separate experiments.

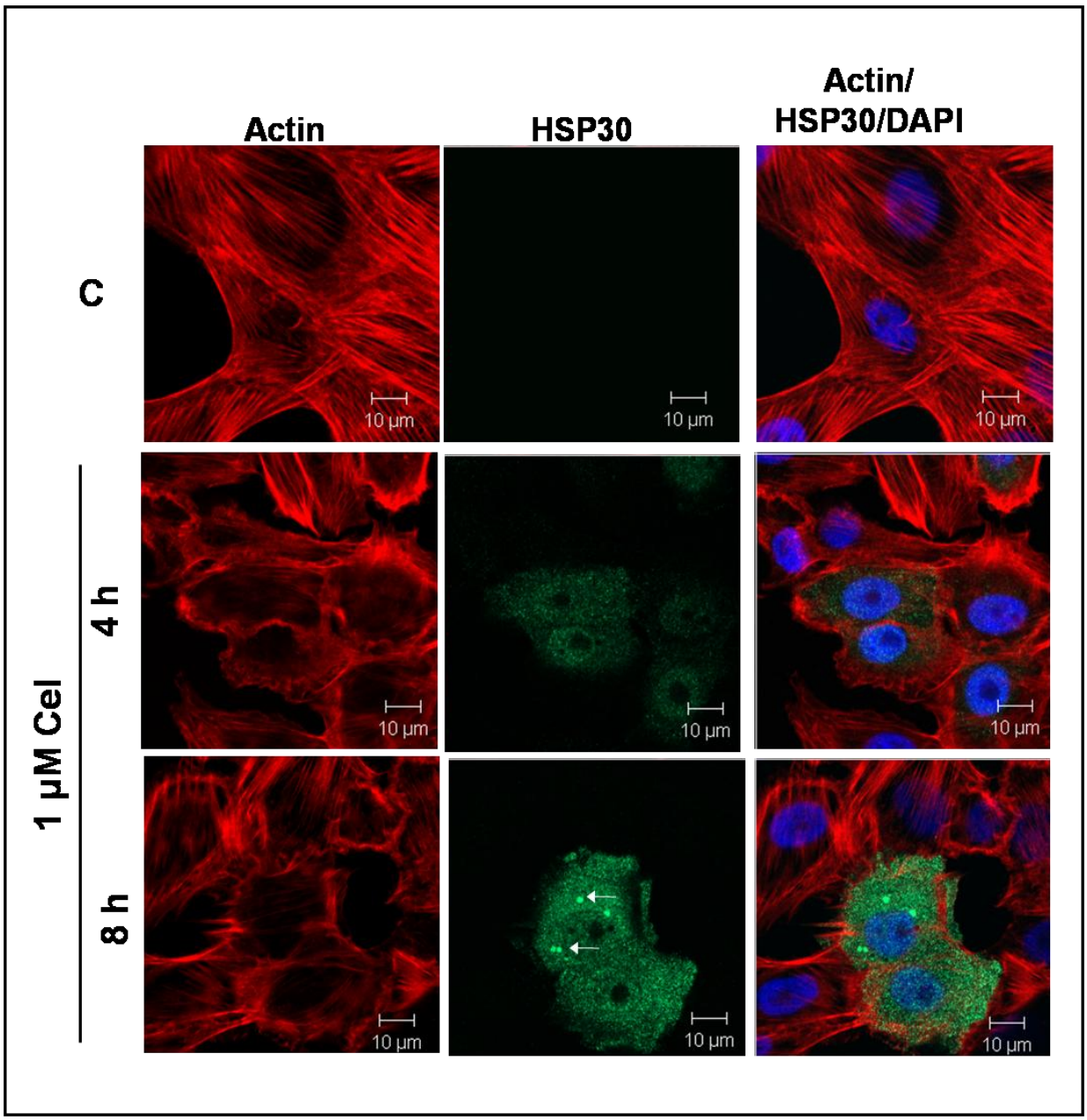
Actin
HSP30
Actin/
HSP30/DAPI
C
1 µM Cel
4 h
8 h
10 µm

Figure 23. The effect of 2.5 µM celastrol on the localization of HSP30. Cells were grown on base-washed glass coverslips and maintained at either 22 ˚C or treated with 2.5 µM celastrol for 4 or 8 h at 22 ˚C. Actin and nuclei were stained directly with phalloidin conjugated to TRITC (red) and DAPI (blue), respectively. HSP30 was indirectly detected with an anti-HSP30 antibody and a secondary antibody conjugated to Alexa-488 (green). The white arrows indicate large circular cytoplasmic foci of HSP30 observed in some cells treated with 2.5 µM celastrol for 4 h. The 10 µm white scale bars are indicated at the bottom right section of each panel. These data are representative of five separate experiments. It should be noted that colocalization of HSP30 with actin was not observed during confocal microscopy. However, the apparent colocalization in Figure 23 is an artifact of printing.

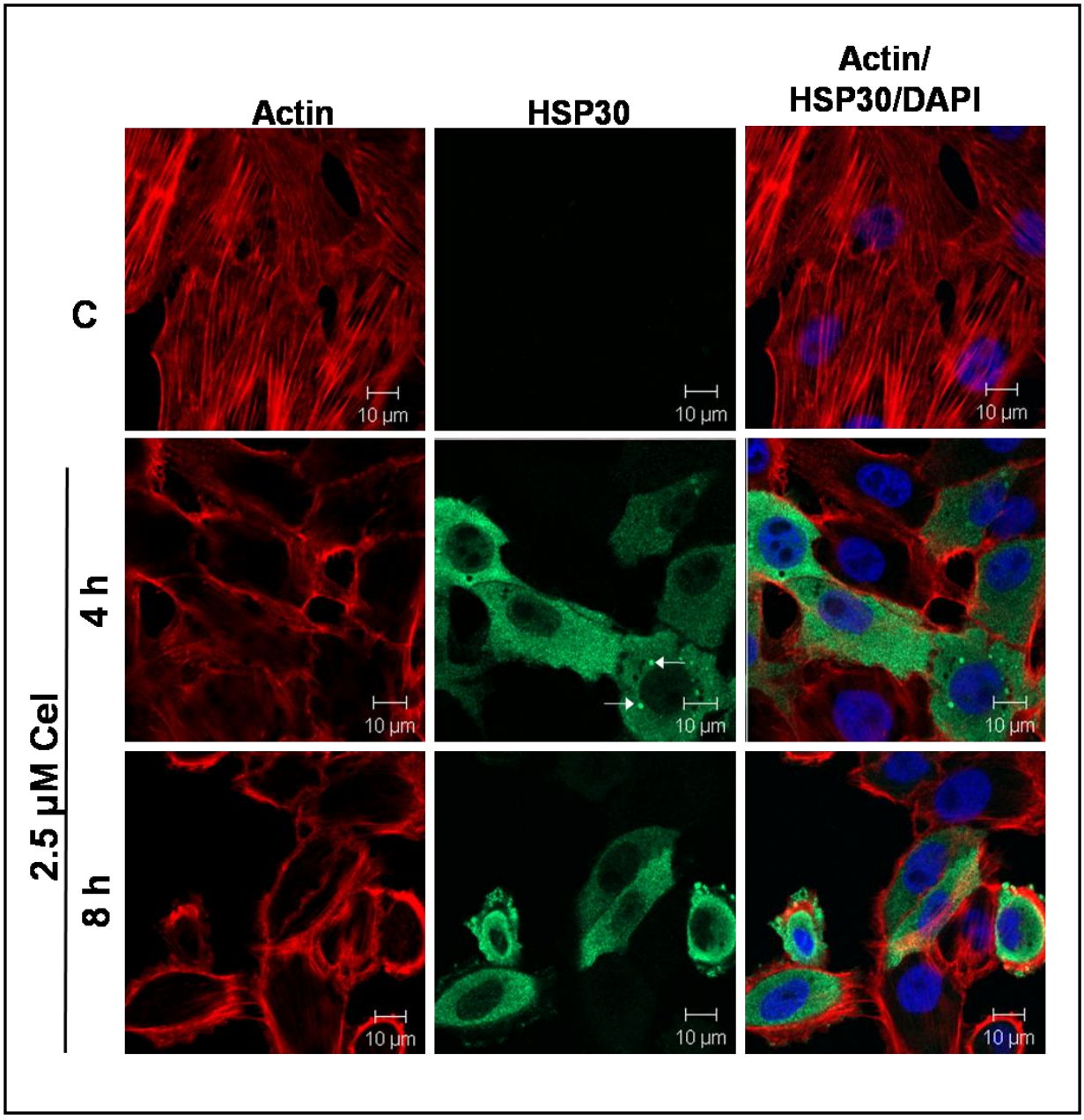
Actin
HSP30
Actin/
HSP30/DAPI
C
2.5 µM Cel
4 h
8 h
10 µm

control cells, treatment with celastrol produced changes to the general morphology and F-actin organization in A6 cells. For example, cells incubated with celastrol were rounder in shape and displayed some disorganization in the cytoskeleton with a loss of control-like stress fibers and staining of actin primarily at the periphery of some cells.

4 Discussion

The present study has shown that celastrol inhibited proteasomal activity and induced *hsp30* and *hsp70* gene expression in *Xenopus laevis* A6 kidney epithelial cells. Initial studies demonstrated that exposure of A6 cells to celastrol enhanced the relative levels of ubiquitinated protein. These results were comparable to MG132-induced ubiquitinated protein accumulation presented in this study and previously in our laboratory (Young and Heikkila, 2009). Additionally, *Xenopus* A6 cells treated with 2.5 μM celastrol exhibited a 58 % to 78 % decrease in chymotrypsin-like activity. Taken together the celastrol-induced increase in the accumulation of ubiquitinated proteins and decreased chymotrypsin-like activity in A6 cells, is an indicator of proteasomal inhibition as reported previously in other systems (Yang et al., 2006; Dai et al., 2009). In comparison to A6 cells, similar results were obtained in mammalian cells, since celastrol increased protein ubiquitination in a dose-dependent manner and inhibited chymotrypsin-like activity by 55 % in human prostate cancer cells (PC-3 and LNCaP) (Yang et al., 2006). In *Xenopus laevis* A6 cells, like other eukaryotic systems, the ubiquitin-proteasome system (UPS) is the primary degradation pathway for misfolded or damaged proteins (Lee and Goldberg, 1998b; Malik et al., 2001). Previous studies have demonstrated that proteasome inhibition results in the accumulation of ubiquitinated cellular proteins targeted for degradation within the cytosol (Bush et al., 1997; Lee and

Goldberg, 1998b; Malik et al., 2001; Liao et al., 2006). Since misfolded proteins possess exposed hydrophobic amino acid residues, increased concentrations of these non-native proteins by means of proteasomal inhibition can result in aggregate formation, which is detrimental to cell function (Hartl, 1996; Lee and Goldberg, 1998b; Hartl and Hayer-Hartl, 2009).

As mentioned above, treatment of *X. laevis* A6 cells with celastrol resulted in the accumulation of *hsp30* and *hsp70* mRNA as well as HSP30 and HSP70 protein. In these experiments, celastrol had no detectable effect on actin levels. These findings are in agreement with previous studies in our laboratory, which demonstrated that proteasome inhibition by MG132 induced *hsp* gene expression in A6 cells (Young and Heikkila, 2009). Previously, the effects of celastrol on *hsp* gene expression were also examined in yeast, mouse and human systems (Westerheide et al., 2004; Cleren et al., 2005; Chow and Brown, 2007; Zhang and Sarge, 2007; Trott et al., 2008; Kalmar and Greensmith, 2009). For example, in HeLa cells, Westerheide et al. (2004) demonstrated that celastrol activated an *hsp70.1* promoter-luciferase reporter gene and induced HSP70 accumulation to levels that were comparable to heat shock. Also, in human neuronal cell lines, celastrol induced increased levels of HSP27, HSP32, HSP70 and HSP70B (Chow and Brown, 2007), while *in vivo* celastrol injections induced increased levels of HSP70 in the striatum of rat models of Huntington's disease and the substantia nigra of mouse models of Parkinson's disease (Cleren et al., 2005).

In *Xenopus*, the stress-induced expression of *hsp* genes is mediated by HSF1 DNA-binding activity (Heikkila, 2003; Voellmy, 2004). Although, the mechanism by which HSF1 is activated is unknown, it is thought that this process is triggered by the

accumulation of misfolded or damaged proteins in the cytosol (Morimoto and Santoro, 1998; Voellmy, 2004; Morimoto, 2008). The current study determined that pretreatment of A6 cells with the HSF1 inhibitor, KNK437, prior to the application of celastrol repressed the accumulation of both HSP30 and HSP70. This suggested that celastrol-induced *hsp* gene expression in *Xenopus* A6 cells was likely controlled, at least in part, at the level of transcription through the activation of HSF1 DNA-binding. These results are in agreement with previous studies in *Xenopus*, demonstrating that pretreatment with KNK437, inhibited heat shock, chemical stress, and MG132-induced *hsp* gene expression (Manwell and Heikkila, 2007; Voyer and Heikkila, 2008; Young and Heikkila, 2009). Additionally, previous studies have investigated the effect of celastrol on HSF1 activity in yeast and mammalian cells (Westerheide et al., 2004; Trott et al., 2008). In yeast, Trott et al. (2008) determined that celastrol activated an *hsp70* promoter-LacZ reporter gene, by inducing HSF1 DNA-binding activity. Furthermore, in HeLa cells expressing an *hsp70.1* promoter reporter construct, studies using gel shift analysis demonstrated that celastrol caused hyperphosphorylation of HSF1. Subsequent chromatin immunoprecipitation *in vivo* experiments verified that celastrol induced HSF1 DNA-binding activity to the endogenonous *hsp70.1* promoter (Westerheide et al., 2004).

In time course experiments with A6 cells exposed to 2.5 µM celastrol, levels of HSP70 and HSP30 were first detectable in cells after 2 and 6 h, respectively. While maximal levels were noted after 18 h. In contrast, continuous exposure of A6 cells to heat shock induced detectable levels of HSP30 and HSP70 after 1 h and maximal levels of HSP accumulation were observed after 2 h (Darasch et al., 1988). Reasons for the different temporal patterns of HSP accumulation in A6 cells subjected to heat shock and

celastrol are unknown. It is possible that the delay in maximal HSP accumulation in A6 cells treated with celastrol may be due to the time required for celastrol entry into the cell and the time required to increase the non-native protein levels that will activate HSF1 DNA-binding activity. In support of this possibility a delayed accumulation of HSPs compared to heat shock was observed in A6 cells subjected to sodium arsenite, cadmium chloride, MG132, or herbymicin A (Darasch et al., 1988; Ohan et al., 1998; Gauley and Heikkila, 2006; Woolfson and Heikkila, 2009; Young and Heikkila, 2009) For example, MG132-treated A6 cells displayed levels of HSP70 and HSP30 after 4 and 8 h, respectively with maximal HSP accumulation occurring after 24 h (Young and Heikkila, 2009). Also, in A6 cells exposed to cadmium chloride, HSP30 and HSP70 were detectable after 5 and 8 h, respectively, with maximal levels of HSPs occurring after 16 h (Woolfson and Heikkila, 2009).

The present study also investigated the pattern of HSP accumulation in *Xenopus* A6 cells recovering from celastrol treatment. Relative levels of HSP30 and HSP70 accumulation remained elevated for 18-24 h after the removal of celastrol. These findings were similar to results described in A6 cells recovering from MG132, in which the relative levels of HSP30 and HSP70 remained elevated for up to 24 h (Young and Heikkila, 2009). Additionally, a prolonged accumulation of HSPs was reported in Chinese hamster ovary cells recovering from proteasomal inhibition (Kovacs et al., 2006). The prolonged accumulation of HSPs in A6 cells recovering from celastrol may be due to continued *hsp* gene transcription or an increase in *hsp* mRNA or HSP stability, as suggested previously for sodium arsenite (Darasch et al., 1988). Nevertheless, it is likely that elevated levels of HSPs are beneficial to celastrol-treated cells since relatively high

concentrations of ubiquitinated cellular proteins that accumulate within the cytosol may require an extended amount of time to re-establish protein homeostasis by degradation (Bush et al., 1997; Lee and Goldberg, 1998b; Liao et al., 2006).

In *X. laevis* A6 cells, concurrent treatment with both mild heat shock and celastrol, induced elevated levels of HSP30 and HSP70 accumulation. In fact, the relative levels of HSP30 displayed in cells treated with both stressors were greater than the sum of the values found with each stressor individually. In comparison to individual treatments, an increased amount of HSP70 accumulation was observed in A6 cells treated concurrently with both stressors for 4 h. However, the relative levels of HSP70 accumulation displayed in cells exposed to both celastrol and mild heat shock for 8 h were not substantially different from those resulting from celastrol alone. Similarly, increased levels of HSP30 and HSP70 accumulation were observed in *Xenopus* A6 cells treated concurrently with 30 μM MG132 and mild heat shock temperatures ranging from 24-30 ˚C (Young and Heikkila, 2009). Additionally, our laboratory reported an increase in *hsp* gene expression in A6 cells when a mild heat shock was combined with low concentrations of cadmium chloride, sodium arsenite, herbimycin A or hydrogen peroxide (Heikkila et al., 1987; Briant et al., 1997; Muller et al., 2004; Woolfson and Heikkila, 2009). The mechanism responsible for increased levels of HSP30 and HSP70 in A6 cells concurrently exposed to celastrol and mild heat shock is unknown. As mentioned previously, celastrol can induce an increase in the relative levels of ubiquitinated protein destined for degradation by inhibiting the proteasome. Additionally, heat shock can induce a generalized unfolding of intracellular proteins. Thus, it is

possible in A6 cells, that a mild heat shock and celastrol treatment in combination will elevate the total level of non-native protein to a threshold level required for HSF1 activation. Evidence supporting the existence of a threshold level for HSF1 activation has been described in a number of systems including mouse T-lymphocytes and testis, intertidal mussels, HeLa cells and *Xenopus* (Sarge, 1995; Lee et al., 1995; Ali et al., 1997; Buckley et al., 2001; Gothard et al., 2003).

The current study also investigated the combined effects of the proteasome inhibitors, celastrol and MG132 on *hsp* gene expression in *Xenopus* A6 cells. Similar to results observed with mild heat shock and celastrol, treatment with low concentrations of celastrol (1 µM) and MG132 (5 µM or 10 µM) resulted in enhanced levels of HSP30 to values higher than the sum of those produced by each stressor individually. Also, levels of HSP70 accumulation were increased in A6 cells exposed to both celastrol and MG132 simultaneously, but were not substantially higher than those observed in cells exposed to MG132 alone. Therefore, the combined stresses of celastrol plus MG132 have a different effect on the pattern of HSP30 and HSP70 accumulation in A6 cells. Previously, our laboratory reported different accumulation patterns of HSP30, HSP70, and HSP110 in *Xenopus* cultured cells treated with sodium arsenite (Gauley et al., 2008). For example, while enhanced levels of HSP70 and HSP110 were observed in A6 cells treated with 10 µM sodium arsenite, increased HSP30 accumulation was first detected in cells incubated with 25 µM concentrations (Gauley et al., 2008). Although, the mechanism responsible for the different levels of HSP30 and HSP70 in A6 cells exposed to combined celastrol

treatment is not known, this phenomenon may reflect specific physiological roles for each HSP during proteasome inhibition.

The effect of celastrol on A6 cell morphology was also examined using phase-contrast microscopy. Treatment with celastrol modified A6 cell structure in a dose- and time-dependent manner. Control cells displayed an elongated morphology and formed a confluent monolayer adherent to the surface of tissue culture flasks and coverslips. In contrast, A6 cells exposed to celastrol exhibited reduced adherence, cytoplasmic retraction, and a rounder cell shape. The effects of celastrol on cellular morphology have been described previously in mammalian cells (Yang et al., 2006; Chow and Brown, 2007). For example, cell shrinkage and rounder cell bodies were observed in human and rodent neuronal cells treated with celastrol (Chow and Brown, 2007). The morphological properties of A6 cells recovering from celastrol were also examined during this study. Compared to the round appearance of cells incubated with celastrol for 18 h, after 4 days of recovery A6 cells were confluent and displayed control-like morphology. The molecular pathway responsible for celastrol-induced morphological changes in A6 cells is unknown. However, reduced NF-kβ activity has been linked to decreased levels of various cell adhesion molecules (CAMs) required for proper attachment of the cytoskeleton to the extra cellular matrix (ECM) including E-selectin, ICAM-I and VCAM-I (Collins et al., 1995; Tozawa et al., 1995; Collins and Cybulsky, 2001). Furthermore, celastrol- mediated inhibition of NF-kβ, has been reported in mammalian cancer cell lines (Lee et al., 2006; Kim et al., 2009; He et al., 2009). Thus, suppression of

NF-kβ activity caused by decreased proteasome function may play a role in the round morphology and reduced adherence of A6 cells exposed to celastrol.

Immunocytochemistry and LSCM were employed to examine the localization of HSP30 in *X. laevis* A6 cells treated with celastrol or MG132. Cells exposed to these stressors displayed HSP30 accumulation primarily in the cytoplasm in a punctate pattern with some staining in the nucleus. The punctate pattern of HSP30 accumulation may represent the stress-induced formation of HSP30 multimeric structures that are required for sHSP function (Ohan et al., 1998; MacRae, 2000; Van Montfort et al., 2001). Additionally, relatively large HSP30 staining foci were detected in some *X. laevis* A6 cells incubated with celastrol or MG132. Similar structures were reported in A6 cells exposed to cadmium chloride, sodium arsenite or MG132 (Voyer and Heikkila, 2008; Woolfson and Heikkila, 2009; Young and Heikkila, 2009). Although the identity of these large structures is unknown, it has been suggested that they are inclusion bodies containing HSP30 bound to unfolded proteins and may be associated with the molecular chaperone function of HSP30 (Fernando and Heikkila, 2000; Heikkila, 2003; Heikkila, 2004; Young and Heikkila, 2009). In support of this concept, previous studies have determined that proteasome inhibition significantly increased the formation of cytosolic aggresomes that are composed of smaller protein aggregates also known as inclusion bodies (Garcia-Mata, 1999). Results previously described with MG132, determined that these foci occurred in response to high concentrations of MG132 (Young and Heikkila, 2009). In contrast, A6 cells treated with relatively low concentrations of celastrol for 8 h also displayed HSP30 staining foci. Lastly, the current study determined that treatment of

A6 cells with celastrol disrupted the actin cytoskeleton with most cells displaying a rounder morphology compared to control cells. It was also noted that treatment with higher concentrations of celastrol caused a collapse in the cytoskeleton with actin staining primarily in the periphery of A6 cells. As mentioned previously, this may be related to celastrol-mediated inhibition of the NF-kβ signalling pathway (Collin et al., 1995; Tozawa et al., 1995; Collins and Cybulsky, 2001).

In summary, the present study has shown for the first time in an amphibian system, that the proteasome inhibitor, celastrol, induced *hsp30* and *hsp70* gene expression, increased the accumulation of ubiquitinated proteins, inhibited chymotrypsin-like activity and disrupted the actin cytoskeleton. Understanding the effect that celastrol has on *Xenopus hsp* gene expression is of importance given the potential therapeutic role for HSPs in various human diseases. This study leaves some unanswered questions about the effects of celastrol on *hsp* gene expression. Therefore, further analysis on the relationship between celastrol-induced proteasome inhibition and the accumulation of HSPs is required. Future studies should examine the effect of celastrol on other *Xenopus hsp* genes such as *BiP, hsp47* and *hsp90*. Mammalian studies have suggested that proteasome inhibition may have an impact on molecular chaperones in the endoplasmic reticulum and HSP90 (Bush et al., 1997; Banerji, 2009) Also, the effect of proteasome inhibition on *hsp* gene expression during animal development has not been investigated. Given the advantages of the *Xenopus* embryonic system including microinjections and transgenic methodology, future experiments should examine the effects of celastrol on *hsp* gene expression during early development. Future research should also investigate

whether celastrol-induced HSP accumulation can have a cytoprotective effect in A6 cells subjected to a thermal challenge. Recently, the acquisition of thermotolerance was reported following proteasomal inhibition by celastrol in mammals and by MG132 in A6 cells (Westerheide et al., 2004;Young and Heikkila, 2009). Previous studies have also shown that celastrol can induce apoptosis through inhibition of the NF-kβ signalling pathway (Lee et al., 2006; Idris et al., 2009; He et al., 2009). Therefore, the potential induction of apoptosis in celastrol-treated *Xenopus* A6 cells and embryos should also be investigated.

References

Abdulle R, Mohindra A, Fernando P, Heikkila JJ. 2002. *Xenopus* small heat shock proteins, HSP30C and HSP30D, maintain heat- and chemically denatured luciferase in a folding-competent state. *Cell Stress Chaperones*. 7:6-16.

Ali A, Fernando P, Smith WL, Ovsenek N, Lepock JR, Heikkila JJ. 1997. Preferential activation of HSF-binding activity and *hsp70* gene expression in *Xenopus* heart after mild hyperthermia. *Cell Stress Chaperones.* 2:229-37.

Ali A, Heikkila JJ. 2002. Enhanced accumulation of constitutive heat shock protein mRNA is an initial response of eye tissue to mild hyperthermia in vivo in adult *Xenopus laevis*. *Can J Physiol Pharmacol.* 80:1119-23.

An B, Goldfarb RH, Siman R, Dou QP. 1998. Novel dipeptidyl proteasome inhibitors overcome bcl-2 protective function and selectively accumulate the cyclin-dependent kinase inhibitor p27 and induce apoptosis in transformed, but not normal, human fibroblasts. *Cell Death Differ.* 5:1062-75.

Anckar J, Hietakangas V, Denessiouk K, Thiele DJ, Johnson MS, Sistonen L. 2006. Inhibition of DNA binding by differential sumoylation of heat shock factors. Mol *Cell Biol.* 26:955-64.

Arrigo AP. 1998. Small stress proteins: Chaperones that act as regulators of intracellular redox state and programmed cell death. *Biol Chem.* 379:19-26.

Balch WE, Morimoto RI, Dillin A, Kelly JW. 2008. Adapting proteostasis for disease intervention. *Science.* 319:916-9.

Baldwin AS. 2001. Control of oncogenesis and cancer therapy resistance by the transcription factor NF-kappaB. *J Clin Invest.* 107:241-6.

Banerji U. 2009. Heat shock protein 90 as a drug target: Some like it hot. *Clin Cancer Res*. 15:9-14.

Baumeister W, Walz J, Zuhl F, Seemuller E. 1998. The proteasome: Paradigm of a self-compartmentalizing protease. *Cell*. 92:367-80.

Bharadwaj S, Ali A, Ovsenek N. 1999. Multiple components of the HSP90 chaperone complex function in regulation of heat shock factor 1 in vivo. *Mol Cell Biol.* 19:8033-41.

Bienz M. 1984. *Xenopus hsp70* genes are constitutively expressed in injected oocytes. *EMBO J.* 3:2477-83.

Birnbaum G, Kotilinek L. 1997. Heat shock or stress proteins and their role as autoantigens in multiple sclerosis. *Ann N Y Acad Sci*. 835:157-67.

Biswas DK , Iglehart JD. 2006. Linkage between EGFR family receptors and nuclear factor kappaB (NF-kappaB) signaling in breast cancer. *J Cell Physiol.* 209:645-52.

Briant D, Ohan N, Heikkila JJ. 1997. Effect of herbimycin A on *hsp30* and *hsp70* heat shock protein gene expression in *Xenopus* cultured cells. *Biochem Cell Biol*. 75:777-82.

Bruce JL, Price BD, Coleman CN, Calderwood SK. 1993. Oxidative injury rapidly activates the heat shock transcription factor but fails to increase levels of heat shock proteins. *Cancer Res*. 53:12-5.

Buckley BA, Owen ME, Hofmann GE. 2001. Adjusting the thermostat: The threshold induction temperature for the heat-shock response in intertidal mussels (G*enus mytilus*) changes as a function of thermal history. *J Exp Biol* . 204:3571-9.

Burggren WW, Warburton S. 2007. Amphibians as animal models for laboratory research in physiology. *ILAR J*. 48:260-9.

Bush KT, Goldberg AL, Nigam SK. 1997. Proteasome inhibition leads to a heat-shock response, induction of endoplasmic reticulum chaperones, and thermotolerance. *J Biol Chem.* 272:9086-92.

Chang FR, Hayashi K, Chen IH, Liaw CC, Bastow KF, Nakanishi Y, Nozaki H, Cragg GM, Wu YC, Lee KH. 2003. Antitumor agents. 228. five new agarofurans, reissantins A-E, and cytotoxic principles from *Reissantia buchananii*. *J Nat Prod.* 66:1416-20.

Chow AM, Brown IR. 2007. Induction of heat shock proteins in differentiated human and rodent neurons by celastrol. *Cell Stress Chaperones.* 12:237-44.

Christians E, Davis AA, Thomas SD, Benjamin IJ. 2000. Maternal effect of HSF1 on reproductive success. *Nature*. 407:693-4.

Clark JI, Muchowski PJ. 2000. Small heat-shock proteins and their potential role in human disease. *Curr Opin Struct Biol.* 10:52-9.

Cleren C, Calingasan NY, Chen J, Beal MF. 2005. Celastrol protects against MPTP- and 3-nitropropionic acid-induced neurotoxicity. *J Neurochem.* 94:995-1004.

Collins T and Cybulsky MI. 2001. NF-kappaB: Pivotal mediator or innocent bystander in atherogenesis? *J Clin Invest*. 107:255-64.

Collins T, Read MA, Neish AS, Whitley MZ, Thanos D, Maniatis T. 1995. Transcriptional regulation of endothelial cell adhesion molecules: NF-kappa B and cytokine-inducible enhancers. *FASEB J.* 9:899-909.

Dai Y, DeSano JT, Meng Y, Ji Q, Ljungman M, Lawrence TS, Xu L. 2009. Celastrol potentiates radiotherapy by impairment of DNA damage processing in human prostate cancer. Int J Radiat *Oncol Biol Phys.* 74:1217-25.

Darasch S, Mosser DD, Bols NC, Heikkila JJ. 1988. Heat shock gene expression in *Xenopus laevis* A6 cells in response to heat shock and sodium arsenite treatments. *Biochem Cell Biol.* 66:862-868.

Daugaard M, Rohde M, Jaattela M. 2007. The heat shock protein 70 family: Highly homologous proteins with overlapping and distinct functions. *FEBS Lett*. 581:3702-10.

Drexler HC, Risau W, Konerding MA. 2000. Inhibition of proteasome function induces programmed cell death in proliferating endothelial cells. *FASEB J*.14:65-77.

Fenteany G, Standaert RF, Lane WS, Choi S, Corey EJ, Schreiber SL. 1995. Inhibition of proteasome activities and subunit-specific amino-terminal threonine modification by lactacystin. *Science*. 268:726-31.

Fernando P and Heikkila JJ. 2000. Functional characterization of *Xenopus* small heat shock protein, HSP30C: The carboxyl end is required for stability and chaperone activity. *Cell Stress Chaperones*. 5:148-59.

Fernando P, Megeney LA, Heikkila JJ. 2003. Phosphorylation-dependent structural alterations in the small HSP30 chaperone are associated with cellular recovery. Exp *Cell Res.* 286:175-85.

Fernando P, Abdulle R, Mohindra A, Guillemette JG, Heikkila JJ. 2002. Mutation or deletion of the C-terminal tail affects the function and structure of *Xenopus laevis* small heat shock protein, HSP30. *Comp Biochem Physiol B Biochem Mol Biol.* 133:95-103.

Fujikake N, Nagai Y, Popiel HA, Okamoto Y, Yamaguchi M, Toda T. 2008. Heat shock transcription factor 1-activating compounds suppress polyglutamine-induced neurodegeneration through induction of multiple molecular chaperones. *J Biol Chem.* 283:26188-97.

Garcia-Mata R, Bebok Z, Sorscher EJ, Sztul ES. 1999. Characterization and dynamics of aggresome formation by a cytosolic GFP-chimera. *J Cell Biol*. 146:1239-54.

Gauley J, Heikkila JJ. 2006. Examination of the expression of the heat shock protein gene, *hsp110*, in *Xenopus laevis* cultured cells and embryos. Comp Biochem Physiol *A Mol Integr Physiol.* 145:225-34.

Gauley J, Young JT, Heikkila JJ. 2008. Intracellular localization of the heat shock protein, HSP110, in *Xenopus laevis* A6 kidney epithelial cells. *Comp Biochem Physiol A Mol Integr Physiol.* 151:133-8.

Gellalchew M, Heikkila JJ. 2005. Intracellular localization of *Xenopus* small heat shock protein, HSP30, in A6 kidney epithelial cells. *Cell Biol Int.* 29:221-7.

Ghosh S, May MJ, Kopp EB. 1998. NF-kappa B and rel proteins: Evolutionarily conserved mediators of immune responses. *Annu Rev Immunol.* 16:225-60.

Goldfarb SB, Kashlan OB, Watkins JN, Suaud L, Yan W, Kleyman TR, Rubenstein RC. 2006. Differential effects of HSC70 and HSP70 on the intracellular trafficking and functional expression of epithelial sodium channels. *Proc Natl Acad Sci U S A.* 103:5817-22.

Gothard LQ, Ruffner ME, Woodward JG, Park-Sarge OK, Sarge KD. 2003. Lowered temperature set point for activation of the cellular stress response in T-lymphocytes. *J Biol Chem.* 278:9322-6.

Groll M, Ditzel L, Lowe J, Stock D, Bochtler M, Bartunik HD, Huber R. 1997. Structure of 20S proteasome from yeast at 2.4 A resolution. *Nature.* 386:463-71.

Hair A, Prioleau MN, Vassetzky Y, Mechali M. 1998. Control of gene expression in *Xenopus* early development. *Dev Genet.* 22:122-31.

Hartl FU. 1996. Molecular chaperones in cellular protein folding. *Nature*. 381:571-9.

Hartl FU, Hayer-Hartl M. 2009. Converging concepts of protein folding *in vitro* and *in vivo*. *Nat Struct Mol Biol.* 16:574-81.

He D, Xu Q, Yan M, Zhang P, Zhou X, Zhang Z, Duan W, Zhong L, Ye D, Chen W. 2009. The NF-kappa B inhibitor, celastrol, could enhance the anti-cancer effect of gambogic acid on oral squamous cell carcinoma. *BMC Cancer.* 9:343.

Heikkila JJ. 2004. Regulation and function of small heat shock protein genes during amphibian development. *J Cell Biochem.* 93:672-80.

Heikkila JJ. 2003. Expression and function of small heat shock protein genes during *Xenopus* development. *Semin Cell Dev Biol.* 14:259-66.

Heikkila JJ, Kaldis A, Morrow G, Tanguay RM. 2007. The use of the *Xenopus* oocyte as a model system to analyze the expression and function of eukaryotic heat shock proteins. *Biotechnol Adv.* 25:385-95.

Heikkila JJ, Ohan N, Tam Y, Ali A. 1997. Heat shock protein gene expression during *Xenopus* development. *Cell Mol Life.* Sci 53:114-21.

Heikkila JJ, Darasch SP, Mosser DD, Bols NC. 1987. Heat and sodium arsenite act synergistically on the induction of heat shock gene expression in *Xenopus laevis* A6 cells. *Biochem Cell Biol.* 65:310-6.

Hershko A, Ciechanover A. 1998. The ubiquitin system. *Annu Rev Biochem.* 67:425-79.

Hietakangas V, Anckar J, Blomster HA, Fujimoto M, Palvimo JJ, Nakai A, Sistonen L. 2006. PDSM, a motif for phosphorylation-dependent SUMO modification. *Proc Natl Acad Sci U S A.* 103:45-50.

Holmberg CI, Tran SE, Eriksson JE, Sistonen L. 2002. Multisite phosphorylation provides sophisticated regulation of transcription factors. *Trends Biochem Sci.* 27:619-27.

Hong Y, Rogers R, Matunis MJ, Mayhew CN, Goodson ML, Park-Sarge OK, Sarge KD. 2001. Regulation of heat shock transcription factor 1 by stress-induced SUMO-1 modification. *J Biol Chem.* 276:40263-7.

Idris AI, Libouban H, Nyangoga H, Landao-Bassonga E, Chappard D, Ralston SH. 2009. Pharmacologic inhibitors of IkappaB kinase suppress growth and migration of mammary carcinosarcoma cells *in vitro* and prevent osteolytic bone metastasis *in vivo*. *Mol Cancer Ther.* 8:2339-47.

Jedlicka P, Mortin MA, Wu C. 1997. Multiple functions of drosophila heat shock transcription factor *in vivo*. *EMBO J.* 16:2452-62.

Jin HZ, Hwang BY, Kim HS, Lee JH, Kim YH, Lee JJ. 2002. Antiinflammatory constituents of *Celastrus orbiculatus* inhibit the NF-kappaB activation and NO production. *J Nat Prod.* 65:89-91.

Jolly C, Morimoto RI. 2000. Role of the heat shock response and molecular chaperones in oncogenesis and cell death. *J Natl Cancer Inst*. 92:1564-72.

Kakizuka A. 1998. Protein precipitation: A common etiology in neurodegenerative disorders? *Trends Genet.* 14:396-402.

Kallio M, Chang Y, Manuel M, Alastalo TP, Rallu M, Gitton Y, Pirkkala L, Loones MT, Paslaru L, Larney S, et al. 2002. Brain abnormalities, defective meiotic chromosome synapsis and female subfertility in HSF2 null mice. *EMBO J.* 21:2591-601.

Kalmar B, Greensmith L. 2009. Activation of the heat shock response in a primary cellular model of motoneuron neurodegeneration-evidence for neuroprotective and neurotoxic effects. *Cell Mol Biol Lett.* 14:319-35.

Katschinski DM. 2004. On heat and cells and proteins. *News Physiol.* Sci 19:11-5.

Kiaei M, Kipiani K, Petri S, Chen J, Calingasan NY, Beal MF. 2005. Celastrol blocks neuronal cell death and extends life in transgenic mouse model of amyotrophic lateral sclerosis. *Neurodegener Dis.* 2:246-54.

Kim DH, Shin EK, Kim YH, Lee BW, Jun JG, Park JH, Kim JK. 2009. Suppression of inflammatory responses by celastrol, a quinone methide triterpenoid isolated from *Celastrus regelii*. *Eur J Clin Invest.* 39:819-27.

Koegl M, Hoppe T, Schlenker S, Ulrich HD, Mayer TU, Jentsch S. 1999. A novel ubiquitination factor, E4, is involved in multiubiquitin chain assembly. *Cell*. 96:635-44.

Kovacs I, Lentini KM, Ingano LM, Kovacs DM. 2006. Presenilin 1 forms aggresomal deposits in response to heat shock. *J Mol Neurosci.* 29:9-19.

Krone PH, Snow A, Ali A, Pasternak JJ, Heikkila JJ. 1992. Comparison of regulatory and structural regions of the *Xenopus laevis* small heat-shock protein-encoding gene family. *Gene*. 110:159-66.

Lang L, Miskovic D, Lo M, Heikkila JJ. 2000. Stress-induced, tissue-specific enrichment of *hsp70* mRNA accumulation in *Xenopus laevis* embryos. *Cell Stress Chaperones.* 5:36-44.

Lang L, Miskovic D, Fernando P, Heikkila JJ. 1999. Spatial pattern of constitutive and heat shock-induced expression of the small heat shock protein gene family, *hsp30*, in *Xenopus laevis* tailbud embryos. *Dev Genet.* 25:365-74.

Lathia JD, Mattson MP, Cheng A. 2008. Notch: From neural development to neurological disorders. *J Neurochem.* 107:1471-81.

Lee, D.H., Goldberg, A.L. 1998a. Proteasome inhibitors: valuable new tools for cell biologists. *Trends in Cell Biology.* 8: 397-403.

Lee, D.H. , Goldberg, A.L. 1998b. Proteasome inhibitors cause induction of heatshock proteins and trehalose, which together confer thermotolerance in *Saccharomyces cerevisiae*. *Molecular and Cellular Biology.* 18: 30-38.

Lee BS, Chen J, Angelidis C, Jurivich DA, Morimoto RI. 1995. Pharmacological modulation of heat shock factor 1 by antiinflammatory drugs results in protection against stress-induced cellular damage. *Proc Natl Acad Sci U S A.* 92:7207-11.

Lee JH, Koo TH, Yoon H, Jung HS, Jin HZ, Lee K, Hong YS, Lee JJ. 2006. Inhibition of NF-kappa B activation through targeting I kappa B kinase by celastrol, a quinone methide triterpenoid. *Biochem Pharmacol.* 72:1311-21.

Lehman NL. 2009. The ubiquitin proteasome system in neuropathology. *Acta Neuropathol*. 118:329-47.

Leung CH, Grill SP, Lam W, Han QB, Sun HD, Cheng YC. 2005. Novel mechanism of inhibition of nuclear factor-kappa B DNA-binding activity by diterpenoids isolated from *Isodon rubescens*. *Mol Pharmacol.* 68:286-97.

Li B, Dou QP. 2000. Bax degradation by the ubiquitin/proteasome-dependent pathway: Involvement in tumor survival and progression. *Proc Natl Acad Sci U S A* . 97:3850-5.

Liao W, Li X, Mancini M, Chan L. 2006. Proteasome inhibition induces differential heat shock protein response but not unfolded protein response in HepG2 cells. *J Cell Biochem.* 99:1085-95.

MacRae TH. 2000. Structure and function of small heat shock/alpha-crystallin proteins: Established concepts and emerging ideas. *Cell Mol Life Sci*. 57:899-913.

Malik B, Schlanger L, Al-Khalili O, Bao HF, Yue G, Price SR, Mitch WE, Eaton DC. 2001. Enac degradation in A6 cells by the ubiquitin-proteosome proteolytic pathway. *J Biol Chem.* 276:12903-10.

Malusecka E, Zborek A, Krzyzowska-Gruca S, Krawczyk Z. 2001. Expression of heat shock proteins HSP70 and HSP27 in primary non-small cell lung carcinomas. an immunohistochemical study. *Anticancer Res.* 21:1015-21.

Manwell LA, Heikkila JJ. 2007. Examination of KNK437- and quercetin-mediated inhibition of heat shock-induced heat shock protein gene expression in *Xenopus laevis* cultured cells. *Comp Biochem Physiol A Mol Integr Physiol* .148:521-30.

Melendez K, Wallen ES, Edwards BS, Mobarak CD, Bear DG, Moseley PL. 2006. Heat shock protein 70 and glycoprotein 96 are differentially expressed on the surface of malignant and nonmalignant breast cells. *Cell Stress Chaperones.* 11:334-42.

Miskovic D, Heikkila JJ. 1999. Constitutive and stress-inducible expression of the endoplasmic reticulum heat shock protein 70 gene family member, immunoglobulin-binding protein (BiP), during *Xenopus laevis* early development. *Dev Genet.* 25:31-9.

Morimoto RI. 2008. Proteotoxic stress and inducible chaperone networks in neurodegenerative disease and aging. *Genes Dev.* 22:1427-38.

Morimoto RI. 1998. Regulation of the heat shock transcriptional response: Cross talk between a family of heat shock factors, molecular chaperones, and negative regulators. *Genes Dev.* 12:3788-96.

Morimoto RI, Santoro MG. 1998. Stress-inducible responses and heat shock proteins: New pharmacologic targets for cytoprotection. *Nat Biotechnol.* 16:833-8.

Muller M, Gauley J, Heikkila JJ. 2004. Hydrogen peroxide induces heat shock protein and proto-oncogene mRNA accumulation in *Xenopus laevis* A6 kidney epithelial cells. *Can J Physiol Pharmacol.* 82:523-9.

Mulligan-Tuttle A, Heikkila JJ. 2007. Expression of the small heat shock protein gene, *hsp30*, in *Rana catesbeiana* fibroblasts. *Comp Biochem Physiol A Mol Integr Physiol.* 148:308-16.

Nakai A. 1999. New aspects in the vertebrate heat shock factor system: HSF3 and HSF4. *Cell Stress Chaperones.* 4:86-93.

Nandi D, Tahiliani P, Kumar A, Chandu D. 2006. The ubiquitin-proteasome system. J *Biosci.* 31:137-55.

Nylandsted J, Brand K, Jaattela M. 2000. Heat shock protein 70 is required for the survival of cancer cells. *Ann N Y Acad Sci.* 926:122-5.

Ohan NW, Tam Y, Heikkila JJ. 1998. Heat-shock-induced assembly of HSP30 family members into high molecular weight aggregates in *Xenopus laevis* cultured cells. *Comp Biochem Physiol B Biochem Mol Biol.* 119:381-9.

Ohan NW, Tam Y, Fernando P, Heikkila JJ. 1998. Characterization of a novel group of basic small heat shock proteins in *Xenopus laevis* A6 kidney epithelial cells. *Biochem Cell Biol.* 76:665-71.

Orlowski RZ. 1999. The role of the ubiquitin-proteasome pathway in apoptosis. *Cell Death Differ.* 6:303-13.

Ostling P, Bjork JK, Roos-Mattjus P, Mezger V, Sistonen L. 2007. Heat shock factor 2 (HSF2) contributes to inducible expression of *hsp* genes through interplay with HSF1. *J Biol Chem.* 282:7077-86.

Parsell DA, Lindquist S. 1993. The function of heat-shock proteins in stress tolerance: Degradation and reactivation of damaged proteins. *Annu Rev Genet*. 27:437-96.

Paul C, Manero F, Gonin S, Kretz-Remy C, Virot S, Arrigo AP. 2002. HSP27 as a negative regulator of cytochrome C release. *Mol Cell Biol.* 22:816-34.

Phang D, Joyce EM, Heikkila JJ. 1999. Heat shock-induced acquisition of thermotolerance at the levels of cell survival and translation in *Xenopus* A6 kidney epithelial cells. *Biochem Cell Biol.* 77:141-51.

Pirkkala L, Nykanen P, Sistonen L. 2001. Roles of the heat shock transcription factors in regulation of the heat shock response and beyond. *FASEB J.* 15:1118-31.

Prahlad V and Morimoto RI. 2009. Integrating the stress response: Lessons for neurodegenerative diseases from C. elegans. *Trends Cell Biol.* 19:52-61.

Rafferty KA. 1968. Mass culture of amphibian cells: methods and observations concerning stability of cell type. In Biology of Amphibian Tumors (ed. M Mizzel), pp. 52-81. New York,NY, USA: Springer Verlag.

Rallu M, Loones M, Lallemand Y, Morimoto R, Morange M, Mezger V. 1997. Function and regulation of heat shock factor 2 during mouse embryogenesis. *Proc Natl Acad Sci U S A.* 94:2392-7.

Rane MJ, Pan Y, Singh S, Powell DW, Wu R, Cummins T, Chen Q, McLeish KR, Klein JB. 2003. Heat shock protein 27 controls apoptosis by regulating akt activation. *J Biol Chem.* 278:27828-35.

Rekwirowicz H, Marszalek A. 2009. Hypoxia-inducible factor-1, a new possible important factor in neoplasia. *Pol J Pathol.* 60:61-6.

Rock KL, Gramm C, Rothstein L, Clark K, Stein R, Dick L, Hwang D, Goldberg AL.1994. Inhibitors of the proteasome block the degradation of most cell proteins and the generation of peptides presented on MHC class I molecules. *Cell*. 78:761-71.

Sarge KD. 1995. Male germ cell-specific alteration in temperature set point of the cellular stress response. *J Biol Chem*. 270:18745-8.

Sethi G, Ahn KS, Pandey MK, Aggarwal BB. 2007. Celastrol, a novel triterpene, potentiates TNF-induced apoptosis and suppresses invasion of tumor cells by

inhibiting NF-kappaB-regulated gene products and TAK1-mediated NF-kappaB activation. *Blood.* 109:2727-35.

So A, Hadaschik B, Sowery R, Gleave M. 2007. The role of stress proteins in prostate cancer. *Curr Genomics.* 8:252-61.

Soligo D, Servida F, Delia D, Fontanella E, Lamorte G, Caneva L, Fumiatti R, Lambertenghi Deliliers G. 2001. The apoptogenic response of human myeloid leukaemia cell lines and of normal and malignant haematopoietic progenitor cells to the proteasome inhibitor PSI. *Br J Haematol.* 113:126-35.

Sun Y, MacRae TH. 2005. The small heat shock proteins and their role in human disease. *FEBS J*. 272:2613-27.

Tam Y, Heikkila JJ. 1995. Identification of members of the HSP30 small heat shock protein family and characterization of their developmental regulation in heat-shocked *Xenopus laevis* embryos. *Dev Genet.* 17:331-9.

Tanabe M, Sasai N, Nagata K, Liu XD, Liu PC, Thiele DJ, Nakai A. 1999. The mammalian HSF4 gene generates both an activator and a repressor of heat shock genes by alternative splicing. *J Biol Chem.* 274:27845-56.

Tanaka M, Asashima M, Atomi Y. 2003. Proliferation and differentiation of *Xenopus* A6 cells under hypergravity as revealed by time-lapse imaging. *In Vitro Cell Dev Biol Anim* .39:71-9.

Tozawa K, Sakurada S, Kohri K, Okamoto T. 1995. Effects of anti-nuclear factor kappa B reagents in blocking adhesion of human cancer cells to vascular endothelial cells. *Cancer Res.* 55:4162-7.

Trott A, West JD, Klaic L, Westerheide SD, Silverman RB, Morimoto RI, Morano KA. 2008. Activation of heat shock and antioxidant responses by the natural product celastrol: Transcriptional signatures of a thiol-targeted molecule. *Mol Biol Cel.l* 19:1104-12.

Tuttle AM, Gauley J, Chan N, Heikkila JJ. 2007. Analysis of the expression and function of the small heat shock protein gene, *hsp27*, in *Xenopus laevis* embryos. *Comp Biochem Physiol A Mol Integr Physiol*. 147:112-21.

Van Montfort R, Slingsby C, Vierling E. 2001. Structure and function of the small heat shock protein/alpha-crystallin family of molecular chaperones. *Adv Protein Chem.* 59:105-56.

Verrey F, Loffing J, Zecevic M, Heitzmann D, Staub O. 2003. SGK1: Aldosterone-induced relay of Na+ transport regulation in distal kidney nephron cells. *Cell Physiol Biochem.* 13:21-8.

Voellmy R. 2004. On mechanisms that control heat shock transcription factor activity in metazoan cells. *Cell Stress Chaperones.* 9:122-33.

Voellmy R, Boellmann F. 2007. Chaperone regulation of the heat shock protein response. *Adv Exp Med Biol.* 594:89-99.

Voyer J, Heikkila JJ. 2008. Comparison of the effect of heat shock factor inhibitor, KNK437, on heat shock- and chemical stress-induced *hsp30* gene expression in *Xenopus laevis* A6 cells. *Comp Biochem Physiol A Mol Integr Physiol.* 151:253-61.

Westerheide SD, Morimoto RI. 2005. Heat shock response modulators as therapeutic tools for diseases of protein conformation. *J Biol Chem.* 280:33097-100.

Westerheide SD, Anckar J, Stevens SM,Jr, Sistonen L, Morimoto RI. 2009. Stress-inducible regulation of heat shock factor 1 by the deacetylase SIRT1. *Science.* 323:1063-6.

Westerheide SD, Bosman JD, Mbadugha BN, Kawahara TL, Matsumoto G, Kim S, Gu W, Devlin JP, Silverman RB, Morimoto RI. 2004. Celastrols as inducers of the heat shock response and cytoprotection. *J Biol Chem.* 279:56053-60.

Whitby FG, Masters EI, Kramer L, Knowlton JR, Yao Y, Wang CC, Hill CP. 2000. Structural basis for the activation of 20S proteasomes by 11S regulators. *Nature.* 408:115-20.

Whitesell L, Mimnaugh EG, De Costa B, Myers CE, Neckers LM. 1994. Inhibition of heat shock protein HSP90-pp60v-src heteroprotein complex formation by benzoquinone ansamycins: Essential role for stress proteins in oncogenic transformation. *Proc Natl Acad Sci U S A* .91:8324-8.

Woolfson JP, Heikkila JJ. 2009. Examination of cadmium-induced expression of the small heat shock protein gene, *hsp30,* in *Xenopus laevis* A6 kidney epithelial cells. *Comp Biochem Physiol A Mol Integr Physiol*. 152:91-9.

Xiao X, Zuo X, Davis AA, McMillan DR, Curry BB, Richardson JA, Benjamin IJ. 1999. HSF1 is required for extra-embryonic development, postnatal growth and protection during inflammatory responses in mice. *EMBO J.* 18:5943-52.

Yamamoto A, Mizukami Y, Sakurai H. 2005. Identification of a novel class of target genes and a novel type of binding sequence of heat shock transcription factor in *Saccharomyces cerevisiae*. *J Biol Chem*. 280:11911-9.

Yamamoto N, Takemori Y, Sakurai M, Sugiyama K, Sakurai H. 2009. Differential recognition of heat shock elements by members of the heat shock transcription factor family. *FEBS.* J 276:1962-74.

Yang H, Landis-Piwowar KR, Chen D, Milacic V, Dou QP. 2008. Natural compounds with proteasome inhibitory activity for cancer prevention and treatment. *Curr Protein Pept Sci.* 9:227-39.

Yang H, Chen D, Cui QC, Yuan X, Dou QP. 2006. Celastrol, a triterpene extracted from the chinese "thunder of god vine," is a potent proteasome inhibitor and suppresses human prostate cancer growth in nude mice. *Cancer Res.* 66:4758-65.

Young JT, Gauley J, Heikkila JJ. 2009. Simultaneous exposure of xenopus A6 kidney epithelial cells to concurrent mild sodium arsenite and heat stress results in enhanced hsp30 and hsp70 gene expression and the acquisition of thermotolerance. *Comp Biochem Physiol A Mol Integr Physiol*. 153:417-24.

Young JT, Heikkila JJ. 2009. Proteasome inhibition induces *hsp30* and *hsp70* gene expression as well as the acquisition of thermotolerance in *Xenopus laevis* A6 cells. *Cell Stress Chaperones*. [E-published ahead of print:DOI 19.1007/s12192-009-0147-4]

Zhang YQ, Sarge KD. 2007. Celastrol inhibits polyglutamine aggregation and toxicity though induction of the heat shock response. *J Mol Med.* 85:1421-8.

Zuo J, Rungger D, Voellmy R. 1995. Multiple layers of regulation of human heat shock transcription factor 1. *Mol Cell Biol.* 15:4319-30.